Cape Peninsula University of Technology

An application of pinch analysis in the design of a stand-alone thermochemical cycle, hydrogen hub sourced from renewables in rural South Africa

By

Daniel Cecil Seragie

Thesis submitted in fulfilment of the requirements for the degree

Master of Engineering: Chemical Engineering

In the Faculty of Engineering

At the Cape Peninsula University of Technology

Supervisor: **Mr. Joe John**

Co-Supervisor: **Prof Daniel Ikhu-Omoregbe**

Bellville Campus

May 2020

DECLARATION

I, **Daniel Cecil Seragie**, declare that the contents of this dissertation/thesis represent my unaided work and that the dissertation/thesis has not previously been submitted for academic examination towards any qualification. Furthermore, it represents my own opinions and not necessarily those of the Cape Peninsula University of Technology.

Signed **Date**

ABSTRACT

Economic and social development are closely related to the accessibility of electricity. Meanwhile, non-grid connected rural areas shoulder the burden of health and environmental risks since extending the grid is considered uneconomical. Renewable hydrogen, hybrid energy systems are viewed as a promising solution in remote areas where grid extension is costly and fuel costs increase parallel to remoteness. Hence, this study applies heat and power pinch analysis in the conceptual design of an isolated, decentralized thermochemical cycle hydrogen & biogas energy hybrid, to satiate the electricity needs of a non-grid rural area in South Africa. This study highlights the value of using heat pinch and PoPA tools as a mid-term supplement to combat increasing energy costs, reduce negative environmental impacts, improve profits, and more importantly as a contribution to ensuring temperatures are kept well below 2℃ above pre-industrial levels.

The hybrid plant was designed to supply electricity to 39 village households, housing 156 inhabitants with daily electrical usage of 273 kWh. A 4-step hybrid CuCl thermochemical process including an electrolysis step coupled with Anaerobic Digestion (AD) was employed in the hybrid design. The 4-step hybrid CuCl cycle process was chosen since it has greater thermal efficiency and practical viability relative to the other thermochemical cycles whilst AD was chosen since the chosen site is rich in biomass.

A Parabolic Trough Concentrator (PTC) to capture solar radiation and a Proton Exchange Membrane Fuel Cell (PEMFC) was combined with the thermochemical plant to convert hydrogen to electricity. Considering the demand, the solar and biogas plant was sized at 30 & 35 kW respectively. Once sized, heat pinch analysis was applied to improve heat distribution coupled with Power Pinch Analysis (PoPA) for effective electricity distribution.

In applying heat pinch analysis and constructing the Grid Diagram (GD), a cooling energy target of 43.86 kW was achieved whilst reducing the total number of heat exchangers from 19 to 12, leaving 5 unsatisfied streams. However, the 5 unsatisfied streams were accepted since reaching its target temperatures were considered insignificant. PoPA was applied whilst maintaining an Available Excess Electricity for the Next Day (AEEND)>Minimum Outsourced Electricity Supply (MOES), thereby ensuring no grid electricity requirement. The initial envisioned operating times and capacity resulted in an oversized system with a daily electricity surplus of 586.99 kWh. This was then revised by shifting operating times to provide an electrical surplus of 12 kWh per day. The original capacity was not changed but the plant power output can be ramped down to achieve continuous operation of the biogas plant, thereby providing an electrical surplus of 8.99 kWh. The process of ramping output up or down is known as cycling.

The solar and biogas plant was initially oversized to 30 and 35 kW respectively, thus accounting for power losses, increased migration to the village considering the available power source and potential

extension to neighbouring villages. Consequently, cycling was recommended to minimize electricity surplus.

The minimum surplus of 8.99 kWh a day was achieved by reducing the power output (cycling) of the solar and biogas plant to 10 kW & 12 kW respectively. PoPA revealed that a biogas plant power output of 12 kW was ideal to ensure continuous power supply should weather conditions thwart effective operation of the solar plant.

A cost estimate was performed revealing a unit cost of $3/kWh & $2/kWh. Consequently, the system was concluded as expensive. However, it has been recommended to scale-up production to ensure a more accurate estimate whilst reducing the unit cost with economy of scale. Furthermore, exploiting economy of scale could further highlight the benefits of using pinch tools to combat rising energy costs and negative environmental impacts associated with power production.

DEDICATION

This is for you, Mommy. Thank You.

ACKNOWLEDGMENTS

I would like to thank Mr. Joe John for his around the clock assistance. Your calming demeanour and encouragement have always kept me sane. Thank You.

Prof Daniel Ikhu-Omoregbe, thank you for the criticism, guidance & advice. It has assisted me in ways that extend beyond this thesis.

I am also thankful for the partial financial support provided by the National Research Foundation of South Africa during this project. Opinions expressed in this thesis and the conclusions arrived at, are those of the author, and are not necessarily to be attributed to the National Research Foundation.

Contents

List of Figures

List of Tables

Nomenclature

PoPA	Power Pinch Analysis
HES	Hybrid Energy System
CC	Composite Curve
HEN	Heat Exchanger Network
PTA	Problem Table Algorithm
GD	Grid Diagram
ΔT_{min}	Minimum Approach Temperature
PCT	Power Cascade Table
SCT	Storage Cascade Table
PoCA	Power Cascade Analysis
MOES	Minimum Outsourced Electricity Supply
AEEND	Available Excess Electricity for the Next Day
FCEV	Fuel Cell Electric Vehicle
BEV	Battery Electric Vehicle
GHG	Green House Gas
PHEV	Plug in Hybrid Electric Vehicle
HEV	Hybrid Electric Vehicle
ICEV	Internal Combustion Engine Vehicle
ICE	Internal Combustion Engine
H_2ICEV	Hydrogen Internal Combustion Engine Vehicle
PV	Photovoltaic
CHP	Combined Heat & Power
AD	Anaerobic Digestion
FC	Fuel Cell
CSP	Concentrated Solar Power
Cp	Heat Capacity

CP	Heat Capacity Flowrate
Vc	Fuel Cell Mean Voltage
Pe	Electric Power
TMC	Total Module Cost
TGRC	Total Grass Roots Cost
FCI	Fixed Capital Investment
FCI_L	Fixed Capital Investment Excluding Land
C_{BM}	Bare Module Cost
C_P^0	Purchased Cost of Equipment at Base Conditions
F_{BM}	Bare Module Factor
A	Size Parameter
K_n	Equipment Correlation Data
F_M	Equipment Material Factor
F_P	Equipment Pressure Factor
B_n	Equipment Constant
C_{BMT}	Total Bare Module Cost
COM	Cost of Manufacture
COMd	Cost of Manufacture Excluding Depreciation
C_{Ol}	Cost of Operating Labour
C_{UT}	Cost of Utilities
C_{WT}	Cost of Waste Treatment
C_{RM}	Cost of Raw Materials
P	Number of Solid Handling Steps
N_{OL}	Number of Operators Per Shift
N_{np}	Number of Non-Solid Handling Steps
$\bar{X}$	Average

CHAPTER 1: INTRODUCTION

1.1 General Overview

Energy is a vital component in every aspect of our daily lives, contributing significantly to both social and economic development. The Energy Information Administration (EIA, 2016) notes that fossil fuels which include liquid fuels, natural gas, and coal will account for 78% of total world energy consumption by 2040. Worldwide, energy demands continue to escalate with population and economic growth, thereby placing strain on current energy reserves. Liquid fuel consumption is expected to decrease from 33% in 2012 to 30% by 2040 however, coal and natural gas consumption will increase by $0.6\%/year$ and $1.9\%/year$ respectively by 2030 (EIA, 2016). Consequently, Shafiee & Topal (2009) predict that coal reserves will last to at least 2112, whilst being the only fossil fuel in the world after 2042. In South Africa, Eskom produces 77% of the country's energy needs by coal, with a reserve of roughly 200 years (Eskom, 2017). Concern surrounding energy security is fast growing since fossil fuels are finite. In support of energy security, Dincer & Rosen (1999), state that the supply of energy must be fully sustainable in achieving sustainable development.

Thwarting sustainable development, fossil fuels contribute significantly to environmental deterioration, as well as being an accelerator of species extinction. Furthermore, fossil fuel induced greenhouse gases (GHG) are gradually increasing, thereby accelerating the trapping of heat radiated from the Earth's surface. Naturally, this raises the temperature of the Earth's surface whilst forcing climate change. Chang (2010) & Muneer *et al* (2005) respectively expect surface temperatures to rise by 1 -2℃ & 6℃ by the year 2100.

It has been stressed that global warming and its resulting climate changes have alarming effects on human health, economics, and the environment (Muneer *et al*, 2005). According to the World Health Organization (WHO, 2017), climate change is expected to cause approximately 250 000 additional deaths per year between 2030 and 2050. Additionally, economic growth will be hindered as a direct result of climate change. Many of the damaging economic consequences will be due to droughts, floods, storms, and the rise in sea level. Consequently, frequent extreme weather conditions may lead to property and infrastructure loss (Wade & Jennings, 2016).

Furthermore, Wade & Jennings (2016) went on to mention that developing countries may lack the capacity to bounce back in response to natural disasters, and recovery time may be prolonged. Despite the loss in economic growth because of climate-sensitive sectors such as tourism, governments will be squeezed into diverting resources from economic growing possibilities towards countering costs of severe weather conditions (Wade & Jennings, 2016).

Although developing nations are expected to bear the brunt of climate change (Stern, 2006), the impact of rising temperatures will be felt globally partly due to the financial, political, and economic integration of world economies (Wade & Jennings, 2016). Renewable energy sources are considered one of the solutions to combatting climate change whilst maintaining sustainability between energy, economy, and social aspects as well.

Envisioned as the low carbon fuel of the future, Muneer *et al* (2005) noted that, hydrogen acting as an energy carrier allows energy produced by renewables to be stored thereby overcoming concerns surrounding the intermittency of renewable energy sources. The above authors added that environmentally friendly hydrogen, for fuel and energy applications, include powering vehicles, running turbines, or Fuel Cells (FCs) to produce electricity and generating heat, which would reduce the use of fossil fuels.

In a perfect world, nations fuelled by hydrogen generated from renewable energy sources serve as a potential solution to sustaining the environment, economy, and human health. Despite the world's energy sector depending mainly on fossil fuels, many countries have adopted policies and procedures paving the way towards a hydrogen economy. As one of the countries, leading the transition into a renewable energy sourced hydrogen economy, Iceland could become a pilot country for the demonstration of the hydrogen economy as it strives towards achieving it by 2030 (Arnason & Sigfusson, 2000).

It is clear that a collective effort is required to combat climate change. However, developing nations are slow in their pursuit of renewable sourced energy options whilst being considered the fastest growing source of CO_2 emissions. According to Dincer & Rosen (1999), CO_2 cumulative emissions from 17 major developing countries will reach 3.6 billion tonnes in 2025 compared to 0.9 billion tonnes in 1985. This is further supported by Pegels (2010), who stated that in the year 2000, developing countries already accounted for 55% of the global greenhouse gas emissions. More specifically, South Africa ranks seventh of the top ten countries that are responsible for more than 85% of the global carbon emissions from coal-fired plants (Pretorius *et al*, 2015).

Recently, South Africa has introduced measures such as the carbon tax act and air quality act to ensure minimum emission standards (MES) in an attempt to reduce greenhouse gases (Pretorius *et al*, 2015). According to the Carbon Report (2015), the South African government has committed to reducing greenhouse gases by 34% in 2020 and 42% by 2025. However, to meet current and projected energy demands, Eskom has invested in the commissioning of two new coal-fired power plants namely the Medupi and Kusile power plants, which appear to be contrary to the above targets. Despite the increasing regulations introduced by the South African government to reduce emissions, it is clear that the energy sector will rely on coal for many years.

Little progress has been made towards providing electricity to much of rural South Africa. According to Pretorius *et al* (2015), in 2011 the number of households living in informal households was approximately 1.25 million, 57% of which did not have access to electricity. Furthermore, the Community Survey (2016) estimated that only 91.1% of households countrywide are using electricity. The remaining households not electrified are those situated in the deep rural areas of South Africa (White & Koopman, 2011).

Moreover, White & Koopman (2011) went on to mention that rising material and increasing electricity costs make extending the grid to non-electrified rural areas uneconomical. This introduces the opportunity for decentralized energy systems, which can be fuelled by renewable sources. Elam *et al* (2003) noted that hydrogen energy systems have the added benefit in locations where conventional energy supply infrastructure does not exist. Consequently, introducing hydrogen technologies in niche applications could result in improvements and possible cost reductions.

Decentralized stand-alone energy systems have emerged as a cost-effective prospect for supplying power to remote rural areas, where grid extension remains uneconomical. In support, Akikur *et al* (2013) stated that, naturally, grid extension is the first option for non-electrified rural areas, however, it becomes uneconomical due to the large investment required relative to the low energy requirements.
Kaundinya *et al* (2009) characterized decentralized power, as an energy system generating power closer to the demand, focussing mainly on meeting local needs. Moreover, they noted that decentralized power may or may not be connected to the electrical grid, the latter acting as an independent/stand-alone system. Naturally, introducing stand-alone power systems in deep rural areas will pave the way to improved standards of living, while reversing social inequity (Kaundinya *et al*, 2009).

Access to electricity is closely related to economic and social development, whereby the lack thereof may lead to negative environmental and health risks. White & Koopman (2011) reported that pollution in non-electrified rural areas increase due to the burning of wood for heat and lighting, whilst simultaneously leading to deforestation. Moreover, they estimated that inhabitants from rural areas spend roughly 3 to 4 times more money on energy, whereby the increased cost is attributed to energy sources such as paraffin, candles, and wood. Consequently, the burning of such fuels reduces the quality of air in confined spaces.
According to Winkler *et al* (2011), access to electricity allows for reduced smoke exposure, reallocation of household time from energy provision to improved education and income. Winkler *et al* (2011), listed more benefits of electrification; lighting allows for greater flexibility with time allocation and better conditions for education, lower transportation, and communication costs with more access to information and improved health care and schools. Furthermore, the introduction of reliable and adequate electricity will reduce the high infant mortality, improve life expectancy, literacy, and fertility rates in poor rural areas (Davidson & Mwakasonda, 2004).

This study introduces a decentralized stand-alone energy system, powered by renewable sources for hydrogen production which could go the distance in improving the welfare of rural area inhabitants, reduce global temperatures with an application in the potential hydrogen economy

1.2 Problem Statement

Non-grid connected rural areas remain at the centre of social injustice, as several developing countries struggle with the cost implications of extending the national electricity grid. Energy demands continue to escalate, placing strain on limited fossil fuel reserves whilst reducing the capacity of the power sector to provide sustainable electricity to rural areas. Coupled with pinch technology for efficient use of resources, renewable energy sources are an attractive prospect for economical electricity supply to a small rural setting. Introducing renewables for electricity supply will pave the way in reversing social injustices and the negative climatic effects from the use of fossil fuels for national grid electricity production.

1.3 Aims & Objectives

This study aims to use pinch analysis to design an efficient thermochemical cycle hydrogen hub as part of a renewable hybrid, capable of providing a sustainable electric supply to an off the grid rural setting in South Africa. Additionally, a cost estimate will be performed alongside the design.

More specifically, to achieve these aims the following will be done:

- Locate appropriate rural setting & scope for an ideal renewable mix to form part of the hybrid.
- Analyse existing thermochemical cycles and fuel cells for hydrogen production along with solar collecting systems.
- Determine the energy requirement for the rural setting.
- Apply PoPA & heat pinch analysis for efficient electricity and heat distribution to a rural setting.
- Capital & manufacturing cost estimate to determine the per-unit cost.

1.4 Delineation

The study focusses on heat pinch analysis and PoPA for effective process heat distribution and reduced electricity wastage. Hence, applying pinch analysis will lead to improved system efficiency. However, the following will not be focused on or included in this research project:

- Electricity, hydrogen, or heat storage.
- Enhancing the efficiency of current FCs and solar collecting systems to improve overall plant efficiency.
- PoPA will assume no power losses hence, 100% efficiency.
- Piping, instrumentation, pumps, and plant layout is not considered in the cost analysis.

1.5 Significance of Research

Considering the high costs associated with generating electricity from renewables, this study applies pinch and hybrid technology to improve the efficient and effective use of renewable sources, to promote the renewable energy market with the hope of attracting NGO’s and government, improving renewable energy policy and widening electricity access to remote rural households, whilst contributing to the possibility of a clean hydrogen economy.

1.6 Expected Outcomes

According to Steinfeld (2005), solar thermochemical hydrogen production has the potential to be cost competitive with water electrolysis via photovoltaics and conventional fossil-based processes. In support Abanades *et al* (2005), Graf *et al* (2008), Holladay *et al* (2009) & Wang *et al* (2012) claim that hydrogen production efficiencies using the thermochemical process have the potential to exceed water electrolysis via photovoltaics and conventional fossil-based processes. Hence, it could have the potential to be cost-effective. Consequently, it is expected that this study provides a basis for competitive solar hydrogen production for the transport and energy sectors in a future hydrogen economy. It is worth noting that this study will present potentially, the first reported thermochemical hydrogen hybrid for electricity supply in a rural setting.

CHAPTER 2: LITERATURE REVIEW

2.1 Chapter Outline

The following section provides relevant background into the research problem. More importantly, it provides the rationale for the adopted approach by discussing alternative renewable sources, hydrogen production methods, heat and power pinch methods whilst motivating the prospect of a hydrogen economy.

2.2 Renewable Energy

Global warming continues to brand its presence as the world suffers through climate change. The rise in oceanic and atmospheric temperatures will continue to cause severe weather conditions and rising sea levels. This, for the most part, is attributed to the release of harmful emissions from the ever-expanding energy and transport sector's dependence on fossil fuels. Renewable energy sources that are clean, safe, abundant, and can always be replenished include solar, wind, biomass, geothermal, and oceanic.

2.2.1 Geothermal Energy

Generated in the Earth's core where temperatures can reach 6650℃ (Nasruddin *et al*, 2016), geothermal energy harnessed as underground water in fissured rocks is heated as it approaches the surface through fractures in the Earth's crust (The NEED Project, 2012), leading to water temperatures of approximately 260℃ (Barnea, 1972). Upon reaching the Earth's surface at a lower pressure, water is flashed off as steam and captured before feeding generators to create electric power.

Nasruddin *et al* (2016) note that only countries located within the Pacific Ring of Fire have the most active, most easily harvested, and economical geothermal sources. South Africa is among the list of countries lacking the potential to harvest geothermal power due to its geological position. Therefore, geothermal energy will not be used as a renewable generator in this study since the chosen rural site is not suited to harvesting geothermal power.

2.2.2 Hydroelectric Power

Although considered renewable, hydroelectricity is not exactly the poster child for being environmentally friendly. The Department of Energy (2019) considers hydroelectric energy as being detrimental to the environment since large areas of land may be flooded when dams are built which disrupts wildlife habitats, residential and farming areas.

Considering the environmental impact and displacement of settlements by huge storage dams, the Department notes that this will likely limit hydropower on a large scale. Additionally, Bigili *et al* (2018) report that large scale hydropower plants are disadvantaged by energy loss due to long transmission lines harming the surrounding ecology, waste of important forest and underground resources, and extended production periods.

Despite the negative environmental effects, hydropower has established itself as the leading global renewable source for electricity generation contributing 71% of all renewable energy (World Energy Council, 2019). This may in part be attributed to small scale hydropower plants that do not generate

pollution, are reliable and flexible, easy to maintain, and are considered more environmentally friendly with the highest potential of electrifying rural areas at a lower cost (Bigili *et al*, 2018).

Africa is the most underdeveloped hydroelectric producing continent (World Energy Council, 2016). More specifically, Aliyu *et al* (2018) acknowledge that hydropower has not been prioritized in South Africa. Loots *et al* (2015) attribute the lack of South Africa's hydropower priority to the fact that South Africa by international comparison, is considered a water scarce country. Banks & Schaffler (2006) agree with this assessment since very low river and dam levels are a regular occurrence making it an unreliable source of energy in South Africa. Considering the geological position of the chosen site, water scarcity & negative environmental impacts of hydropower, hydropower cannot be employed as a renewable generator in this study.

2.2.3 Oceanic Renewable Energy

Considered vast and powerful, Pele & Fujita (2002) goes so far as to mention that the ocean stores enough energy to meet and exceed worldwide energy demands. According to Esteban & Leary (2010), there are presently four methods for harvesting renewable energy from the ocean which include wind, tides, waves, and thermal differences between deep and shallow waters.

2.2.3.1 Tidal Barrages & Tidal Current Turbines

Harvesting energy from tides is achieved by converting the tide's inherent potential or kinetic energy into electricity using tidal barrages and tidal current turbines respectively (Rourke *et al*, 2010).

Exploiting the rise and fall of the ocean's surface, Rourke *et al* (2010) noted that, a tidal barrage fills a basin built across a bay or estuary at high tide and allows the captured water to flow through turbines to produce electricity once the tide has receded sufficiently, to generate a substantial hydrostatic head across the barrage. The authors added that extracting energy using tidal current turbines involves only the use of turbines running in water to convert the kinetic energy of tidal currents into electrical energy.

According to Rourke *et al* (2010), building large tidal barrages across a bay or estuary may change the flow of tidal currents thereby affecting the marine life within the estuary. Silva *et al* (2017) add that, tidal barrages reduce aquatic habitat connectivity limiting fish movements, especially for migrating species. The same holds with respect to progress for tidal current turbines, which is still in its infancy since it is unprofitable (Melikoglu, 2018).

2.2.3.2 Ocean Thermal Energy Conversion (OTEC)

Covering over 70% of the Earth's surface, Khan *et al* (2017) reported that the ocean absorbs and stores solar energy in its surface layer equivalent to the energy stored in 250 billion barrels of oil.

As the surface layer is heated, a temperature differential is created between the surface and deep seawater (Zhang *et al*, 2018). Volatile working fluids such as ammonia, propane, various refrigerants, and ammonia-water mixtures are employed in a process known as Ocean Thermal Energy Conversion

(OTEC) to create electricity via a vapour power cycle operated between the temperature differential (VanZwieten *et al*, 2017).

OTEC is considered viable in tropical regions, in environments with temperature differences of about 20℃ between the surface and deep water no more than 1000 m apart, located within ocean 25 km from the shore (Esteban & Leary, 2012). OTEC has since progressed but remains an immature technology relative to tidal barrages and tidal currents.

2.2.3.3 Wave Energy Converters (WECs)

Oceanic waves exist as a result of wind blowing over the surface of the ocean to create reserves of extractable potential and kinetic energy (Khan *et al*, 2017). Considered one of the most promising renewable energy sources, wave energy presents potential for a reliable energy output which is available 90% of the time at a given site thereby casting a shadow over the 20-30% availability of solar and wind (Pele & Fujita, 2002). Additionally, further advocating for wave energy is its energy density of 2-3 kW/m^2, which is significantly higher than the energy density of wind and solar of 0.4-0.6 kW/m^2 and 0.1-0.2 kW/m^2 respectively (Lopez *et al*, 2013).

Melikoglu (2018) reports that wave energy can be harvested directly from surface waves or pressure fluctuations below the surface, thereby leading to the development of Wave Energy Converters (WECs) which are classified according to location, size and working principle (Lopez *et al*, 2013). WECs may be located at different distances relative to the coast since wave power increases with ocean depth (Lopez *et al*, 2013).

According to Pele & Fujita (2002), most of the wave potential can be found where the strongest winds exist at the temperate latitudes of 40° and 60° north and south, on the eastern boundaries of the ocean. Despite the significant energy densities for wave energy at the various temperate latitudes, wave energy remains at an early stage in its deployment due to technological and financial constraints (Uihlein & Magagna, 2016). Regardless of South Africa's significant coastline, the chosen rural location cannot harness wave power since it is located away from the coastline.

2.2.3.4 Pressure Retarded Osmosis (PRO) & Reverse Electrodialysis (RED)

A release of free energy occurs, driven by the difference in chemical potential between them when two water bodies of varying salinity encounter one another at river mouths (Silva *et al*, 2016). Schaetzle & Buisman (2015) along with Silva *et al* (2016) agree that two energy extracting technologies exist with significant developmental progress namely; Pressure Retarded Osmosis (PRO) and Reverse Electrodialysis (RED).

Osmotic energy can be harvested and converted into useful energy using PRO. This technology uses semipermeable membranes, to allow water to flow from a dilute solution to a concentrated one (Hefler *et al*, 2014). This movement from low to high concentration allows for an increased static head on the

concentrated side, which feeds a turbine to convert the mechanical energy into electricity (Jia *et al*, 2014).

Cipollina *et al* (2018) note that RED uses a series of anionic and cationic membranes stacked in an alternating manner between an anode and cathode which takes advantage of the selective migration of ions through these membranes (Embadi *et al*, 2016). Cipllina *et al* (2018) added that the generated ionic current is converted to an electronic one, which flows through an external circuit connected to the anode and cathode.

Despite the vast potential of oceanic energy, powering the rural location using this renewable source will require long transmission lines since it is not located close to the ocean. The investment cost and topology of deep rural areas disallow any economical use of oceanic energy. Renewable sources inherent to the location will likely be more technically and cost-effective.

2.2.4 Wind Energy

Today, wind energy is considered as the fastest growing energy industry in the world (Banks & Schaffler, 2006) with commercial operations in more than 90 countries around the world, bringing the global capacity to 539 123 MW (Global Wind Report, 2017).

The Global Wind Report (2017) accepts wind power as becoming a fully commercialized unsubsidized technology, successfully competing with its heavily subsidized fossil and nuclear counterparts. Pegels (2010) agrees that wind energy is one of the affordable renewable energy technologies being nearly competitive with conventional energy in Europe since conditions are favourable and fossil fuels are expensive. However, the author adds that the price of wind energy in South Africa is not sufficient to make it commercially attractive especially since wind speeds are not comparable to sites in Europe.

However, South Africa is considered to have an abundance of wind resources with a potential capacity ranging from 500 to 56 000 MW (Aliyu *et al*, 2018), whilst having a coal fed generational capacity of 43 776 MW (Power Africa, 2019). Acknowledging the potential of South Africa's wind energy to supersede its current fossil dependent energy system serves as motivation for the country to be a leader in wind power generation.

Although wind energy is considered a part replacement for the fossil energy sector since it mitigates GHG emissions, adverse environmental impacts associated with its use have emerged and are described below.

Firstly, wind turbines generate mechanical and aerodynamic noise, the former, due to advanced mechanical design has been effectively reduced (Wang & Wang, 2015). The continuous droning of a moving turbine is considered to be a potential mental stressor, causing a nuisance, decreased wellbeing, and sleep disturbance (Abbasi *et al*, 2014). Secondly, the visual impact of turbines affecting the scenery will likely continue to rise with the rapid growth of the wind industry. An additional impact on its

surroundings is the risk of harm to birds and bats which get injured or killed in flight as they collide with the turbines.

Moreover, Abbasi *et al* (2014) stated that wind turbines cause electromagnetic interference by distorting radio and television transmissions whilst generating their own electromagnetic radiation. Lastly, wind turbines modify surface-atmosphere interactions and the transfer of energy, momentum, mass, and moisture within the atmosphere (Wang & Wang, 2015). Consequently, this may affect the local hydrometeorology and may affect atmospheric dynamics (Abbasi *et al*, 2014) with satellite data showing a warming trend of up to 0.72℃ per decade (Wang & Wang, 2015).

Wind sources can potentially be harnessed for the site since it was found that there are reasonable wind speeds in the region. However, it won't be used considering the negative effects associated with wind turbines. Biomass coupled with solar sources were chosen for the hybrid system. More specifically, the choice of biomass superseded that of wind sources, considering the negatives of wind while biomass allows for the involvement of unskilled labour.

2.2.5 Biomass

Considered carbon neutral (Vassilev *et al*, 2015), biomass can be classified as forest biomass (extracted from forests), woody biomass (extracted from grass and croplands), non-woody biomass (extracted from grass and croplands), waste biomass (extracted from domestic, commercial, industrial or medical waste), and invasive plant biomass (Visser *et al*, 2019). Furthermore, Banks & Schaffler (2006) lists several forms it can be used as:

- Direct heating, cooking or to generate electricity (Direct combustion in boilers, gasification, fluidized bed gasification)
- Indirectly in biological processes to produce methanol, ethanol, and creating a liquid fuel that can be used for transport or cooking applications.
- High oil-containing crops can be used for biodiesel.
- Biomethane/gas obtained in the Anaerobic Digestion (AD) of biomass.

Vassilev *et al* (2015) reported that approximately 95-97% of the world's bioenergy is used in direct combustion. In agreement, WBA Global Bioenergy Statistics (2017) transcribes that bioheat is the most important use of biomass globally with more than 90% of biomass use attributed to heating. Furthermore, the report adds that biomass is the third largest renewable electricity generating source contributing 10.3% of the global energy supply in 2014, whilst having an annual growth of 2.3%.

However, Mamphweli & Meyer (2009) acknowledge that the burning of this resource has socio-environmental implications including GHG emissions and the accumulation of tars and soot on windows.

Despite the socio-environmental implications in the scenario above, Eskom (2019) recognized that bioenergy reduces emissions of $NO_x$and SO_x during power generation, having the added benefit of being

renewable with a reduction in fuel costs when wastes are used. Conversely, possible reasons attributed to South Africa's slow bioenergy growth are listed by Eskom (2019) & Aliyu *et al* (2018) as;

- High capital cost for biomass power plants.
- Fast-growing crops require a large land area.
- Fuel transportation can be expensive.
- Dedicated fast-growing crops will compete with other agricultural activities for land and hence lead to expensive fuel.
- Water shortage in South Africa, since dedicated crops and biofuel processes, require significant process water.
- Food security, since emphasis, may potentially be given to energy crop and not food crop
- Planting a single crop on a large scale may affect land quality.

An extensive list of advantages and disadvantages of biomass and biofuels can be found in Vassilev *et al* (2015).

Moreover, biomass is an additional contender to generate electricity, especially in rural areas. According to Mohammed *et al* (2014), most inhabitants in rural areas are farmers who could provide bio-feedstock for energy generation from decentralized applications or as part of hybrid energy systems.

2.2.6 Solar Energy

Kabir *et al* (2018) describe solar energy as being capable of satisfying worldwide energy demand if harvesting and distribution technologies were readily available whilst Khan & Arsalan (2016) added that the amount of solar radiation received in one day is capable of satisfying worldwide energy demand for more than 20 years.

Africa is considered to have the highest solar radiation levels with a potential Concentrated Solar Power (CSP) and Photovoltaic (PV) energy amounting to roughly 470 & 660 PWh respectively (Kabir *et al*, 2018). More specifically, according to Banks & Schaffler (2006), South Africa is considered to have amongst the highest solar radiation levels in the world with daily solar radiation varying between 4.5 and 7.5 kWh/m^2, requiring only 3000 km^2 of land to meet the country's energy demand. In support, the Department of Energy (2019) noted that South Africa has an average solar radiation of 220 W/m^2 compared to about 150 W/m^2 in parts of the US and about 100 W/m^2 for Europe. Solar is the resource with the largest theoretical potential in South Africa, amounting to 8,500,000 $PJ/year$ as suggested by Howells, cited in Winkler (2005), which casts a shadow over the coal reserve estimated at 1298000 PJ (WWF, 2012).

A few solar power applications include heat & power, refrigeration, and cooling, rural electrification, methanol production, desalination, and hydrogen production (Modi *et al*, 2017). This is expected since Kanan & Vakeesan (2016) consider solar power the best renewable option for future demand based on availability, cost-effectiveness, accessibility, capacity, and efficiency.

Kabir *et al* (2018) support this assessment by noting that, GHG emissions associated with solar power are minimal with the most feasible solutions to global warming, solar would minimize premature mortality rates, lost workdays and overall healthcare costs by replacing fossil fuels, improve job opportunities especially in comparison to fossil fuels, no importation of fossil fuels and hence money will remain in the local economy, low operating costs with lower susceptibility to price fluctuations like that of fossil fuels and since it can be distributed it is less likely to large scale failure. Kanan & Vakeesan (2016) add that solar systems can be used in industrial, residential, and rural settings. As an example, Kabir *et al* (2018) report that the introduction of 113 533 US household solar systems resulted in the reduction or avoidance of 696 544 metric tons of CO_2 emissions.

Acar & Dincer (2019) note that a hydrogen economy is necessary to reduce emissions and combat global warming whilst achieving energy security. In their paper, the authors comparatively investigate different hydrogen production sources based on economic, environmental, social, and technical performance and found that solar has the highest average ranking amongst other renewable sources.

Since solar power is inexhaustible and abundant, the harnessing thereof in central or decentralized power systems will support the continued economic and population growth. Hence, solar energy was chosen to operate as part of the hybrid system with biomass producing biogas.

2.3 Process Integration

Global primary energy consumption continues to rise with economic and population growth. Up from 1.2% in 2016, the primary energy consumption growth averaged at 2.2% in 2017, with the largest increments starting with natural gas followed by renewables and oil (BP Statistical Review of World Energy, 2018). Considered the world's fastest growing energy sources the EIA (2013), states that renewable and nuclear power increases $2.5\%/year$ whilst BP Statistical Review of World Energy (2018), reported the highest recorded renewable growth rate of 17% in 2017. However, despite this positive progress in ensuring low carbon economies, fossil fuels are still projected to supply nearly 78% of the global energy consumption (EIA, 2016). The South African context, according to the BP Statistical Review of World Energy (2018), fossil fuels, and renewable sources accounted for 95% and 1.7% of the primary energy consumption respectively.

South Africa's reliance on fossil fuels has led it to become a global carbon emitter, contributing roughly 35% of Africa's emission, making it the 13th highest carbon emitter in the world (BP Statistical Review of World Energy, 2018). Using the climate data platform provided by the World Resources Institute (2018), total CO_2e amounted to 530 Mt in 2014 with the energy sector contributing to 85% of the CO_2e. However, South Africa admits that a global solution with cooperative efforts of all countries is required to address the causes and impacts of climate change, which led the Government to consider the long term GHG emissions mitigation potential.

Consequently in 2008, as part of their moral and legal obligation to make a fair contribution to the global mitigation effort under the United Nations Framework Convention on Climate Change (UNFCCC) and

its Kyoto Protocol, South Africa announced that emissions should peak during the period from 2020 to 2025, remain stable for a decade and decline thereafter (National Climate Change Response White Paper, 2011). According to the National Climate Change Response White Paper (2011), during the peaking period a range with a lower limit of 398 Mt CO_2e and upper limits of 583 & 614 Mt CO_2e should exist. However, as of 2014, South Africa's GHG emissions already reached 91% of the first upper limit, as highlighted by their UNFCCC commitments.

However, South Africa remains committed to the Kyoto Protocol which should effectively ensure temperatures are kept well below 2℃ above pre-industrial levels, noting that an average global temperature increase of 2℃ translates to up to 4℃ for South Africa by the end of the century (South Africa's Intended Nationally Determined Contributions, 2015). As of 2018, a new assessment introduced by the Intergovernmental Panel on Climate Change (IPCC) has shifted the temperature threshold of 2 to 1.5℃, which is considered more likely to provide a sustainable and equitable society (IPCC, 2018). However, adding to an already dire situation, the National Climate Change Response White Paper (2011) reports that by mid-century the South African coast will warm by 1-2℃ and the interior by 2-3℃ which by the year 2100, could increase to 3-4℃ and 6-7℃ respectively.

The recently proposed Climate Change Bill provides an opportunity for the South African government to legally enforce climate change mitigation measures and emissions management, thereby establishing South Africa as a progressive nation in the fight against climate change. In the short term, energy efficiency provides a large potential for mitigation (Winkler & Marquand, 2009) which could assist companies in fulfilling their legal obligations once the Climate Change Bill is passed by the legislature. Pinch analysis has been proven to be an effective tool to boost energy efficiency and hence an effective tool for mandatory mitigation.

Initially, pinch analysis was introduced as a tool for heat integration and has since been adapted to multiple fields of resource conservation. According to Aziz *et al* (2017), these fields include mass pinch, oxygen pinch, Total Site Heat Integration (TSHI), production planning, hydrogen pinch, water pinch, financial management, CO_2 emissions pinch, biomass supply chain, emergy analysis, waste management pinch, and power pinch. An overview of the development within process integration can be found in Klemes *et al* (2013) and Klemes *et al* (2018)

More specifically, process heat integration has diverged into two complementary categories namely pinch analysis and Mathematical Programming (MP) (Klemes *et al*, 2013). According to the authors, the former relies on thermodynamic and/or physical insights whilst MP extrapolates those ideas to create mathematical expressions for solving advanced process integration problems. Hence, MP will not be used in this project considering the envisioned simplicity of the process.

Heat pinch analysis has seen significant development in addition to the expansion of pinch analysis across multiple fields. Its development includes the introduction of TSHI, pressure drop considerations, synthesis of utility systems based on steam networks, and applying heat transfer enhancement. Further

development within these categories can be found in Klemes *et al* (2013), Klemes & Kravanja (2013), and klemes *et al* (2018). Klemes *et al* (2018) describe TSHI as the integration of several processes instead of unit operations. Pressure drop targetting has been included in the development of integration to allow for a specified pressure drop for each stream (Klemes *et al*, 2013) since not considering pressure drop may lead to an inoperable system (Chew *et al*, 2015). Morever, Klemes & Kravanja (2013) note that utility systems synthesis was introduced since different rules were necessary for the placement of special equipment within pinch analysis. Lastly, Heat-Transfer Enhancement (THE) was applied to process integration. According to Klemes *et al* (2020), THE involves modifying heat transfer equipment to increase the rate of heat transfer of the specified equipment to achieve higher loads, improve energy conservation and productivity. However, the basic heat pinch analysis technique will be used in this research whilst these developments won't be included considering the design stage of the project.

Principally based on the laws of thermodynamics, heat pinch analysis introduces process heat integration by providing a systematic approach to optimally integrate energy inherent to a process. Consequently, heat pinch analysis provides an opportunity to comply with mandatory GHG mitigation since it reduces CO_2emissions whilst simultaneously considering technical and economic constraints (Aziz *et al*, 2017). Following a simple approach, heat pinch analysis maximises heat recovery by using heat flows inherent to a process to create optimal heat recovery networks. John (2014), acknowledges that the objective of heat pinch analysis is to match hot and cold process streams to create a heat exchanger network (HEN) that minimizes dependence on external hot and cold utilities. In support, Tantimuratha *et al* (2000) reported that heat pinch analysis is used to achieve minimum utility usage, minimum heat transfer area of the HEN, and the minimum number of units. Therefore, a decrease in capital and running costs is expected once pinch analysis is applied to the hybrid system.

2.3.1 Industrial Experience

Pinch analysis achieves maximum heat integration by setting practically attainable theoretical targets for both grassroots and retrofit HEN design, hence marking its presence in the industrial sector. Ebrahim & Kawari (2000) reported that by the year 2000 BASF, the German chemical company already started more than 150 pinch projects since they were able to achieve an energy saving of over 25% in their main factory at Ludwigshafen. The implementation of pinch tools by authors Dunn & El-Halwagi (2003) in retrofitting a polymer and monomer production process resulted in a 10% reduction in site utility costs, whilst achieving a 25% reduction in energy usage with a payback period of less than one year in a speciality chemicals production process. One of the earliest applications of pinch technology was its implementation by Imperial Chemical Industries (ICI) which led to a saving of over 1 million pounds per year on energy and capital costs (Kemp, 2007).

2.3.2 Heat Pinch Analysis

Pinch tools may be applied to multiple industries with a flexible application to both grassroots and retrofitting, producing significant savings whilst achieving attractive payback periods typically less than

two years (Dunn & El-Halwagi, 2003). This is achieved by following a systematic procedure as highlighted by the subsequent summarised list;

- Extract the necessary temperatures, heat capacities and enthalpies from the appropriate material and energy balances after hot and cold streams have been identified.
- Select the minimum approach temperature.
- Using Composite Curves (CCs), energy targets are identified. Alternatively, the Problem Table Algorithm (PTA) can be used. March (1998), notes that pinch analysis provides these targets to ensure minimum energy consumption or maximum energy recovery.
- Once the energy targets are established, the HEN can be designed using the grid representation method more commonly known as the Grid Diagram (GD).
- Lastly, operational and capital costs associated with HEN can be estimated.

2.3.3 Data Extraction

According to March (1998), to identify potential changes in a process that could lead to financial savings, the first step in applying pinch analysis is to extract thermal data from the process. Since pinch analysis considers heat flows from one stream to the next, identifying hot and cold streams becomes the first step in extracting the necessary thermal data. The author describes streams that require heating as cold streams whilst those that need cooling are known as hot streams.

Data extraction becomes reasonably straightforward once hot and cold streams are identified accompanied by a consistent mass and energy balance. However, challenges often present themselves at this stage. Kemp (2007) recognized these challenges as he mentioned that difficulties arise once mixing or a change of composition occurs with direct heat transfer. Additionally, processes are not likely to operate at steady state as per the design mass and energy balance. In support both Smith (2005) and Kemp (2007), agree that flow rates, compositions, temperatures, and specific heat capacities are much easier to obtain from grassroots plants since the information can be extracted directly from design data.

Conversely, the performance will often differ significantly from an existing plant's design data. To mitigate the challenges inherent to data extraction for existing plants, Kemp (2007) suggests constructing a mass and energy balance on a plant's current conditions. Once a reliable heat and mass balance can be produced, hot and cold streams may be extracted.

2.3.4 Energy Targetting

Once reliable thermal data is extracted from the plant, pinch analysis is applied to set energy targets in an attempt to minimise external energy consumption. Traditionally, energy targets are set using CCs as shown in Figure 1. Alternatively, the PTA may be used.

The hot and cold CCs are constructed on a temperature-enthalpy plot, thereby providing the available heat, and utility demand for the process. Moreover, in doing so, the maximum energy recovery is obtained for a given temperature difference. Constructing CCs, involve the addition of enthalpy changes

of the hot and cold streams in the respective temperature intervals (March, 1998). The hot and cold CCs overlap one another separated by a minimum temperature difference. The overlapping of the hot and cold CCs is an indication of the maximum process heat recovery whilst, the sections of the CCs that do not overlap indicate the need for a heating or cooling utility.

However, John (2014) adds that a more convenient method known as the PTA can be used instead of CCs for setting targets algebraically.

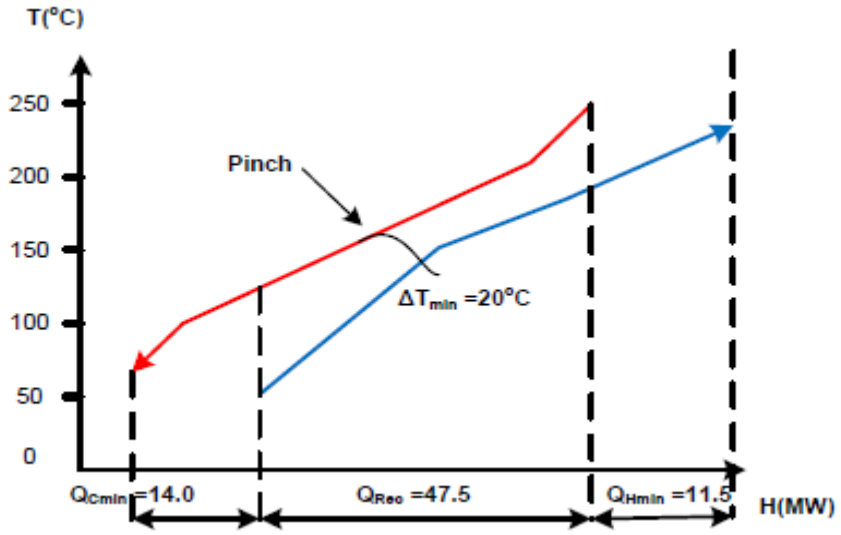

Figure 1: Example of Composite Curves (John, 2014)

2.3.5 Pinch Principle

The minimum approach temperature (ΔT_{min}) is known as the pinch. It determines how closely the hot and cold composites can be from one another without violating the second law of thermodynamics, implying that none of the heat exchangers may have a temperature crossover.

John (2014) states that the selection of the initial minimum temperature difference is industry-specific which is easily obtainable in literature. Since the pinch governs the degree at which the CCs overlap, significant consideration has to be placed on deciding the minimum approach temperature. As a result, the targets are highly dependent on the choice of ΔT_{min}.

In lowering the pinch, thereby vertically shifting the CCs closer to one another, the overlapping is increased thus maximising the energy recovery and consequently reducing utility usage. However, in doing so the HEN area has to increase, to increase the driving potential between exchanging streams thus increasing capital costs. Conversely, by increasing the ΔT_{min}, energy recovery is reduced thereby increasing the demand for utility usage. Consequently, utility costs increase. This introduces the concept of area targeting ahead of the actual network design. March (1998) reports that the manipulation of ΔT_{min} allows for trade-offs between capital and energy to obtain an optimum ΔT_{min} ahead of network design.

Furthermore, the pinch divides the process into two systems; above the pinch, only the hot utility is required, conversely below the pinch only the cold utility is required. As a result, three rules have been established for practical HEN design using pinch technology:

- No external heating below the pinch
- No external cooling above the pinch
- No heat transfer across the pinch

John (2014) emphasizes that the violation of any of these rules will lead to inefficient HEN design, since the usage of cold utilities above the pinch would require additional hot utility, similarly using hot utilities below the pinch would result in more cold utilities.

2.3.6 Heat Pinch Design Method

Focus is now placed on HEN design once the appropriate thermal data has been extracted followed by energy targeting considering both capital and energy costs. Based on pinch analysis principles, the systematic HEN design procedure known as the Pinch Design Method translates the modifications obtained in the targeting stage into a HEN that achieve energy targets within practical limits (March, 1998). The Pinch Design Method uses the GD to represent HENs.

March (1998) describes the GD, noting that, hot streams run horizontally from left to right decreasing in temperature whilst cold streams run horizontally below from right to left increasing in temperature. Heat transfer between matched streams is indicated using vertical lines joined by circles.

The author adds that the pinch divides the process into two, a dashed line splitting the process into two regions is used to illustrate this. All stream temperatures as well as the pinch point obtained from the CCs are indicated accordingly. As a result, the system below the pinch is located on the right whilst the system above the pinch is located on the left. Hot and cold streams are matched by applying the three rules; therefore, no cooler is placed on the left-hand side of the GD, and conversely, no heaters are placed on the right-hand section of the GD.

Furthermore, no process heat exchangers are placed between the hot streams on the left of the pinch and the cold streams on the right of the pinch, thus concluding the design of HEN that achieves the energy target (March. 1998).

2.4 Power Pinch Analysis (PoPA)

Rozali *et al* (2013) describe PoPA as a technique used for optimizing power allocation in hybrid power systems, by setting minimum outsourced electricity targets and maximum storage targets during start-up and normal operations. Aziz *et al* (2017) add that, PoPA reduces electricity demand by integrating renewable energy sources to determine the plant capacity. Hence, PoPA will be used in conjunction with heat pinch analysis to improve the efficiency of the hybrid system and thus costs. This introduces the opportunity for the renewable system to potentially have a unit cost that may be competitive relative to traditional fossil fuels.

Analogous to the CCs presented for heat pinch analysis, Wan Alwi *et al* (2012) proposed PoPA to optimally size hybrid power systems using graphical tools. The authors introduced Power Composite Curves (PCCs) to determine the MOES and the AEEND for start-up operation. Additionally, they extended the PCCs to the Continuous Power Composite Curves (CPCC) to determine the amount of MOES required for daily operation.

Expanding on the graphical tools presented by Wan Alwi *et al* (2012), Rozali *et al* (2013) presented numerical tools analogous to the PTA used in heat pinch analysis. These tools included the Power Cascade Table (PCT) & Storage Cascade Table (SCT). In constructing the PCT and SCT, Rozali *et al* (2013) note that these tools can be used to determine the minimum target for outsourced electricity, the amount of excess electricity for storage during start-up and daily operations, the amount of transferrable power, maximum storage capacity, surplus electricity to supply to the grid, amount of outsourced electricity needed at each time interval and the time interval where the maximum power demand occurs. The PCT tool is especially important for the rural hybrid system since it allows the designer to size the system in a way so that it doesn't require grid electricity for start-up or during operation. This is done by ensuring that the lowest AEEND>MOES is achieved.

However, the numerical tools similar to that of the graphical tools assumed 100% efficiency for power transfer and storage. Upon considering power losses, Rozali *et al* (2013) found that the targets obtained using these tools had an error of 15-25%.

Acknowledging power loss constraints, Rozali *et al* (2013b) extended PoPA to consider power losses associated with conversion, transfer, and storage in the SCT to provide more realistic energy targets for off-grid hybrid systems thereby reducing the possibility of undersized energy systems. However, this will not be considered in this project.

According to Aziz *et al* (2017), PoPA comprises of three main steps which include;

- An analysis of potential renewable energy sources.
- Power sources and demands data extraction.
- Construction of the PCT and SCT.

2.4.1 Power Cascade Table (PCT)

The Power Cascade Analysis (PoCA) is executed using the PCT tool. Applying PoCA allows one to determine the amount of electricity that can be stored and transferred to subsequent days for off-grid systems and the amount of electricity that can be mutually transferred using grid-connected systems (Rozali *et al*, 2013).

A brief methodology, describing the construction of the PCT has been extracted from Rozali *et al* (2013) and presented below.

- Calculating and tabulating the net electricity surplus/deficit from the difference between the sum of electricity sources and demands in the intervals they exist, is the first step in constructing the PCT. A net surplus indicates storable energy whilst a net deficit indicates that electricity needs to be supplied from storage or outsourced electricity.
- Once tabulated, the surplus and/or deficits are cumulated from the first to the last time interval in a separate column. The absolute value of the largest negative electricity flow (if any exist) is then cascaded cumulatively to the net electricity surpluses/deficits to generate the MOES and AEEND.
- According to Wan Alwi *et al* (2012), as cited in Rozali *et al* (2013), two possible scenarios for daily operations exist. One wherein the AEEND is less than, or equal to MOES. Excess electricity from the previous day is stored and used to reduce external electricity needed for the following day. The second scenario is when the AEEND exceeds the MOES,and storing electricity more than that equivalent to the MOES will require infinite storage. Consequently, the difference between AEEND and MOES highlights surplus electricity. Excess electricity can be sold to the electricity grid for on-grid systems.

2.4.2 Storage Cascade Table (SCT)

Once the MOES and AEEND have been determined, Rozali *et al* (2013) recommend constructing the SCT to determine the amount of electricity that can be transferred from each source, external electricity requirement at each time interval and storage capacity. Extracted from the authors, the subsequent list provides a brief methodology used to construct the SCT. The SCT plays a significant role in sizing the storage since the renewable hybrid system will not depend on grid electricity.

- Similar to the PCT, columns for time, time interval, electricity sources, and demands are constructed. The column that follows titled “amount of electricity transfer”, involves allocating the maximum amount of electricity transferred as restricted by the lowest value between the sources and demands during each time interval.
- The net electricity surplus/deficit is then repeated to determine the storage capacity during start-up.
- Once tabulated, the surplus/deficit column is cascaded cumulatively downward each time interval in a separate column, titled storage capacity.
- The largest positive value is an indicator of the maximum storage whilst the sum of the negative values provide the outsourced electricity requirement. This process is repeated during operation, however, in the case that MOES exceeds AEEND, the cascade begins with the AEEND.
- The process is repeated if the AEEND exceeds MOES. However, for daily operation, once the surplus/deficit is cascaded, the maximum storage is the largest positive value less the surplus electricity as determined by the difference between AEEND and MOES.

A detailed methodology is provided by Rozali *et al* (2013), the numerical techniques of which have been extrapolated from the graphical techniques presented by Wan Alwi *et al* (2012).

2.5 Hydrogen

Considering the climatic, economic, and finite implications of the current fossil-fuelled energy and transportation sectors, has led to the emergence of a potential hydrogen economy to ensure sustainable development. In 1970, Bockris inspired the hydrogen economy, picturing it to be one wherein hydrogen would be used to transport energy from renewables over large distances to be stored and supplied to cities. Bockris added that hydrogen as an energy carrier can be used in FCs for electricity generation and combusted cleanly in air to provide energy for space heating, replace the natural gas industry and power aircraft, trains, and ships (Bockris, 2002).

Hydrogen generated from thermochemical cycles using solar as its source will be fed to a FC to generate electricity as part of a hybrid system along with biogas. Although the hydrogen economy may be considered as advanced technology in the rural context, this study can act as a baseline for decentralized renewable energy systems that could subscribe to a potential hydrogen economy.

2.5.1 Hydrogen Applications

Hydrogen has already established its importance within the ammonia, petroleum and to a lesser extent other chemical industries, with an estimated consumption of 500 billion $Nm^3/year$ (Dupont, 2007). Ramachandran & Menon (1998), reported that the majority of hydrogen produced is used as a chemical reactant, accounting for 50, 37, and 8% for ammonia production, petroleum processing, and methanol respectively. Ball & Weeda (2015) report similar figures whilst acknowledging that hydrogen use and production for industry has only existed since 1920. Hydrogen as a fuel source for FC powered vehicles is seen as an additional emerging application which Ball & Weeda (2015) emphasize will play a critical role in advocating for the potential hydrogen economy.

2.5.2 Powertrains

Thomas (2009) & Morrison *et al* (2018) note that Fuel Cell Electric Vehicles (FCEVs) and Battery Electric Vehicles (BEVs) are the two most promising options to reduce GHG emitted within the transportation sector. Although, Plug in Hybrid Electric Vehicles (PHEVs) and Hybrid Electric Vehicles (HEVs) are considered strong contenders for decarbonization, and are enthusiastically promoted by many authors such as Romm (2006), Chan (2007) & Pollet *et al* (2012), only FCEVs and BEVs will be further discussed since it produces no emissions at the tailpipe.

It has been envisioned by King (2008), and a few authors such as Pollet *et al* (2012) & Morrision *et al* (2018) to name a few, that FCEVs and BEVs will coexist to decarbonize the transport sector.

2.5.3 Infrastructure

On the surface, hydrogen-fuelled vehicles seem counterintuitive since an electricity infrastructure already exists providing an easier transition into an electric fuelled economy. However, like FCEVs,

BEVs still require significant infrastructure investment. Ball & Weeda (2015) along with Andwari *et al* (2017) report that a network of electric charging points is still needed whilst Offer *et al* (2010) notes that a BEV recharging infrastructure can grow quicker owing to the existing power grid with lower risk than hydrogen infrastructure. Ball & Weeda (2015) share this sentiment since the modular nature of charging infrastructure is easy to build up initially. However, they also recognize that at some point FCEV refuelling station costs and investment will drop below that of charging stations because of the fast refuelling times whilst charging stations need continuous investment as the BEV fleet increases.

2.5.4 Refuelling Times

Thomas (2009) reports an average refuelling time of 3.3 min for a FCEV, whilst Ball & Weeda (2015) improve FCEV customer acceptance by providing refuelling times of 3-5 min for a range of 400-500 km. On the other hand, BEVs become less attractive to customers since charging times can inconveniently take up to 8 hours to fully charge from standard domestic and public outlets (Pollet *et al*, 2012), (Ball & Weeda, 2015) whilst Thomas (2009) records a charging time of more than 42 hours to fully charge a BEV with a range of 320 km. Although Offer *et al* (2010) note that the problem can be partly solved by introducing schemes such as battery swopping but the charging logistics and potential situations wherein owners are incapable of charging between trips pose a risk to customer mobility.

2.5.5 Range

According to Balat (2008), hydrogen is considered to have the highest energy content of all conventional fuels which stores approximately 2.6 times more energy per unit mass than gasoline with five times more energy per unit mass than Nickel Metal Hydride (NiMH) batteries and two times more than advanced Lithium-ion batteries (Thomas, 2009). In support, Dunpont (2007) reported that a kg of hydrogen carries roughly the same energy as 3 kg of petrol and produces three times as much energy as the same mass of natural gas and six times that of coal when combusted.

Considering the relatively low energy density of batteries, constraints exist on battery range since they will in turn be larger, heavier, and more expensive. Offer *et al* (2010) provides an example that a BEV with a range of 200 km requires roughly 150 kg of lithium-ion cells or more than 500 kg of lead-acid batteries. Alternatively, increasing the range of FCEV increases its mass negligibly, whilst increasing the range of BEVs will increase its structural and component mass significantly since most of the battery power will be used in moving the heavy load of the vehicle and battery (Thomas, 2009). Ball & Weeda (2015) noted that increasing BEV range above normal driving conditions of 150 km would be very costly. However, they add that a range of 60 km which covers up to two-thirds of daily mileage is sufficient for daily commuters since on average less than 20% of trips exceed a range of 60 km. Nevertheless, considering the relative energy density of FCEVs, it is considered more suitable for a greater range of road vehicles. As such, BEV popularity decreases with range constraints.

2.5.6 Versatility of Hydrogen Fuel

FCEVs and BEVs are not without their disadvantages, cost being a significant factor in its widespread use. Within ideal limits, authors Sainz *et al* (2012) & Morrison *et al* (2018) report that FCEV and BEV costs are estimated to converge by 2030. Morrison *et al* (2018) however, went on to note that FCEVs become cheaper than BEVs by 2040. According to IEA (2007) cost predictions reported in a comparative analysis performed by Offer *et al* (2010) in 2030, capital costs for Internal Combustion Engine Vehicles (ICEVs), FCEVs and BEVs are 2200, 7000 & $6200 respectively whilst running costs amount to 19, 14 & 27 $\$/GJ^{-1}$ respectively. Offer *et al* (2010) concludes that, with respect to capital costs, ICEVs are still more affordable but by 2030 the lifecycle costs of FCEVs will be consistent with that of conventional petrol vehicles.

Significant FCEV & BEV market penetration will be slow, especially for developing countries such as South Africa since costly FCEVs or BEVs are potentially not financially optional for the majority of the population. Consequently, adhering to the climate obligations of the Kyoto Protocol will become a steeper hill to climb.

Nevertheless, unlike BEVs that need to be bought from a car dealer, Internal Combustion Engines (ICEs) can easily be converted to operate on dual fuel with petrol and hydrogen fuel. Balat (2008) & Dunpont (2007) agree that hydrogen can be used as a fuel directly in an ICE to create a Hydrogen Internal Combustion Engine Vehicle (H_2ICEV) with tests displaying efficiency improvements of up to 25% more than ICEs. The H_2ICEV introduces an opportunity to use existing ICEV infrastructure (White *et al*, 2006) whilst extracting from the experience attained with transport, fueling, and storage, all of which are directly transferrable to FCEVs (Verhelst & Wallner, 2009) thereby speeding up the envisioned hydrogen economy. Verhelst (2014) summarizes the advantages of $H_2ICEV's$ as follows;

Reduction in urban air pollution, reduction in global CO_2 emissions, improved efficiency relative to ICEVs, fuel flexibility, and don't rely on rare materials that cannot be mass-produced at affordable prices.

Adding to the attraction of H_2ICEVs are the lower requirements for hydrogen purity relative to fuel cells and hence cheaper fuel (Verhelst, 2014) whilst changing between fuel modes doesn't require stopping the vehicle (Sainz *et al*, 2012). The technically feasible application of ICEV conversion creates a bridging technology that allows a cheaper alternative to buying costly new BEVs to combat urban air pollution, whilst providing peace of mind of changing fuel operation in the event of low hydrogen.

2.5.7 Hydrogen Safety

Hydrogen as a fuel is easily reduced to a threat to life when people consider its role in the Hindenburg disaster of 1937 and the destruction of a "Hydrogen" bomb which is known to be much more devastating than the atomic bombs detonated during World War 2. These two examples highlight the misinformation used to degrade public confidence in hydrogen fuel as a potential solution.

As cited by Lovins (2005), Dr. Addison Bain, a NASA scientist addressed the unwarranted misconception of hydrogen's role in the Hindenburg disaster. According to an investigation carried out by Dr. Addison Bain, the disaster would have remained unchanged even if the dirigible were lifted by non-flammable helium and that 62 lives were saved because of the safety attributes of hydrogen. Lovins (2005) continues to note that it is likely that nobody aboard was killed by burning hydrogen which swirled harmlessly above them but the deaths of the other 33 people were attributed to them jumping out or by the burning diesel oil, canopy, and debris.

Moreover, introducing a paradigm shift in public perception, Lovins (2005) emphasizes that there is no connection between ordinary hydrogen gas, "whose chemical reactions make it useful as a fuel, and the special isotopes whose thermonuclear reactions power hydrogen bombs", nor can hydrogen gas create conditions required for nuclear fusion in a hydrogen bomb.

Attributes that may have contributed to the survival of many passengers on the Hindenburg include its low density and hence high diffusivity allowing it to burn above the passengers. Dunpont (2007) and Sharma & Ghoshal (2015) agree that the density of hydrogen is roughly 6.9% that of air making it four times as diffusive as natural gas, and 12 times as diffusive as gasoline. As a result, in an event of a potential hydrogen leak, hydrogen would rapidly dissipate from its source reducing the risk of fire or explosion (Dunpont, 2007). Alternatively, gasoline fumes or propane will accumulate near the floor thereby increasing the risk to people since they are typically near the floor (Lovins, 2005). Assuming gasoline or propane was used on the Hindenburg may have resulted in a lower than 65% survival since these fuels would have accumulated closer to the passengers. Extrapolating this information, it can be assumed that a hydrogen explosion in a vehicle would result in an upward wake whereas a gasoline result would explode sideways increasing the risk for people typically situated on the ground. It can be concluded that hydrogen fuel is safer than alternative fuels considering its low density and high diffusivity (Dunpont, 2007), (Sharma & Ghosal, 2015).

An additional attractive characteristic of hydrogen is that it burns with little heat radiation and therefore cannot sear skin from a distance (Dunpont, 2007). Emitting only one-tenth the radiant heat of a hydrocarbon fire and 7% cooler than gasoline, victims generally aren't burnt unless they are in the flame nor are they chocked by smoke (Lovins, 2005).

Motivating hydrogen as a more environmentally friendly fuel, Balat (2008) points out that it is non-toxic and a leak would not harm the environment.

Furthermore, Lovins (2005) & Balat (2008) agree that hydrogen is more easily detonable than other fuels when confined but unlike other fuels, it is very difficult to detonate if unconfined. Lovins (2005) admits that hydrogen ignites easily, requiring 14 times less energy than natural gas. However, he suggests that the dangers of easy ignition are moot considering that even natural gas can be ignited by a static-electricity spark whilst leaking hydrogen is more likely to burn than explode, even inside a

building. This is the case since it burns at concentrations far below its lower explosive limit, whilst ignition requires a fourfold higher minimum concentration than that of gasoline.

To conclude the greater relative safety of hydrogen, Lovins (2005) reports a demonstration comparing a hydrogen fire to that of a gasoline fire in a vehicle. In the demonstration, a hydrogen leak was created at a high-pressure location resulting in a vertical flame that raised the interior temperature of the car by at most 0.6-1.1℃. Furthermore, the outside temperature nearest the flame rose by no more than a car would experience when parked under the sun. This would have left any passenger relatively unharmed. Using the *same* vehicle with a 2.5-fold lower energy leak from a hole in a gasoline line destroyed the car's interior which would have killed anyone inside.

2.6 Hydrogen Production

Global warming continues to brand its presence as the world suffers through climate change. The use of fossil fuels acts as the main link to feeding global warming and remains the most popular energy source in fueling nations. However, its diminishing reserves and environmental causality threatens sustainable growth. Consequently, renewable sources and technologies will become unavoidable. Solar power has emerged as a game-changer in establishing a fossil-free energy source, especially in countries with high solar radiation such as South Africa. The subsequent section will discuss solar-powered water-splitting technologies for hydrogen production since the author believes that a hydrogen economy should be adopted in the future.

2.6.1 Direct Water Thermolysis

The single-step thermal dissociation of water is known as water thermolysis (Yilmaz *et al*, 2016). This method is considered to be years away from becoming engineering practice (Wang *et al*, 2012) since it has little technical and economic viability with no commercial or pilot scale solar water thermolysis plant in existence (Yilanci *et al*, 2009).

The main reason for its immaturity is the need for high temperatures exceeding 2500℃ to ensure decomposition. Consequently, sustainable heat sources are unachievable (Nikolaidis & Poullikas, 2017). Furthermore, the required temperature is too high for existing materials and construction equipment (Wang *et al*, 2012). Yilanci *et al* (2009) add that there is partial separation with the risk of hydrogen and oxygen recombining, requiring expensive separation technology. This product mixture increases the chances of an explosion (Yilmaz *et al*, 2016) with very low overall efficiency levels (Yilanci *et al*, 2009). Hence, this solar method is not seen as a viable option.

2.6.2 Photoelectrolysis

Photoelectrochemical also known as photoelectrolysis or photolysis is not to be categorized as water electrolysis. Unlike water electrolysis, photoelectrolysis requires at least one light-absorbing electrode, and only part or no external electricity is needed for the electrode redox reactions (Wang *et al*, 2012). Principally based on the conversion of photon energy into electricity, photolysis is described as a process wherein sunlight is absorbed by semiconducting materials to directly decompose water into hydrogen

and oxygen (Yilmaz *et al*, 2016). Sufficient voltage will be generated to split water molecules as the semiconductor photoelectrode is submerged in an aqueous electrolyte and exposed to sunlight (Yilanci *et al*, 2009).

To its credit, photolysis integrates solar absorption and water electrolysis into a single photoelectrode eliminating the need for a separate power generator and electrolyzer with a believed maximum theoretical efficiency of 38% (Yilanci *et al*, 2009). However, the challenges limiting its near term implementation shadows its advantages as highlighted in the subsequent list;

- Sunlight absorbing electrodes are subject to electrochemical corrosion and hence limit its efficiency (Wang *et al*, 2012), (Yilmaz *et al*, 2016).
- Solar to hydrogen conversion efficiency of materials do not meet requirements for practical application due to limited usable solar spectrum.
- Short lifespan.
- Require large land space (Yilanci *et al*, 2009).

However, considering its challenges, Yilmaz *et al* (2016) report that photolysis is still in an investigative stage, and its implementation is only expected in the long term. Hence, it will not be applied in this study.

2.6.3 Biohydrogen Production

Biophotolysis or Photobiological processes has gained significant interest in recent years due to the increased need for sustainable development and waste minimization (Nikolaidis & Poullikkas, 2017). It is considered sustainable since it uses renewable solar energy as its primary source, does not release carbon dioxide during combustion (Yilmaz *et al*, 2016), and contributes to recycling since it can use various waste materials as feedstock (Nikolaidis & Poullikkas, 2017).

Photobiological hydrogen is produced by processes similar to that found in plant and algal photosynthesis (Yilanci *et al*, 2009), i.e., through their hydrogenase or nitrogenase enzyme system (Nikolaidis & Poullikkas, 2017) to decompose water into hydrogen and oxygen using solar energy under anaerobic conditions. Moreover, it is carried out by microalgae and cyanobacteria (Yilmaz *et al*, 2016). According to Ngoh & Njomo (2012) and Yilanci *et al* (2009), biological hydrogen production can be classified broadly as either direct or indirect biophotolysis, photofermentation, and dark fermentation. The former three are considered light-dependent and dark fermentation a light-independent process.

Yilanci *et al* (2009) note that biological processes can be advantageous since it takes place at ambient temperature and pressure. Additionally, Ngoh & Njomo (2012) acknowledge that the low catalyst cost and low energy requirement for reactors offer a great economical advantage over other hydrogen processes. However, the authors mention that the two main disadvantages of biological processes are the low hydrogen production rate and yield.

Authors, Nikolaidis & Poullikkas (2017) & Ngoh & Njomo (2012) agree that significant surface area requirement and hence low energy density create economic restrictions for biological hydrogen. Additional constraints are placed on dark fermentation since generated hydrogen must be removed as produced since increased pressure lower production rates. Nevertheless, Nikolaidis & Poullikas (2017) considers dark fermentation advantageous relative to the other biological processes since it is a simple process, requiring minimum land that can be produced all day because it is independent of light sources using a wider range of feeds.

However, Yilmaz *et al* (2016) and Yilanci *et al* (2009) ranks photobiological hydrogen production as an immature technology, currently in the early development state of laboratory-scale testing. Similarly, Nikolaidis & Poullikas (2017) adds that direct biophotolysis processes are still at the conceptual stage.

According to Yilanci *et al* (2009), the immaturity of these processes can be attributed to its low efficiency in practice since trees and crops convert solar energy at efficiencies below 1%. Whilst Ngoh & Njomo (2012) attaches the immaturity of these processes to a poor understanding of biochemistry, cellular metabolism, and lack of fundamental research on the mechanism of hydrogen production.

2.6.4 Solar Water Electrolysis

It is widely agreed by several authors that electrolysis for water splitting is an established and well-known method, with decades of commercialization and development as well as active engineering research (Nikolaidis & Poullikkas, 2017, Wang *et al*, 2012, Acar & Dincer, 2019, Ngoh & Njomo, 2012, Nicodemus, 2018). It is considered an economical, technically feasible, and reliable option for hydrogen production due to its long history (Acar & Dincer, 2019, Chi & Yu, 2018).

Aided by Figure 2, Wang *et al* (2012) describe the process of water electrolysis for hydrogen production as one wherein an electric current splits water to produce hydrogen. Direct current passes through the immersed anode and cathode thereby producing hydrogen on the surface of the cathode when the electric potential is sufficiently high.

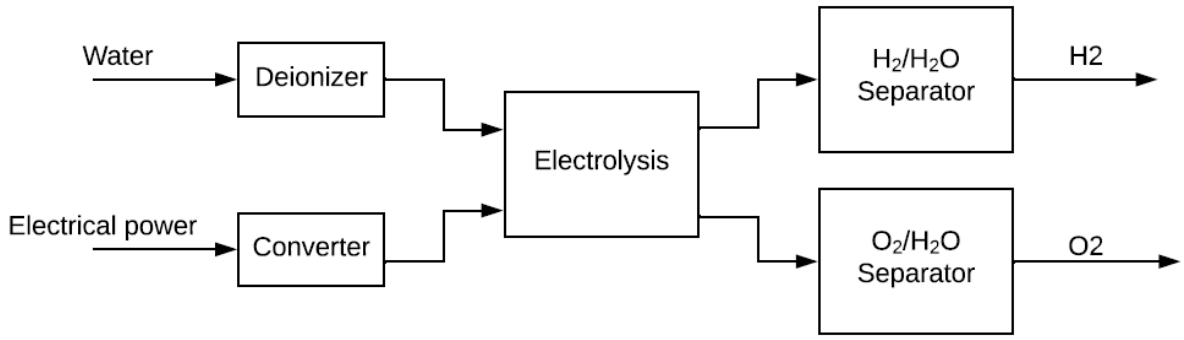

Figure 2: Water Electrolysis BFD (Nikolaidis & Poullikkas, 2017)

It is seen as an advantage that hydrogen generated from water electrolysis has a high purity of 99.9% such that it finds application in the electronic, metallurgical, food, float glass, fine chemical, and

aerospace industries (Chi & Yu, 2018). Furthermore, Wang *et al* (2012) list the advantages of water electrolysis.

- Flexible with respect to various power-generating technologies.
- Engineering maturity.
- A major benefit of all-day operation regardless of sunlight fluctuations.
- The electrolytic facilities do not need to occupy the same space as its sunlight dependent energy conversion technologies.

Considering the flexibility of water electrolysis Bartels *et al* (2010), as cited by Nikolaidis & Poullikkas (2017) present a hydrogen cost estimate from various electricity sources in Table 1.

Table 1: Hydrogen Cost Comparison (Nikolaidis & Poullikkas, 2017)

Energy Source	Hydrogen Production (kg/day)	Capacity Factor (%)	Hydrogen Cost ($/kg)
Nuclear	1000	97	4.15
Solar Thermal	1000	40	7.00
Solar PV	1356	28	10.49(a)
Wind	62,950	65	6.46(a)
	38,356	76	5.10
	1400	28	5.78-23.27(b)
	50,000	41	5.89-6.03(c)
(a) Based on electrolyzer cost of $500/kW, (b) Based on PV cost varying from $\$0.75/W_{Peak}$ to $\$5/W_{Peak}$ and an electrolyzer cost of $450/kW, (c) cost of $6.61/kg assumes electricity/hydrogen cogeneration whilst $6.77/kg is only the cost for hydrogen production			

However, despite these advantages, the high electricity consumption by electrolyzers prevents it from being cost-competitive with other large scale technologies (Nikolaidis & Poullikkas, 2017). Yilmaz *et al* (2016) share this view as they contemplate the challenges facing the widespread use of water electrolysis as being the reduction of energy consumption, costs, and system maintenance, to increase efficiency, safety, durability, and reliability.

Nicodemus (2018) provides an analysis to explore and compare the economic potential of producing solar hydrogen via thermochemical cycles and water electrolysis using solar photovoltaic electricity. In this paper, the author established that thermochemical cycles unlike water electrolysis have not yet been commercialized. However, Nicodemus (2018) went on to mention that the large scale deployment of thermochemical cycles will lead to significant reactor and heat recovery cost reductions, with PV water electrolysis having an insignificant cost-benefit of improving electrolyzer efficiency relative to the benefits of technological improvements in thermochemical cycles.

Lastly, the author concludes that PV electrolysis is the best near-term option and thermochemical cycle hydrogen production has a higher initial expense but has greater long term potential for cost reductions with a faster cost route to $\$2H_2/kg$.

2.6.5 Thermochemical Cycles

Solar thermochemical hydrogen production was introduced to be a better alternative to solar water electrolysis, considering that the latter only provides an overall efficiency of 24% heat to hydrogen (Funk, 2001). Graf *et al* (2008), Holladay *et al* (2009), and Wang *et al* (2012) believe that solar thermochemical hydrogen production, heat to hydrogen conversion efficiencies have the potential to exceed photovoltaic electrolysis and conventional based fuels and hence lower production costs. In support, Abanades & Flamant (2006) report photovoltaic efficiencies of no more than 20-25% whilst finding that the most investigated thermochemical cycles at the time generated efficiencies of 40-50%. Similarly, Rosen (2010) highlights electrolyzer efficiencies at roughly 24% with thermochemical hydrogen using nuclear heat-generating efficiencies of up to 50%. Coupled with heat pinch analysis, since thermochemical cycles involve heat flows, it is assumed that the system efficiency can be improved even further.

Wang *et al* (2012) reports a maximum PV water electrolysis overall efficiency of 16% with estimated thermochemical efficiencies that could reach 40-56% for Zn/ZnO cycles, 39-45% for Fe_3O_4/FeO cycles, 35-46% for hybrid sulfur cycles, and 40-60% for S-I and CuCl cycles which have the potential to compete with the current more favourable steam reforming.

According to Funk (2001), the search for potentially efficient cycles started worldwide in the 1960s with the number of proposed thermochemical cycles now exceeding 800 cycles (Sayyaadi & Boroujeni, 2017). However, authors Rosen (2010), Ghanderhariun *et al* (2010), Wang *et al* (2012), Nikolaidis & Poullikkas (2017), and Sayyaadi & Boroujeni (2017) all agree that the copper-chlorine cycle is one of the most promising cycles. Additional promising cycles include the sulphur-iodine cycle (Rosen, 2010) and the magnesium-chlorine cycle (Nikolaidis & Poullikias, 2017).

2.6.5.1 Process Overview

These cycles or reagents are used in a closed-loop chemical process, wherein they undergo a series of chemical reactions, in which water, the only material input is decomposed into hydrogen and oxygen (Ghandehariun *et al*, 2010). In addition to water, solar power, the source of heat as the other input is used to drive these endothermic chemical reactions. The $CuCl$ cycle is described in detail below.

Without emitting GHG's or releasing harmful pollutants, the $CuCl$ thermochemical cycle uses a series of continuous recycled intermediate copper and chlorine compounds to form a closed internal loop (Ozbilen *et al*, 2016). Naterer *et al* (2011a) present the four-step hybrid $CuCl$ process which will be described below with the accompanying conceptual schematic represented by Figure 3. The details of each process step are summarized in Appendix A.

Step 1

Starting with the electrolysis step, $CuCl$ is oxidized during the electrochemical reaction in the presence of hydrochloric acid (HCl) to liberate hydrogen gas as shown in the first reaction. $Cu(I)$ is oxidized to

$Cu(II)$ at the anode whilst hydrogen ions are reduced at the cathode. Temperature conditions for this step may range between 25-100℃ (Ozbilen *et al*, 2016) with cell voltages below 1 volt (Naterer *et al*, 2011a).

$$2CuCl(aq) + 2HCl(aq) \rightarrow H_2(g) + 2CuCl_2(aq)$$

Step 2

Hydrogen is collected, and aqueous $Cu(II)$ chloride is fed to a dryer to remove its water at a temperature below 100℃ (Naterer *et al*, 2011a)

$$CuCl_2(aq) \rightarrow CuCl_2(s)$$

Step 3

Once dried, solid $Cu(II)Cl$ is fed to the hydrolysis reactor along with superheated steam to undergo an endothermic non-catalytic gas-solid reaction thereby producing copper oxychloride (Cu_2OCl_2) and hydrochloric gas which is pumped back to *step 1*. This reaction operates between 350 & 400℃ (Naterer *et al*, 2011a), as follows:

$$2CuCl_2(s) + H_2O(g) \rightarrow Cu_2OCl_2(s) + 2HCl(g)$$

Step 4

Solid copper oxychloride is then fed to a reactor maintained at 500℃ (Naterer *et al*, 2011a), wherein it undergoes thermal decomposition as shown below to produce *CuCl* which is recycled back to *step 1* whilst the liberated oxygen is extracted from the process.

$$Cu_2OCl_2(s) \rightarrow 2CuCl(l) + \frac{1}{2}O_2(g)$$

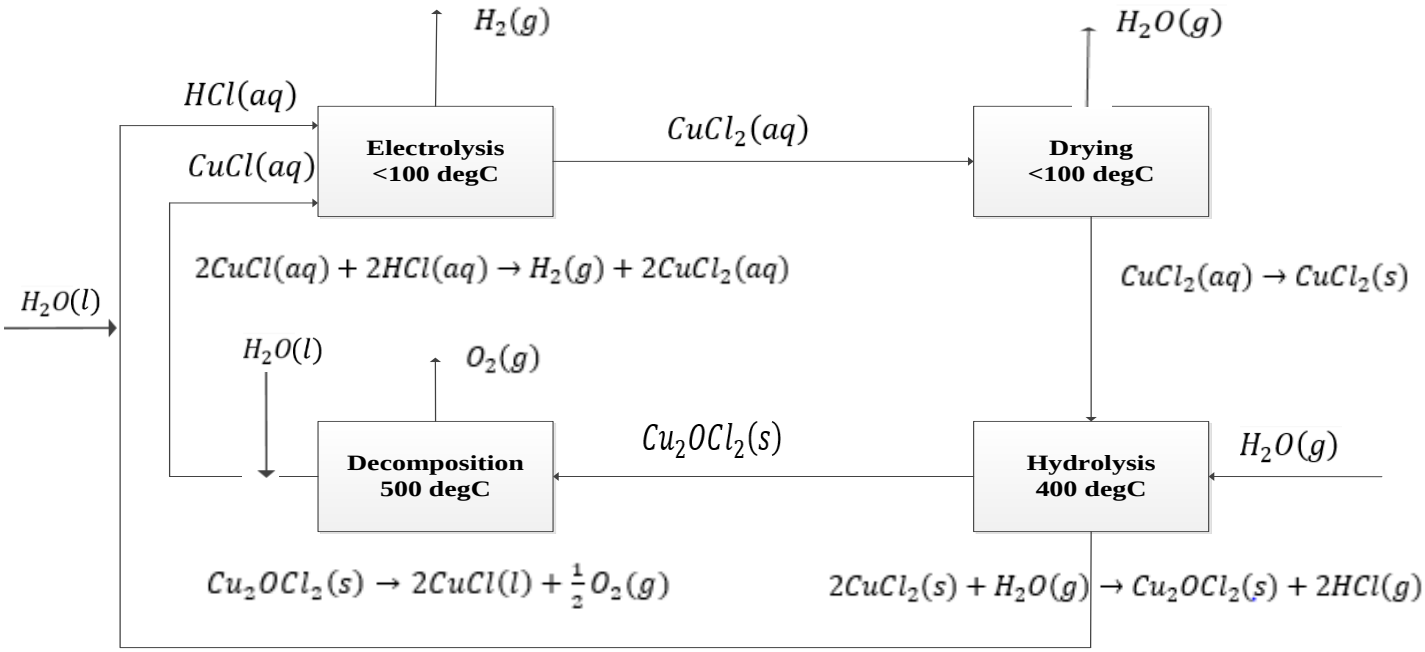

Figure 3: Cu-Cl Thermochemical Cycle Process BFD

Prior to the thermochemical reactions, solar heat is concentrated and harnessed by solar collecting devices such as solar tower systems, solar dish systems, and parabolic trough systems. These solar harnessing technologies are distinguished by the way they concentrate solar radiation (Ghandehariun *et al*, 2010). As a footnote, Wang *et al* (2012) report that solar towers capable of concentrating thousands of suns as well as tens of megawatts of irradiance with heliostats or reflection mirrors can reach a temperature range of 500-1000℃

According to Ghandehariun *et al* (2010), tower systems also known as central receiver systems use an array of heliostats (two-axis tracking parabolic mirrors) that focus sunlight onto a solar receiver mounted on top of a centrally located tower as shown by Figure 4.

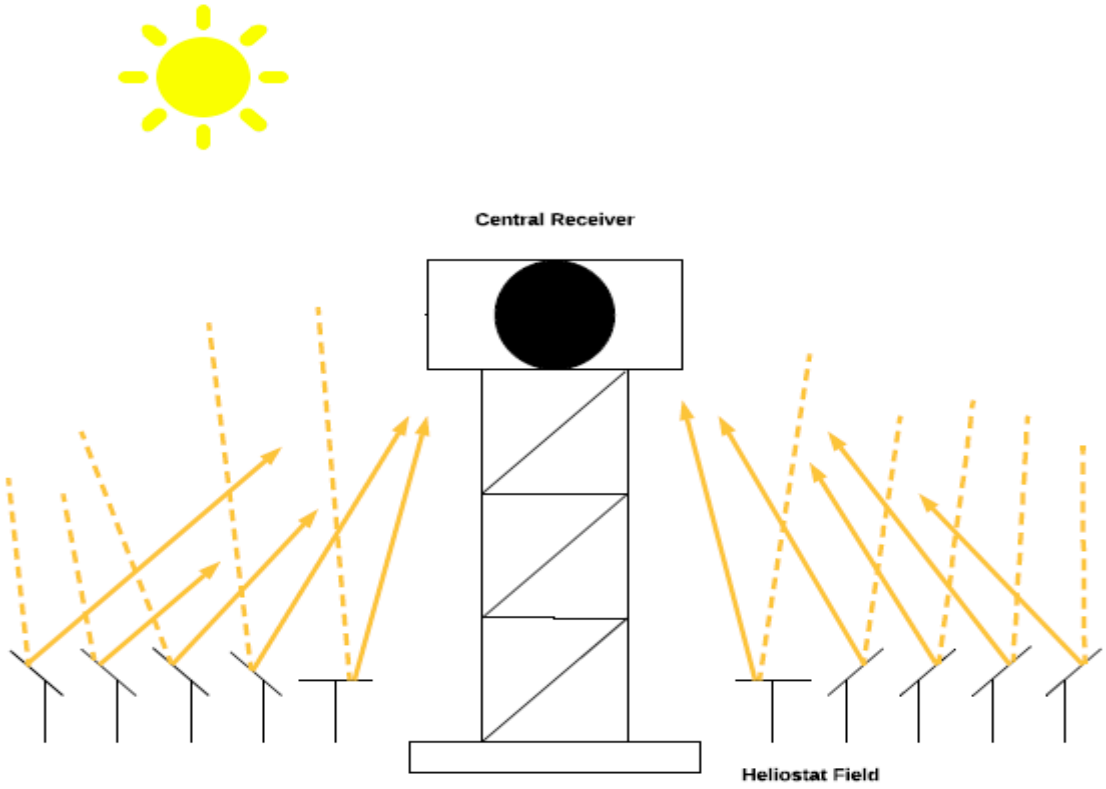

Figure 4: Tower System (Ghandehariun *et al*, 2010)

Ghandehariun *et al* (2010), described dish systems (Figure 5) that use paraboloidal mirrors to concentrate sunlight on a solar receiver positioned at their focus.

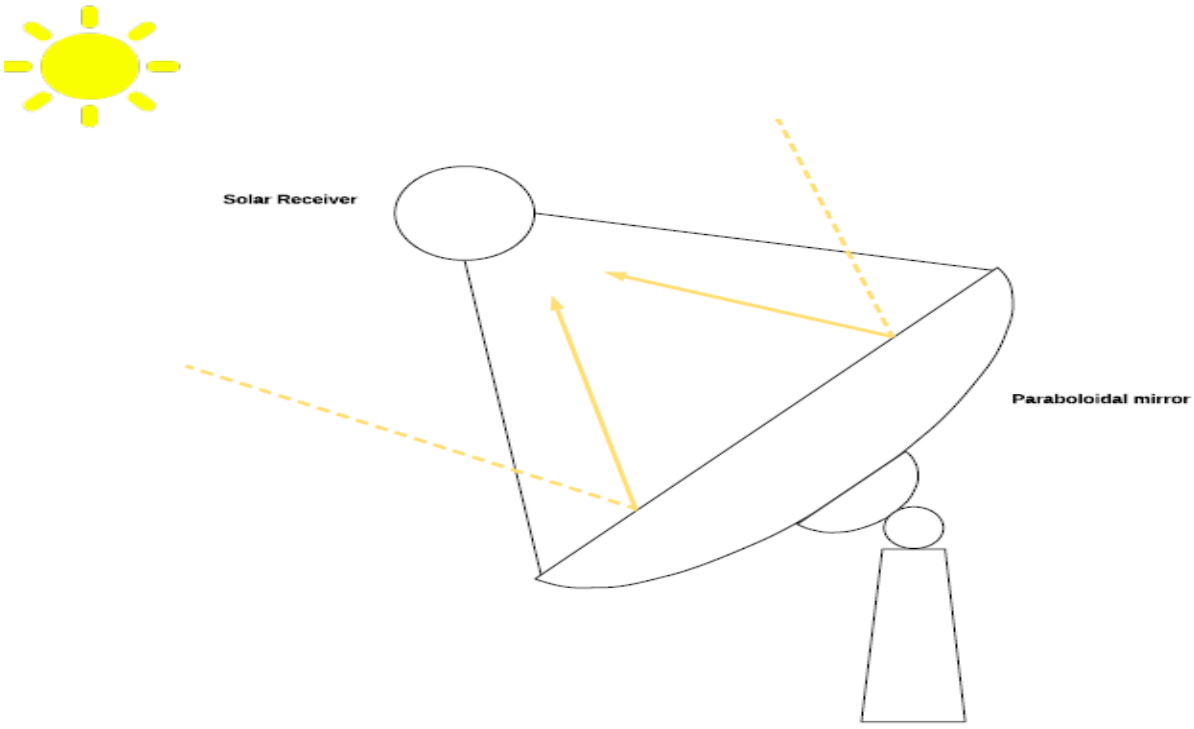

Figure 5: Dish System (Ghandehariun *et al*, 2010)

Trough systems as shown in Figure 6, use linear, two-dimensional parabolic mirrors to focus the sun's rays onto a tubular receiver positioned along their focal plane with the ability to track the sun as it moves across the sky (Ghandehariun *et al*, 2010).

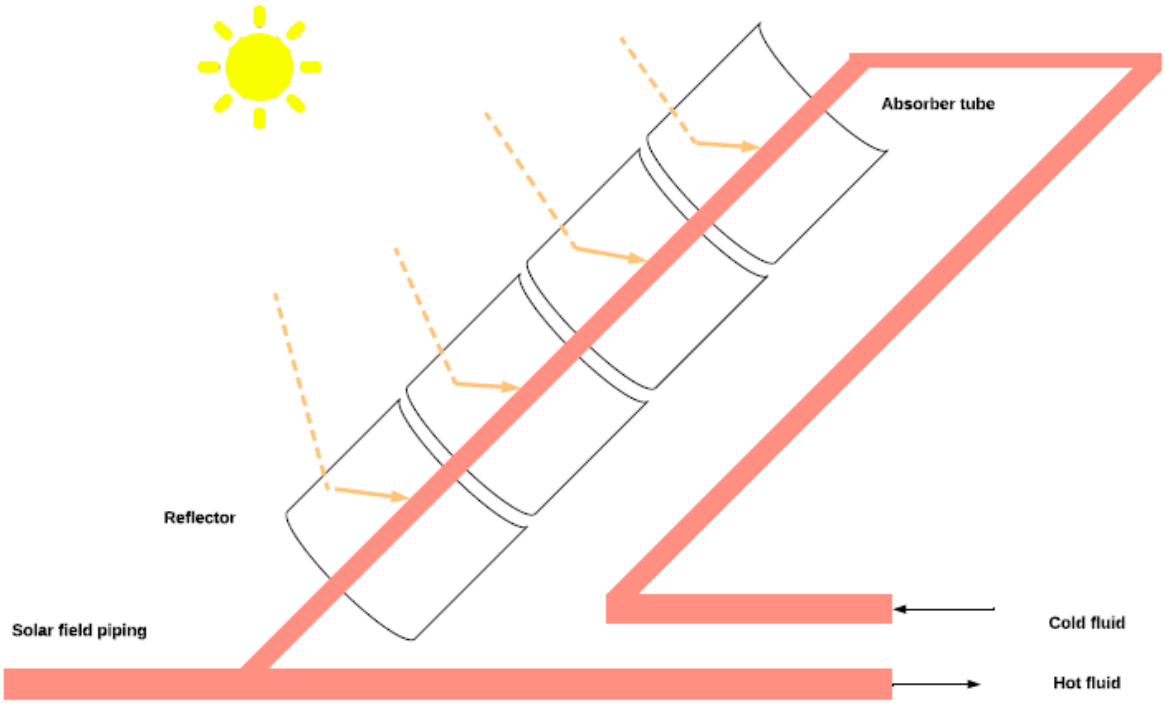

Figure 6: Trough Parabolic System (Ghandehariun *et al*, 2010)

In the case of the trough parabolic mirror system which will be used in this study, the solar radiation is concentrated by the parabolic mirrors onto a receiver pipe filled with molten salts that serve as the heating fluid (Ghandehariun *et al*, 2010). Pregger *et al* (2009), notes that the receiver could be a heat exchanging device whilst Ghandeheriun *et al* (2010) added that the receiver could be a chemical reactor, thereby exposing reactants directly to incoming solar radiation. Nevertheless, the heated molten salts are then fed to a hot tank for heat storage which can be used as feed to the thermochemical process on-demand (Ghandehariun *et al*, 2010) which consists mainly of heat transfer and chemical reactor units (Wang *et al*, 2012). Once cooled, the molten salts are pumped back to cold storage and fed to the parabolic troughs to close the loop. Nikolaidis & Poullikkas (2017) provides an example of the molten salt flow for the thermochemical process as represented by Figure 7.

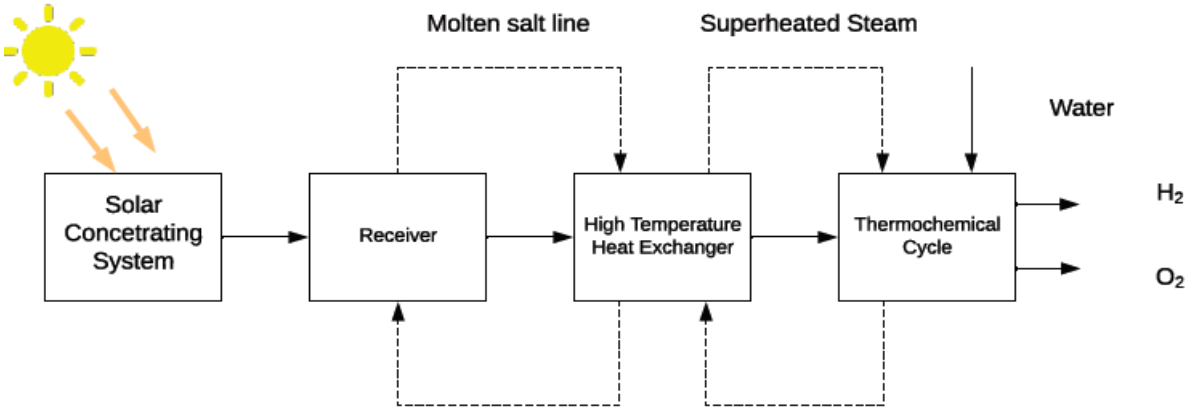

Figure 7: Molten Salt Flow Configuration (Nikollaidis & Poullikkas, 2017)

2.6.5.2 Advantages & Disadvantages of Solar Thermochemical Cycles

Considering the solar concentration field and the land requirement to house the necessary unit operations, Pregger *et al* (2009) believe that the land consumption and environmental impacts on local flora and wildlife during the build-up of these facilities are the main environmental issues associated with this process.

Regardless, solar thermochemical cycle water splitting may be one of the ultimate alternatives for CO_2 free production of hydrogen (Abanades *et al*, 2006) creating an opportunity to ensure a sustainable and secure energy future. Unlike finite fossil fuels. No environmental pollution, since cycles allow complete internal recycling of chemicals (Gandehariun *et al*, 2010).

The introduction of these cycles in the multistep dissociation of water, allow water to be split into hydrogen and oxygen using much lower temperatures relative to the direct thermolysis. As a result, a wider range of heat sources can be used (Rosen, 2010). Unlike direct thermolysis, thermochemical cycles allow for oxygen and hydrogen liberation at different stages and hence avoid the risk of handling the explosive hydrogen-oxygen mixture (Yadav & Banerjee, 2016).

Unfortunately, Pregger *et al* (2009) and Ghandeherin *et al* (2010) acknowledge that the biggest challenge for many of these thermochemical cycles is the high-temperature requirement that restricts availability and flexibility of existing solar thermal technologies as well as material resistance to concentrated acids at high temperatures. However, alternative low-temperature cycles have been and continue to be developed to accommodate solar heat sources and are more readily integrated with existing technologies (Ghandehariun *et al*, 2010).

Although already addressed, as a closing motive Sayyaadi & Boroujeni (2017) report that one of the positive points of thermochemical cycles is being more efficient and cost-effective compared with other methods.

2.6.5.3 Associated Costs

Presently, steam reforming of natural gas is considered the most techno-economic hydrogen production method (Graf *et al*, 2008, Ngoh & Njomo, 2012). Nikolaidis & Poillikas (2017) share this sentiment by presenting an appealing hydrogen cost ranging between 1.34-2.27 $\$/kgH_2$ for conventional hydrogen production methods. Conversely, Sayaadi & Boroujeni (2017) estimate the cost of hydrogen from a CuCl thermochemical plant to be 6.33 $\$/kgH_2$. Graf *et al* (2008) performed economic comparisons and found the cost of hydrogen using hybrid-sulfur and metal oxide thermochemical cycles to range between 5.73-8.23 $\$/kgH_2$ and 5.14-18.82 $\$/kgH_2$ respectively.

It has been predicted by authors Pregger *et al* (2009) that hydrogen production using fossil fuels will remain the most affordable method till at least 2030.

However, Steinfeld & Palumbo (2001) believe that solar technologies will represent viable economic paths earlier if the costs of fossil energy properly account for environmental damages resulting from burning fossil fuels.

Moreover, Funk (2001) notes that a better understanding of process thermal efficiency, capital costs, and thermodynamic irreversibilities may lead to lower production costs. Consequently, Sayaadi & Boroujeni (2017) apply pinch analysis in a conceptual design of a thermochemical cycle plant and in doing so improve the thermal efficiency and thereby costs. Hence, the introduction of pinch analysis in this project. Wang *et al* (2012) conclude that large production scales are more suitable for thermochemical cycles to minimize energy losses due to multiple reactions and unit operations which may lead to competitive hydrogen prices. Summarized in Table 2, Nikolaidis & Poullikas (2017) present the costs of hydrogen using various cycles whilst Ngoh & Njomo (2012) present projected costs in Table 3.

Table 2: Cycle Hydrogen Cost Comparison (Nikolaidis & Poullikas, 2017)

Heat Source	Cycle	Max Temperature (℃)	Efficiency (%)	Production Rate (kg/day)	H_2 Cost ($/kg)
Nuclear	$S-I$	850	45	800,000	2.45-2.63
	$Cu-Cl$	550	45	7000	2.17
Solar	ZnO/Zn	1727	20.8	6000	7.98
	Fe_3O_4/FeO	1627	17.4	6000	8.40
	Fe_2O_3/Fe_3O_4	1327	18.6	6000	8.40

Table 3: Small Scale Cycle Hydrogen Cost Comparison (Ngoh & Njomo, 2012)

Current Solar process designs and small-scale pilot plants	Cost (euro/ton of hydrogen)
Hybrid sulphur cycle	1900
Sulphur-iodine cycle	2000
Metal/metal oxide cycle	3500
High-temperature electrolysis	4667
Methane cracking	1767
Methane steam reforming	1633

2.7 Fuel Cells

In simple terms, FCs are known as combined heat and power energy conversion devices that transform chemical energy directly into electrical energy and heat (Inci & Turksoy, 2019). Mekhilef *et al*, 2012) describe FCs as devices consisting of four main parts; anode, cathode, electrolyte, and the external circuit. Hydrogen is oxidized at the anode into protons and electrons, while the cathode reduces oxygen to oxide species and reacts to form water. The authors add that electrons travel through the external circuit to deliver electric power whilst protons or oxide ions depending on the electrolyte, are transported through the ion-conductor electron-insulating electrolyte. Figure 8 highlights the operating principle.

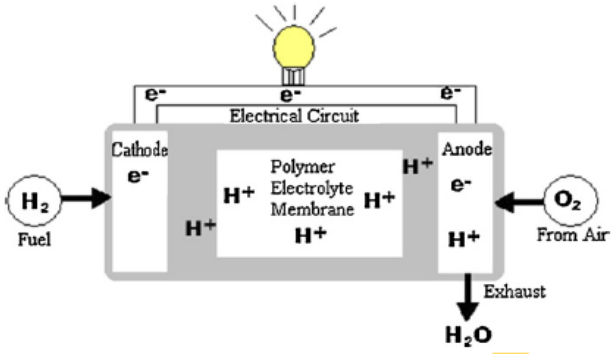

Figure 8: PEM Fuel Cell (Mekhilef *et al*, 2012)

Multiple fuel cells exist. Ogungbemi *et al* (2019) classifies fuel cells on the type of electrolyte and reacting substances whilst they are considered different according to their operating temperature, efficiency and electrolyte into 6 major types (Mekhilef *et al*, 2012):

Alkaline Fuel Cell (AFC), Phosphoric Acid Fuel Cell (PAFC), Solid Oxide Fuel Cell (SOFC), Moltencarbonate Fuel Cell (MCFC), Proton Exchange Membrane Fuel Cell (PEMFC) and Direct Methanol Fuel Cell (DMFC).

According to Daud *et al* (2017), Ogungbemi *et al*, (2019), and Dodds *et al* (2015), the PEMFC is the most promising and most advanced fuel cell technology. They have a low operating temperature, low noise, quick start-up capability, light mass, and high power density (Daud *et al*, 2017). Considered the most advanced fuel cell technology, PEMFC powers around 90% of systems shipped to date and are mostly used in residential heating systems (Dodds *et al*, 2015). Considering these reasons, the PEMFC is used in this study to convert hydrogen to electricity to feed the demand of the rural setting.

Inci & Turksoy (2019) consider solar PV, wind turbines, and fuel cells as the most promising clean energy generators. In support, Parra *et al* (2019) note that PV and wind energy have experienced significant growth since the beginning of this century. Wilberforce *et al* (2016) report that, in 2005, renewables accounted for 16.5% of the global primary energy whilst Parra *et al* (2019) projected renewable energy generation growth of 45% worldwide between 2013 and 2020, whilst contributing 40% of the total power generation by 2040. However, Inci & Turksoy (2019) consider fuel cells a superior alternative for improved power balancing and voltage/frequency regulation in comparison to

wind and PV. In agreement, Wilberforece *et al* (2016) claim that fuel cells represent the most promising technological advancement relative to other renewable energy technologies to assist in managing climate change.

Parallel to the aim of this project, Mekhilef *et al* (2012) acknowledge fuel cells as a promising alternative to provide energy to rural areas with no access to the power grid. Dodd *et al* (2015) claim that stationary CHP is currently the most established market for fuel cells and has experienced rapid commercial growth since 2009. Appreciable growth in 2012, ensured a near double shipment of fuel cell systems compared to the previous year, totaling 45 700 units with stationary fuel cells experiencing the largest growth (Wilberforce *et al*, 2016). According to these authors, fuel cell technology is slowly penetrating the market as a practical option that competes with conventional combustion engine generators, batteries, and power plants.

Fuel cells have become attractive and their impressive growth rate can be attributed to many advantages, summarized in the table below. Moreover, Dodds *et al* (2015) present Table 5 to provide a comparative assessment of the major pollutants produced by emerging energy systems including fuel cells, condensing boilers, and CHP engines.

Table 4: Advantages of FCs

Advantage	Reference	Advantage	Reference
Simple usage	Inci & Turksoy, 2019	Reliable operation	Inci & Turksoy, 2019
Simple design	Mekhilef *et al*, 2012	Quieter operation	Arsalis, 2019
Flexible application on all scales	Mekhilef *et al*, 2012 Dodd *et al*, 2015	Operation during blackout	Dodd *et al*, 2015
Modularity	Inci & Turksoy, 2019 Dodds *et al*, 2015	Reduced dependence on grid power	Dodd *et al*, 2015
Low/zero emissions	Inci & Turksoy, 2019 Mekhilef *et al*, 2012 Daud et al, 2017	Highest efficiency compared to conventional distributed energy systems	Wang *et al*, 2018 Arsalis, 2019 Inci & Turksoy, 2019 Daud *et al*, 2017
Higher power to heat ratio	Arsalis, 2019	Simple routine maintenance requirements	Arsalis, 2019

Table 5: Pollutants Comparison (Dodds *et al*, 2015)

Emissions	Fuel Cell	Condensing boiler	CHP engine
NO_x	1-4	58	30-270
CO	1-8	43	10-50
NO_x	1-3	13	No data
NO_x	0-2	2	No data
Averaged over eight sources. All emissions are given in g/MWh of fuel input.			

Mekhilef *et al* (2012), provided Table 6 to indicate the efficiency superiority of fuel cells compared to conventional distributed energy systems.

Table 6: Efficiency Comparison (Mekhilef *et al*, 2012)

	Reciprocating diesel engine	Turbine Generator	PV	Wind Turbine	Fuel Cell
Efficiency (%)	35	29-42	6-19	25	40-85
Capital Cost ($/kW)	200-350	450-870	6600	1000	1500-3000

However, fuel cells are not without their limitations. Fuel cell capital costs remain a challenge. Regardless, their mass production has decreased its costs in recent years and the relative cost gap is rapidly narrowing. Dodds *et al* (2015) add that residential system prices have dropped by 85% in the last ten years in Japan and over 60% over the last four years in Germany whilst the high capital costs are offset by lower running costs resulting from lower consumption of grid electricity. Mekhilef *et al* (2012) add that pulse demands and impurities of gas streams shorten the life span of fuel cells. Moreover, the lower power density per volume, lower accessibility, and lower durability are additional challenges.

Adding to the web of disadvantages, Wang *et al* (2018) note that the main challenges in commercializing fuel cells are repair and maintenance costs of fuel cells (due to low reliability) can lead to increased costs and decreased availability. Dodds *et al* (2015) agree that durability was one of the major issues challenging the widespread use of fuel cells, reporting lifetimes of 10000 hours (~ 2 years) using intermittent operation. However, they add that recent improvements particularly by Japanese manufacturers have improved the lifespan of some fuel cells to 40000 hours (10 years) with leading Japanese residential systems expected to operate for 60-80000 hours for PEMFCs and up to 90000 hours for SOFCs.

2.8 Hybrid Energy Systems

Hybrid Energy Systems (HESs) integrate multiple energy conversion devices to fulfil an energy requirement. More generally, hybrid systems are defined as either a combination of two or more energy conversion devices or two or more fuels for the same device, thereby overcoming limitations inherent to either (Manwell, 2004). Combining two or more renewable energy sources as part of a hybrid system ensures a sustainable electrical supply by overcoming the fluctuating nature of renewable sources.

Nema *et al* (2009) highlight, that hybrid systems powered by renewables show most promise when applied to remote areas where grid extension and fuel costs increase with remoteness. Contributing to the economic allure of hybrid systems, Nema *et al* (2009) adds that, HESs has shown its potential to significantly reduce the total lifecycle costs of stand-alone power supply whilst providing a more reliable electric supply. Additionally, Zhou *et al* (2010) report that the economic feasibility is improved due to the increase in system efficiency and reduction in energy storage requirements. More importantly, if not most important, renewable sourced HESs provide a cleaner energy supply relative to conventional sources.

In support, Erdinc & Uzunoglu (2012) report that large distances increase the cost of electrifying rural homes but add that, irregular topography raises the costs as well. These authors too, accept stand-alone HESs as a promising solution for electrification in these areas. Furthermore, remote areas typically use petroleum products for transport, electricity, and heating and unless subsidised, inhabitants of these regions incur higher costs for petroleum products since the cost of transporting these goods increases with remoteness (Abdin *et al*, 2015).

Abdin *et al* (2015) encourage HESs in these remote areas since it will diversify the energy mix, improve energy security, reduce fuel import costs, and reduce fossil fuel dependency. The authors don't believe that electricity costs should increase similar to the trend in fossil-fuelled energy prices since renewable sources are not affected by exhaustion or political instability. Hence, introducing HESs will ensure equality, improved quality of life, improved education, improved life expectancy, and reduced mortality.

HESs not only reduces the cost with respect to grid extension and imported fuels. Koutroulis *et al* (2006) as cited in Turkay & Telli (2011), verified that hybrid systems have a lower cost compared with using one renewable source. Similalry Turkay & Telli (2011) by their analysis, confirmed that non-hybrid systems are not feasible.

Depending on a single source may cause components in stand-alone systems to be oversized (Turkay & Telli, 2011) which increases the design costs. To ensure continuous electric supply, HESs are introduced to overcome seasonal variations. Again, single renewable sources cannot achieve this which affects the system's energy performance causing batteries to be discarded too early (Zhou *et al*, 2010). Adding to the attraction of HESs, Nema *et al* (2009) reports that it has been demonstrated that HESs significantly reduce the total lifecycle cost with a more reliable and stable electric supply.

Storage systems in HESs are considered optional (Nema *et al*, 2009), however, to ensure a stable electric supply, Manwell (2004) believes that energy storage is useful in hybrid systems. He believes that it can be used to overcome the deficit in load and the renewable energy source. It is especially important as a contingency if there is a surge in demand during the evening or inconvenient weather conditions (Turkay & Telli, 2011). Becalli *et al* (2008) & Agbossou *et al* (2001) as cited in Turkay & Telli (2011) believe that introducing hydrogen production combined with fuel cells will ensure stabilised electrical power with quick load switching. Yilanci *et al* (2009) & El-Shatter *et al* (2002) also believe that hydrogen production is the best solution for hybrid systems due to its high efficiency, quick load response, and fuel flexibility. Douglas (2016) compares hydrogen FC systems and battery packs. He notes that larger battery banks could be expensive whilst affordable small battery banks have limited charge and discharge capacity. He adds that batteries degrade over time and become less efficient whilst FC hydrogen storage systems have the potential to be optimised and operate without interruption pending the size of hydrogen storage.

2.9 Chapter Summary

Section 2.2 reviews potential renewable energy sources to generate electricity for the chosen rural site. The reviewed list included; geothermal energy, hydroelectric energy, oceanic energy, wind energy, bioenergy, and solar energy.

Geothermal energy was rejected as a potential energy source considering the geological position of the chosen site relative to the Pacific Ring of Fire hence, making this source uneconomical. Hydroelectric power was considered detrimental to the environment despite being considered a renewable energy source. Additionally, South Africa is considered a water scarce country thus it was not selected for the chosen site. A review on oceanic energy highlighted it's vast amount of potential energy capable of exceeding worldwide energy demands. This included analysing its harvesting technologies such as tidal barrages and tidal current turbines, OTEC, WECs, PRO, and RED. However, the investment costs, location, and topology of the deep rural areas discouraged any potential for this renewable energy source to be employed for the chosen site. Despite the chosen site having adequate wind resources, a review of the negative effects of wind turbines and the lack of village inhabitant participation lead to the rejection of wind as an energy source. Biomass as a renewable energy source was considered a potential addition to the hybrid system since bio feedstock is available, it allowed for the employment of unskilled labour and the participation of farmers located in the deep rural areas. Lastly, solar was considered the best option to form part of the hybrid system since the review on solar energy revealed that it is an abundant renewable source in South Africa whilst being the best renewable option based on availability, cost-effectiveness, accessibility, capacity, and efficiency.

Despite progress in ensuring low carbon economies as the world battles with global warming, fossil fuels are still projected to be a majority contributor of energy globally. Whilst the world is taking the necessary steps in reducing fossil fuels as its main source of energy, energy efficiency has proven itself as a useful avenue for mitigation. Pinch analysis, more specifically heat pinch analysis and PoPA have emerged as useful tools in minimising the warming effect whilst simultaneously reducing capital and operational costs. Hence, its introduction to this project.

Hydrogen and battery technology are considered as a potential secondary energy source for low carbon economies especially in the transport sector. However, hydrogen was encouraged over batteries in the review since it is a favoured choice by the author. Promoted through the transport sector, hydrogen was considered superior to batteries based on the long-term costs associated with the infrastructure required to charge car batteries and refuel hydrogen vehicles. The review comparatively analyses the refuelling times of electric vehicles versus hydrogen vehicles and shows the latter's superiority based on its significantly shorter refuelling times. Moreover, the range of each powertrain was considered thereby revealing the range constraints associated with electric vehicles whilst typical internal combustion vehicles has the capability of being converted to hydrogen vehicles with an option of dual-fuel operation. Consequently, hydrogen as a fuel source was concluded capable of being more capable of aiding the transition from fossil fuels to renewable energies. A review of hydrogen safety was performed to abate

any misconceptions surrounding the safety of using hydrogen. The purpose of this section was to promote hydrogen use since it could ease the transition from fossil fuels and highlight its ability to penetrate the transport sector considering that it is a major contributor to global warming.

Section 2.6 consists of a review of renewable-based hydrogen production methods. Direct water thermolysis, photoelectrolysis, biohydrogen production solar water electrolysis and thermochemical cycles were considered as this section narrows down on the most suitable production method for the rural site. Thermochemical cycles and solar water electrolysis were shown to be most suitable largely due to the immaturity of the rest of the production methods. However, in comparing these two technologies, thermochemical cycle hydrogen production has shown to have potential for greater overall efficiency and its large-scale deployment will lead to significant cost reductions relative to the insignificant cost-benefit for improving electrolyzer efficiency. Hence, thermochemical cycles are preferred over solar water electrolysis.

In reviewing fuel cells for the conversion of hydrogen to electricity for the chosen rural site, it was found that the PEMFC was the better option since it is the most promising and most advanced fuel cell technology. Therefore, the PEMFC was the chosen technology for hydrogen conversion in this study.

A HES was chosen in this study since the review revealed that these systems have a lower cost compared to using a single energy source. The review has magnified the ability of a HES to overcome seasonal variations whilst emphasising its promise in remote rural areas where grid extension is uneconomical.

Considering the economic applicability of HESs in rural settings, introducing a thermochemical and biogas HES to the chosen rural site in this theoretically based study could lead to an improved quality of life. In using hydrogen as a fuel, this study could serve as a cog for a potential hydrogen economy made up of multiple decentralized renewable hybrid systems.

CHAPTER 3: PROBLEM DESCRIPTION

3.1 Chapter Outline

This section presents the conceptual diagram and the selection process for the major sections of the hybrid energy system. The selection process includes choosing the ideal rural setting, thermochemical cycle, biomass conversion process, FC, solar collector, and thermochemical plant. Appendix I provides the BFD that combines these systems before heat integration. Furthermore, a stream legend has been included in Appendix N, providing the descriptions of every numbered stream.

3.2 Conceptual Diagram

Figure 9 represents a summarised version of the potential heat and power distribution site to be designed for the South African rural setting.

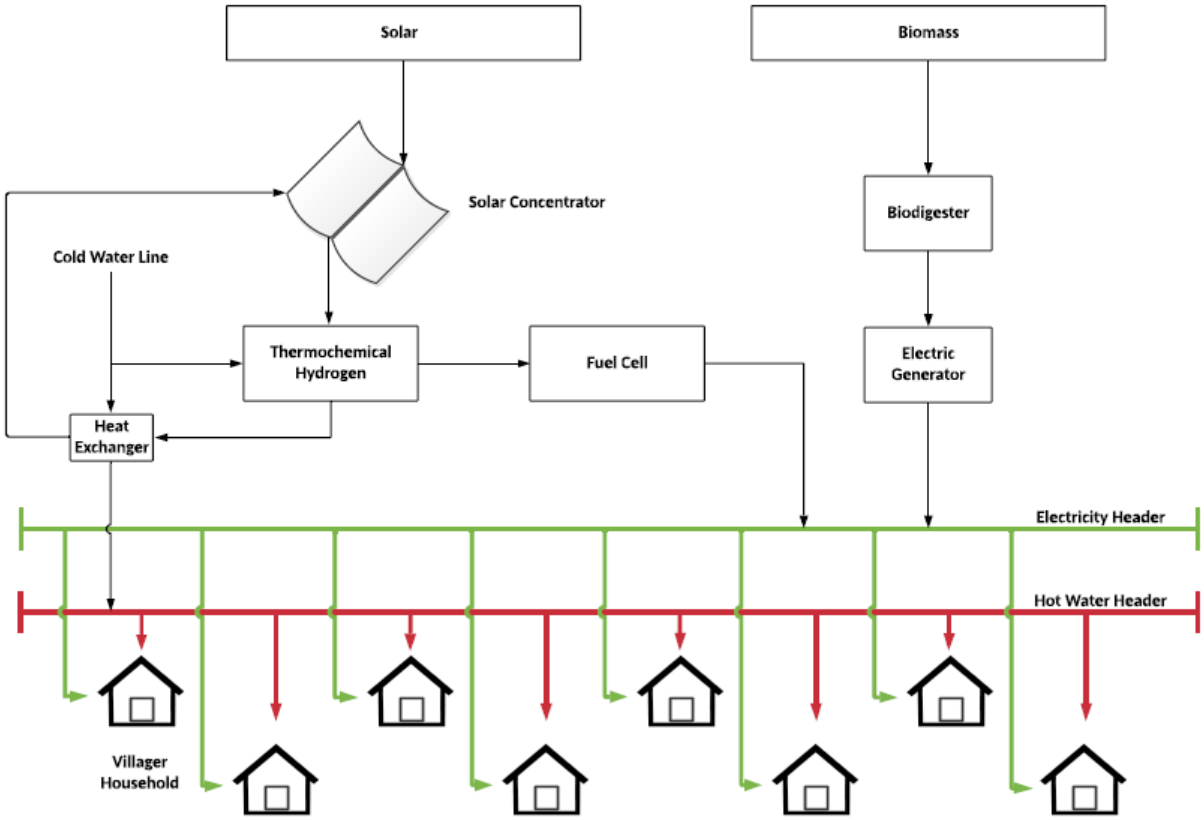

Figure 9: Summarised Heat & Power Generation & Distribution Network

Furthermore, the conceptual diagram shown in Figure 9 has been updated to represent the integrated conceptual diagram given in Appendix C.

3.3 Rural Setting Selection

An ideal location not connected to the central utility with an assumed sustainable water supply and sufficient solar radiation has been located. Focussing on agriculture to ensure food security, this community has the potential to use waste crops as feed for bioreactors to generate combined heat and power. Hence, focus in this section is placed on locating rural areas in South Africa, using markers of high solar radiation, wind concentration, number of traditional dwellings, number of agricultural

households, and access to electricity and water. Government generated statistics will be used to locate these rural areas in tandem with solar radiation maps, wind atlases, and regional agricultural statistics.

The chosen rural location is assumed to have no access to electricity and made up of traditional dwellings. Furthermore, it is assumed to be an agricultural setting. A stretch of land equivalent to 4 km^2 was assumed, however, this can be scaled to accommodate more inhabitants. It was also assumed that the rural setting was well endowed with biomass resources; therefore, it has enough biomass resources to ensure sustainable operation of the biomass plant. The daytime solar resource is assumed satisfactory for constant operation despite radiation levels decreasing as the day progresses.

3.3.1 Provincial Selection

Narrowing the search, the General Household Survey generated by Statistics South Africa (2017), reports that the use of electricity as a source of energy for cooking was lowest in more rural provinces such as Limpopo (60.2%), Mpumalanga (72.4%) and Eastern Cape (74.8%). The generated stats show that in 2017, 5.5% of South African households lived in traditional dwellings whilst being most common in Eastern Cape (22.3%) and Kwazulu-Natal (14.4%). Furthermore, Limpopo, Mpumalanga, and the Eastern Cape have the least common refuse removal, and this can be partly attributed to the remoteness of various rural areas. The focus will be placed on the Eastern Cape region since only 85.4% of households in the province use electricity for lighting, making it the smallest user of electricity for lighting in South Africa. Furthermore, the Eastern Cape has the highest proportion of agricultural households (27.9%) with a significant number of household's agriculture activity focussed on grain and food crops (Community Survey, 2016). This emphasizes the potential of biomass feedstock for electricity in the region.

3.3.2 Municipality Selection

Divided into two metropolitan municipalities (Buffalo City & Nelson Mandela Bay), the Eastern Cape consists of six district municipalities further divided into 31 local municipalities (Municipalities of South Africa, 2019) as showed in Figure 10.

Figure 10: Eastern Cape Municipalities (Municipalities of South Africa, 2019)

Table 7 gives a representation of the number and percentage of traditional dwellings along with the number and percentage of people that do not have access to electricity in the six district municipalities, the data of which were collected from the community survey 2016 and compiled by Wazimap (2019).

Table 7: Number of Traditional Dwellings & Electricity Access by Municipality (Wazimap, 2019)

Municipality	Traditional dwelling (by household)		No access to electricity (by population)	
	No	%	No	%
Alfred Nzo	195975	53	230851	26.6
Amathole	81230	38	125072	14.2
Chris Hani	75773	39	41163	4.9
Joe Gqabi	24728	26	55937	15.5
OR Tambo	169603	54	177801	12.2
Sarah Baartman	2764	2	25916	5.4

These regions were further dissected to determine the highest number of households within each municipality that do not have access to electricity and are tabulated in Table 8 below.

Table 8: Electricity Access by Municipality (Eastern Cape Socio Economic Consultative Council, 2017)

Municipality	Region within municipality	Number of households not using electricity
Alfred Nzo	Matatiele	21200
Amathole	Mbahashe	21800
Chris Hani	Encobo	9890
Joe Gqabi	Elundi	14400
OR Tambo	Ngquza Hill	13900
Sarah Baartman	Kouga	3030

Alfred Nzo has been chosen as the representative municipality considering it has the highest number of traditional dwellings by household and the largest population with no access to electricity. Table 8 shows that Matatiele local municipality has amongst the highest number of households not using electricity and hence will be further analysed to find the representative region for this study.

According to Wazimp (2019), Matatiele is further divided into 26 wards. The Matatiele Local Municipality (2018) identifies Ward 22 as one of the wards with no access to electricity whilst Wazimp (2019) reports that 58.2% of households in Ward 22 are traditional dwellings. Hence this provides an opportunity to use Ward 22 to fulfil the aim of this project.

Only a portion of Ward 22 will be used for electrification. There are 38.4 people per square kilometre in Ward 22 (Wazimap, 2019) with an average of 4 people per household (Matatiele Local Municipality, 2018). Using this information, the area size and number of households for electrification in line with the aim of this project will be subsequently calculated.

- $\frac{4\ \cancel{people}}{household} \times \frac{1\ km^2}{38.4\ \cancel{people}} = \frac{4\ km^2}{38.4\ households} \sim \frac{4\ km^2}{39\ households}$ Eq 3-1
- $\frac{39\ households}{\cancel{4\ km^2}} \times 4\ \cancel{km^2} = 39\ households$ Eq 3-2

As suggested, 39 households covering an assumed 4 km^2 stretch of land will be used for this project. It is worth noting that, there are 8 villages in ward 22 (Mataiele Local Municipality, 2018). However, these 39 households are assumed to be traditional dwellings without electricity, situated within Ward 22 in areas that inhabit the resources identified in the subsequent sections.

3.3.3 Solar Resource

The Eastern Cape regions given in Table 8, will need to be refined to assess its solar radiation levels. Suri *et al* (2015), presents Figure 11, highlighting South Africa's solar radiation levels.

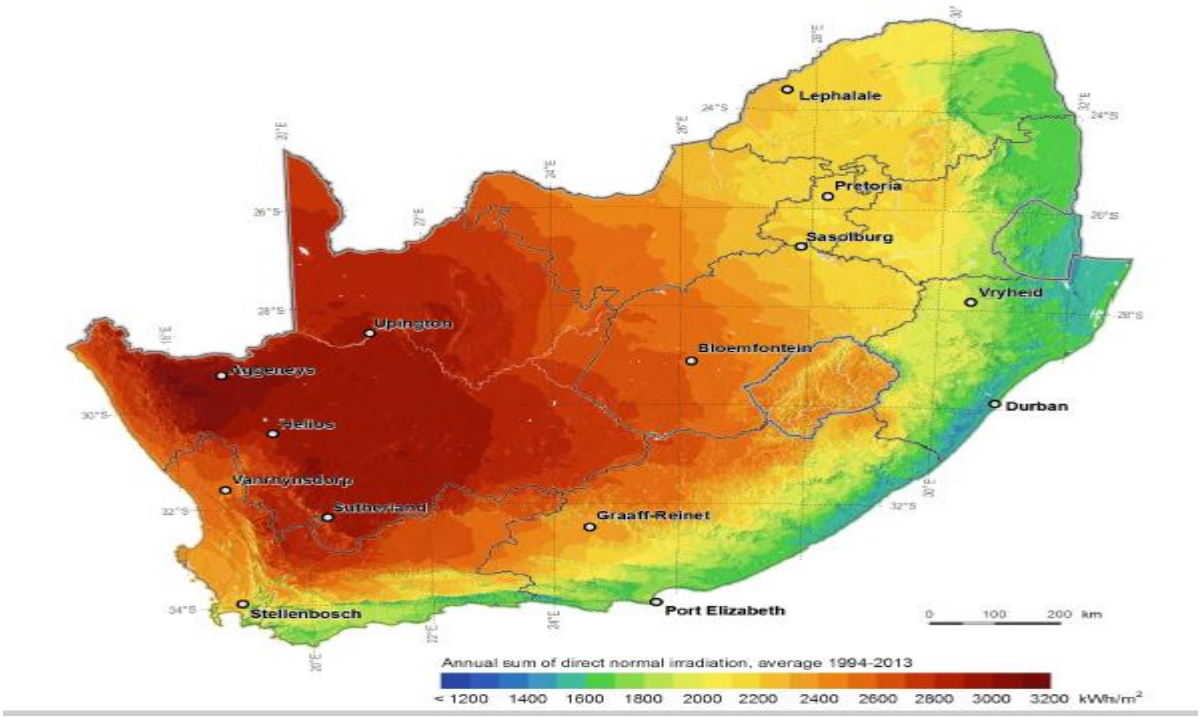

Figure 11: South African Solar Radiation Map (Suri *et al*, 2015)

Superimposing Figure 10 onto Figure 11 it was found that the Matatiele region has the best solar radiation levels amongst those given in Table 8.

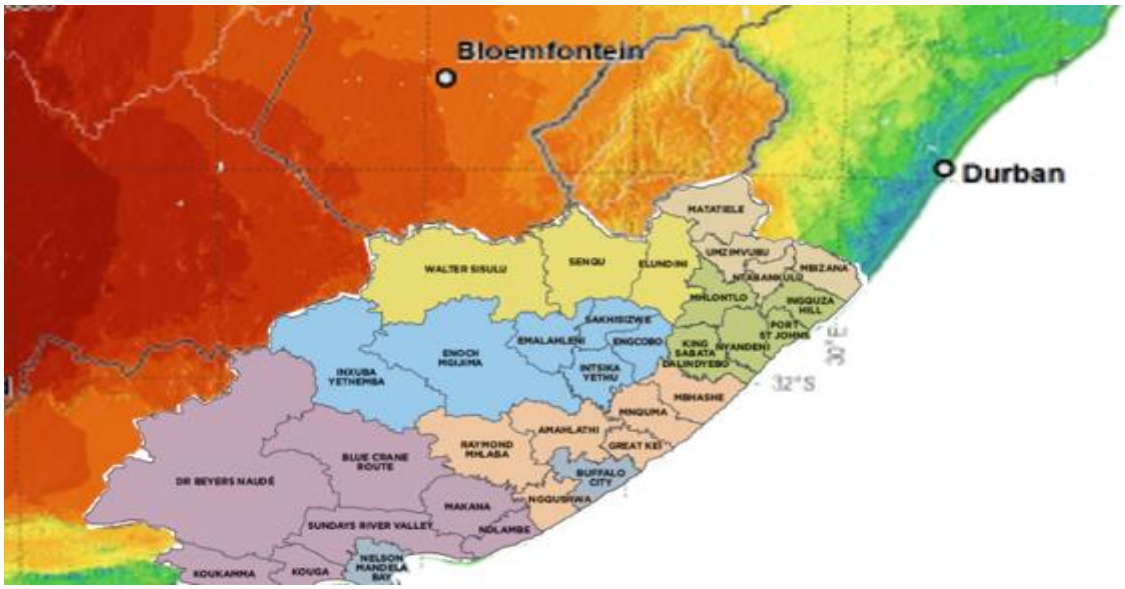

Figure 12: Superimposed Solar Map

It is observed that the Matatiele region experiences solar radiation ranging between 2200 and 2600 kWh/m^2

3.3.4 Wind Resources

This procedure is repeated using the wind resource map given by Figure 13 as presented by Wind Atlas for South Africa (2019).

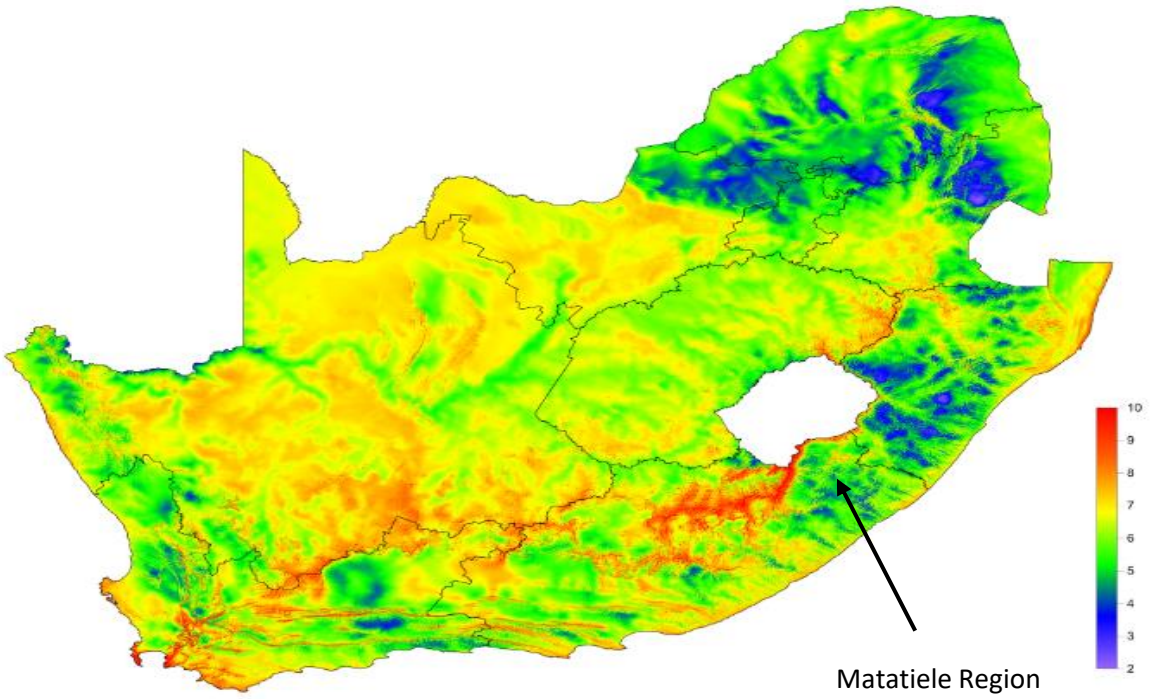

Figure 13: South African Wind Map m/s (WASA, 2019)

It is observed that wind speeds range between 2 & 10 m/s, averagely ranging between 5 & 7 m/s according to the legend.

3.3.5 Biomass Resources

According to the Bioenergy Atlas for South Africa (2016), the most feasible cultivated crops in the Matatiele region is sweet sorghum as shown in Figure 14. Additionally, cow dung may also be used since many of these rural areas have significant informal cattle populations.

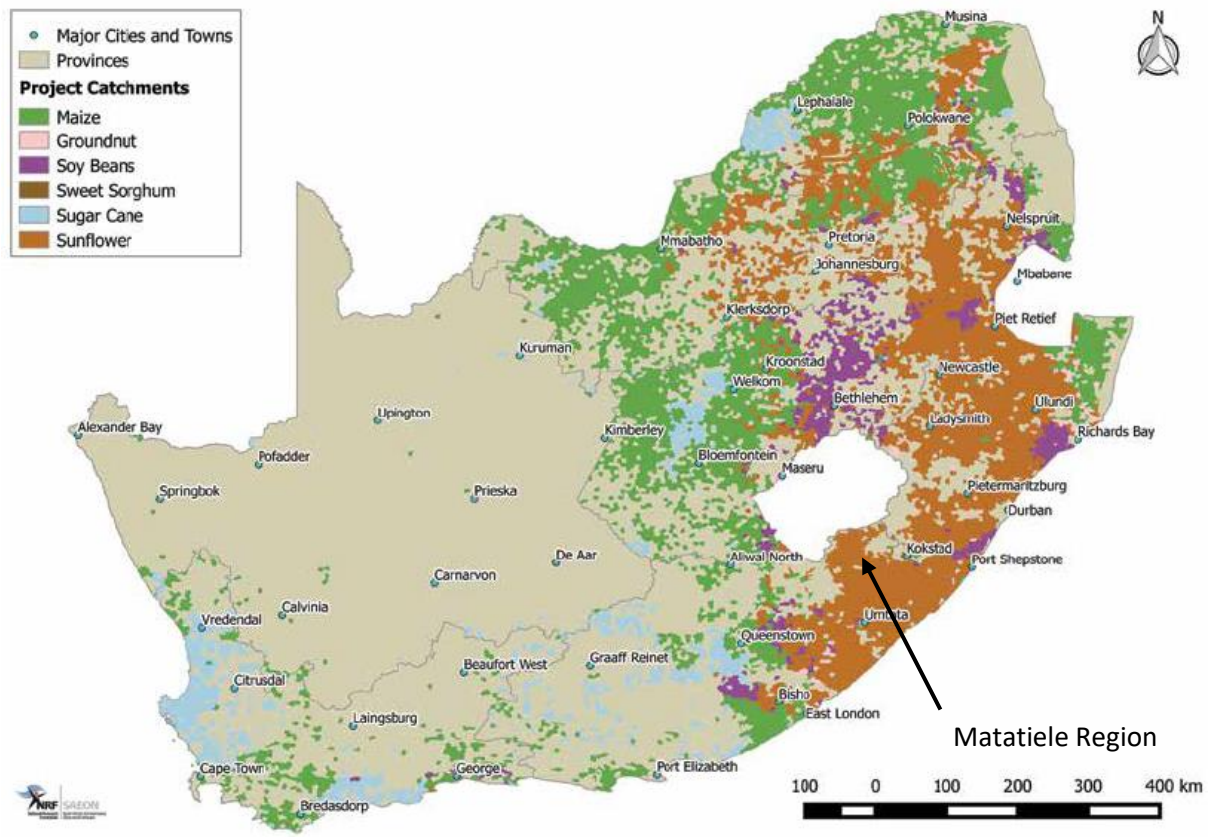

Figure 14: Feasible Bioenergy in South Africa (Bioenergy Atlas for South Africa, 2016)

In addition to sweet sorghum, the Matatiele Integrated Development Plan (2017) notes that the most common farming activities in the region are livestock production, poultry production, grain, and food crops and vegetable production, with cattle, sheep and goat farming making up the main livestock farming opportunities. This introduces an opportunity to use animal dung to create biogas or direct combustion of biomass.

3.3.6 Water Resources

According to the Matatiele Integrated Development Plan (2017), the Mzimvubu river that flows through the Eastern Cape has the highest mean annual runoff in South Africa and equates to almost 15% of the total river flow in the country. Since 44.3% of the population in Ward 22 use river water to satiate their water needs (Wazimap, 2019), it is considered safe to assume that those that make use of river water use this river or its tributaries. It is also safe to assume that if such a large percentage of the population make use of river water, river water is in abundance. The table below highlights the different sources of water that are used in this ward and hence acts as a representation of the water source possibilities to feed the renewable energy hub.

Table 9: Ward 22 Water Resources (Wazimap, 2019)

Population	Households	Number of People per km^2	Traditional Dwellings %	Service Provider %	Dam %	River %	Borehole %	Other %
6287	1827	38.4	58.2	16.5	8.6	44.3	15.4	15.2

3.3.7 Resources Concluding Data

The extracted data presented in Table 10 below, summarises the necessary information required to begin the design of the renewable hub in this rural setting.

Table 10: Section 3.3 Data Summary

Population	Households	Area	Solar Radiation Levels	Wind	Biomass	Water
156	39	4 km^2	2200-2600 kwh/m^2	5-7 m/s	Sweet sorghum, waste crops & animal dung	Mzimvubu river, Service provider, Dam & Borehole

3.4 Thermochemical Cycle Selection

This section provides the rationale behind the selection of the used cycle. According to Naterer *et al* (2011a), more than 200 possible thermochemical cycles have been proposed, whilst Sayyaadi & Boroujeni (2017) report more than 800 thermochemical cycles for producing hydrogen from water as the feed. However, Masin & Lewis (2006) acknowledge that most of these existing cycles use aggressive chemicals with high-temperature requirements above 850℃ which are associated with engineering and construction material challenges. Hence, an optimum cycle with a lower temperature range is chosen.

Naterer *et al* (2011a) reported that the most promising cycles are sulfur-based cycles, copper-chlorine (Cu-Cl), iron-chlorine (Fe-Cl), copper sulfate (Cu-SO_4), cerium-chlorine (Ce-Cl), vanadium-Chlorine (V-Cl), and the hybrid chlorine cycle. However, most of these cycles involve temperatures above 850℃. Consequently, the most promising cycles were in the lower temperature region with evidence of successful proof-of-principle work. It should be noted that the chosen cycle was based on evidence from existing literature and evaluations and no laboratory testing was performed.

According to Andress *et al* (2009), a cycle is considered successful once its final efficiency is greater than 30% so as to compete with the efficiency of hydrogen from water electrolysis. Naterer *et al* (2011a) add that most international efforts are focussed on the Sulfur-Iodine (S-I), hybrid Sulfur, and Copper-

Chlorine (Cu-Cl) cycles. In accordance with the efficiency threshold for a successful cycle previously stated, Andress *et al* (2009) noted that approximately 43% net efficiency is envisioned with the CuCl cycle which is a significant improvement over that of electrolysis.

The CuCl cycle is considered one of the most successful cycles (Sayyaadi & Boroujeni, 2017) and will, therefore, be used in this study. More specifically, the hybrid CuCl cycle. Lewis *et al* (2009) describe the hybrid cycle to involve a partial substitution of a thermal process with that of an electrolytic one since it improves the efficiency of the cycle. They add that the S-I process requires high temperatures ranging between 825-900℃, uses aggressive chemicals with no viable demonstration. Hence it will not be used.

Alternatively, the hybrid CuCl process has been selected since it has a much lower operating temperature (maximum 530℃), has lower demands on construction materials, contains common chemical agents, full completion of reactions, uses a relatively low electrochemical voltage and most importantly since these immediate compounds are recycled, no pollutants are released into the environment (Naterer *et al*, 2011a). Furthermore, Lewis & Masin (2009) reported that this cycle consists of no competing reaction whilst having high yields and possess engineering feasibility.

To dissect the CuCl cycle even further, Naterer *et al* (2011a) adds that, multiple variations of this cycle exist i.e. 5-step, 4-step, and 3-step cycles. However, after evaluating the 3 different types of CuCl cycles, the authors suggested the 4-step hybrid cycle since it is anticipated to have greater thermal efficiency and practical viability. Hence, given these reasons the 4-step hybrid Cu-Cl is used in this study.

3.5 Bioenergy Process Description

Section 3.3 highlights that the chosen location is well-endowed with sweet sorghum, whilst common farming activities include livestock production. A biogas production process to form part of the hybrid system was chosen for this study considering, that sweet sorghum, waste crops, and manure presents an opportunity for feasible biogas production. A block flow diagram of the process along with its motivation is presented in this section.

AD is the process of choice instead of wind to operate as part of the hybrid system. The main reason for this choice is because procurement and transportation of biomass for the AD allow for the involvement of unskilled labour which can be found in the village. Moreover, waste from farmers could be used thus allowing for more integration of the power system with the villagers.

According to Xu *et al* (2018), AD is the process wherein anaerobic microbes are used to convert biomass and organic wastes into biogas in the absence of oxygen. Abdeshahian *et al* (2016) listed the advantages of AD to include reduction of odour release, a decrease of pathogens whilst the treated organic waste can be used as fertilizer. In support, Khalid *et al* (2011) add that, AD prevents the release of methane into the environment whilst the burning thereof releases only carbon-neutral carbon dioxide and hence reduces environmental pollution.

An opportunity for co-digestion exists since the location is rich in sweet sorghum, manure, and waste crops. Khalid *et al* (2011) support co-generation since it improves biogas yields, whilst improving digestion rate and stability. Zhang *et al* (2016) note that digestion performance is optimized since nutrients in the various wastes balance the bacterial community. Moreover, the authors went on to mention that, cow manure as used in this project is considered an effective substrate since it assists in maintaining a stable pH value during AD. The authors conclude that co-digestion of sorghum and cow manure significantly accelerates the AD process, improves the digestion of sorghum stem whilst maintaining a stable pH value. Co-digestion is used in this process considering its ability to accelerate the production rate of methane gas.

Cavinato *et al* (2010) reported findings that the thermophilic range of temperature should be used for co-generation instead of the mesophilic range due to its comparatively superior performances. In their experimental work, the authors show that biogas production rate and methane content is improved once proper process temperatures are used. These authors prove that a temperature of 55℃ is ideal to ensure a general improvement of the digester. Hence this temperature will be used for the biogas production process. This temperature will be achieved using solar heat as extracted by the solar collector. The conceptual schematic of the biogas plant below is a modified version of that presented by Cavinato *et al* (2010).

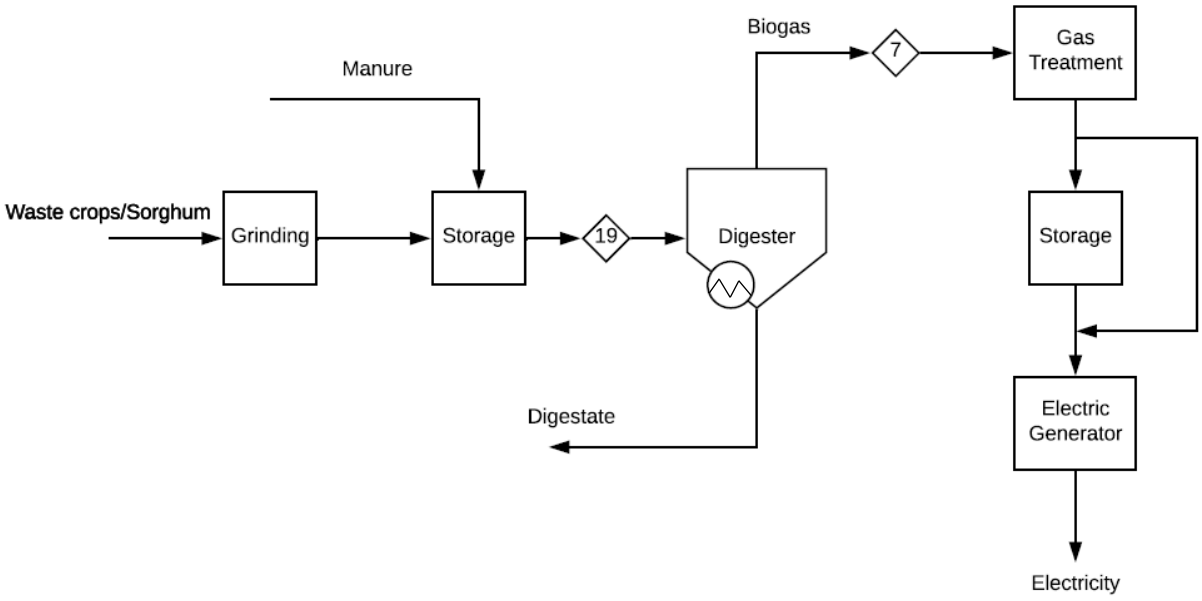

Figure 15: Modified Biogas Plant (Cavinato *et al*, 2010)

Waste crops & sorghum are manually fed to a grinder which can either be an automatic mechanical unit operation or manually ground using a machete. Esposito *et al* (2012) suggest the grinding step to reduce the size of the influent substrate since increasing the available surface area improves the degradation rate and accelerates the digestion process. The ground substrate can be fed using a conveyor or have the grinder within a chute feeding the storage unit. Manure, waste crops and sorghum are fed to the storage unit.

From the storage unit, the influent mixture is pumped to the digester which operates at 55℃. A preheating step may be included before the digester. Thermal preheating will be included since Esposito *et al* (2012) presents findings that suggest that a preheating step may improve biogas yield. The digestate, generated in the digester can be extracted and used as fertilizer with the potential of being sold.

According to Xu *et al* (2018), the generated biogas consists of 60-70% methane, 30-40% carbon dioxide, and traces of other gases such as hydrogen and hydrogen sulphide. Consequently, the generated gas will need to undergo treatment to remove hydrogen sulphide and carbon dioxide. A scrubber containing steel wool is used to adsorb the hydrogen sulphide whilst the gas can be bubbled through water to absorb carbon dioxide. Once treated, the biogas is fed to a storage unit before being used in an electric generator for electricity generation.

3.6 Fuel Cell Selection & Description

Hydrogen produced from the thermochemical process is fed to a FC to create electricity. However, the FC can operate as a Combined Heat and Power (CHP) unit since heat is an output. Consequently, this presents an opportunity for usable heat for process integration. A brief description and rationale for the chosen FC is presented in this section. Furthermore, the efficiency definition is provided since the demand and electrical efficiency is used to estimate the hydrogen input, hence cascading backward, to size the hybrid system.

As reported in Section 2.7, Daud *et al* (2017), Ogungbemi *et al* (2019) and Dodds *et al* (2015) acknowledge the PEMFC as the most promising and advanced FC technology. According to Daud *et al* (2017), the benefits of the PEMFC include *low operating temperature, low noise, quick-start capability, light mass, and high-power density*. Mekhilef *et al* (2012) add that electrodes in the PEMFCs *are easier to seal compared with other FCs whilst having a longer life with the most affordable manufacturing costs*. Furthermore, they add that these low operating FCs operate between 60 and 100℃ since operating at temperatures above 100℃ will vaporize the water, resulting in the dehydration of the membrane and hence a reduction in proton conductivity through the membrane. As such, Spiegel (2019) suggests maintaining the temperature at 90℃ which is beneficial for the reason highlighted above whilst, higher temperatures allow for faster kinetics and a voltage gain that is greater than the voltage loss due to the negative thermodynamic relationship between the open-circuit voltage and temperature.

Mekhilef *et al* (2019) describe the FC operation. The authors state that hydrogen is fed to the anode where it is activated by the catalyst to form protons and electrons. Inherently semi-permeable, the membrane allows protons to pass through it whilst forcing electrons to flow through the external circuit and generate electricity. The electrons return to the cathode compartment where it reacts with oxygen and the protons to form water. Heat is dissipated as a by-product of the electrochemical reaction. To maintain the FC at 90℃, it is assumed that natural convection and radiation will suffice. The half and overall reactions are presented below on the FC schematic.

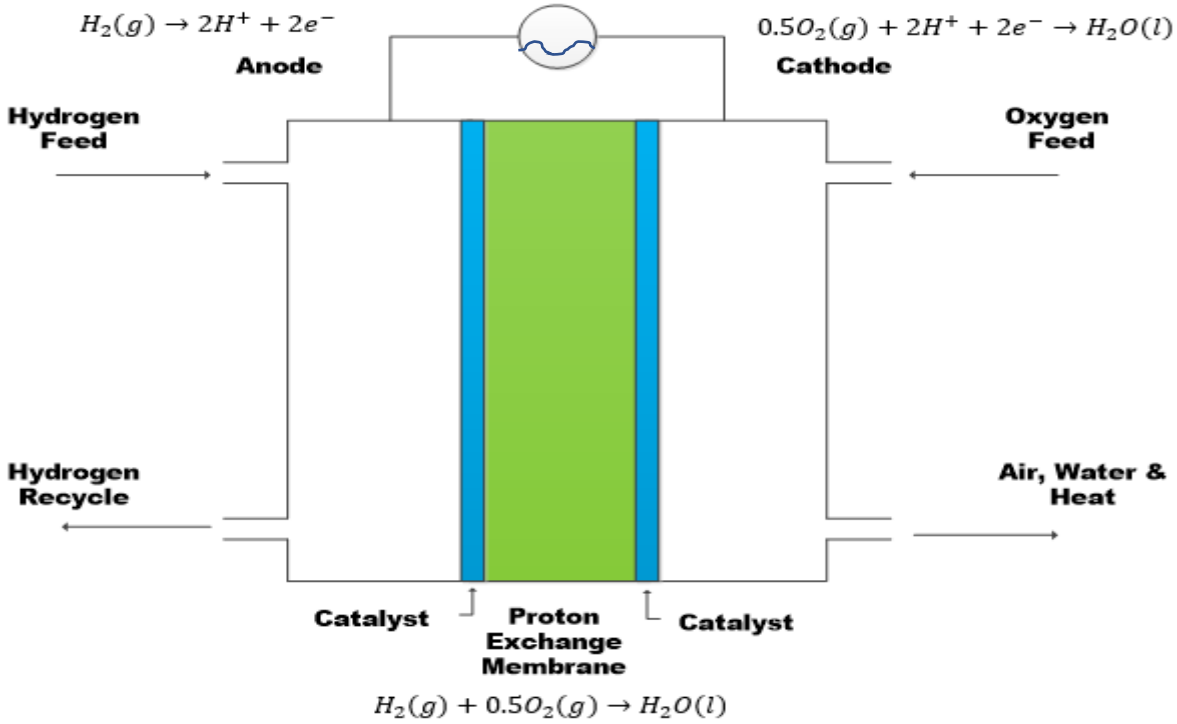

Figure 16: PEMFC & Half Reactions (Mekhilef *et al*, 2012)

Mekhilef *et al* (2012) found that PEMFCs have an electrical efficiency ranging between 53-58% with a CHP efficiency ranging between 70-90%. The latter, a good indication of the process integrating ability of the output heat. An electrical efficiency of 54% will be assumed and used to calculate the FC feed and stoichiometric air requirement. Hence, the mass flow rate of the heating stream is defined and used in the pinch analysis section.

3.7 Solar Collector Selection & Description

Concentrated Solar Power (CSP) technologies are used to extract sunlight by using mirrors to reflect and concentrate sunlight onto receivers that collect solar energy and convert it to heat (Guney, 2016). Fundamentally, a large area of naturally available solar energy is concentrated onto a small area (Khan & Arsalan, 2016). Ogunmodimu & Okoroigwe (2018) notes that four solar concentrators exist which include, Parabolic Trough Concentrators (PTC), Linear Fresnel Reflectors (LFR), Solar Towers (ST) and Parabolic Dish Concentrators (PDC). These four CSP technologies are analysed and the appropriate one is selected below.

Despite solar PV being a more commercially developed and initially affordable technology than CSP, Khan & Arsalan (2016) highlights that CSP achieves greater economic returns and is best suited for large scale applications. The authors add that, in comparison to solar PV, CSP systems can provide electricity in the absence of sunlight.

Selecting an appropriate CSP was challenging considering the relative advantages and disadvantages of the four CSP technologies. The PTC was chosen for this study since it is the most proven, affordable system (Ghandehariun *et al*, 2010) capable of achieving an operating temperature of 550℃ (Khan &

Arsalan, 2016) which exceeds the maximum required temperature of 500℃ required by the thermochemical process. Moreover, Ghandehariun *et al* (2010) add that the overall thermal efficiency, in this context defined as the fraction of incoming solar energy delivered to the collection tube is about 78%. High solar efficiencies are important in reducing the CSP area whilst increasing the capability of achieving the high temperatures required by the thermochemical cycles.

According to Guney (2016), the working fluid allows for storage during periods of low or no solar radiation. In this process, the working fluid will only be stored to preheat the biomass feed during the evening and early morning. Ghandehariun *et al* (2010) recommend nitrate mixtures as the working fluid since it can produce heat at a constant rate due to their high heat capacity per unit volume, are stable at high temperatures (up to 600℃), are relatively inexpensive, widely available, non-flammable, minimal environmental impact, low vapor pressure and has low corrosion rates with typical piping materials. More specifically, the authors recommend a $NaNO_3/KNO_3$ (60/40) mixture, proven to achieve a working temperature up to 565℃. Hence, the 60/40 $NaNO_3/KNO_3$ mixture will be used as the working fluid in this study.

Kaygusuz (2011) found that solar resource in excess of 1800 $kWh/m^2\ y$ is required for economical CSP operation. Since the selected region as shown in Section 3.3.3 has an estimated solar resource range of 2200-2600$kWh/m^2\ y$, CSP is considered a viable option. It is assumed that adequate solar radiation reaches the CSP and hence will operate at the operating temperature of 540℃ during the day and no conversion ratios will be used to estimate the extracted heat from the CSP.

Furthermore, Kaygusuz (2011) notes that approximately 20 m^2 of land is required per megawatt of electricity produced. Section 5.3 assumes a power rating of 30 kW (0.03MW) for the solar plant, therefore, the total CSP land requirement is calculated as follows;

- $Land\ Requirement = 0.03\ MW \times 20\ m^2\ /MW = 0.6\ m^2$ Eq 3-3

The calculation assumes that the plant will operate at 30 kW, however, it is later found to be oversized. However, this capacity is used since at some point the solar plant can operate at its maximum capacity. This could hold if energy demand increases and/or the biogas plant is not operating.

According to Kaygusuz (2011), the PTC is line focussing and uses a mirrored surface of a linear parabolic concentrator to focus solar radiation directly to an absorber pipe, housing the molten salts running along the focal line of the parabola. The heated molten salts are fed to a hot tank before feeding the thermochemical cycle process. Cooled molten salts are returned from the process to a cold tank and then pumped to the solar collectors as shown in the modified BFD presented below by Ghandehariun *et al* (2010).

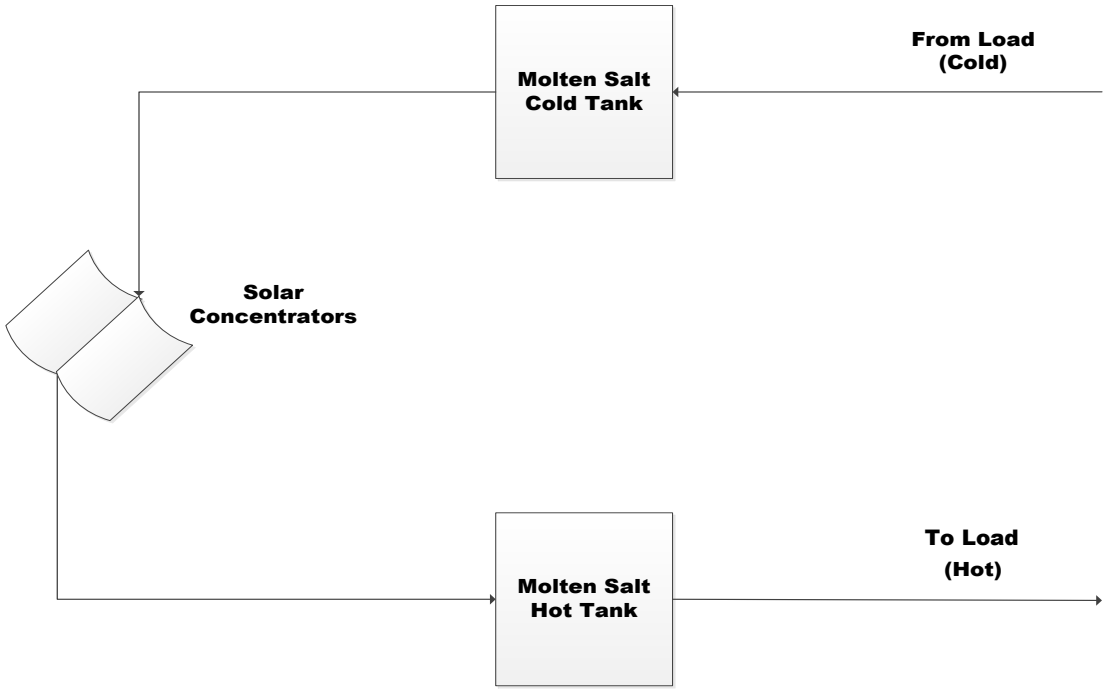

Figure 17: Solar Concentrator Plant Section (Ghandehariun et al, 2010)

3.8 Equipment Concluding Data

A summary of the necessary data as required for the design of the process collected in Sections 3.4-3.7 has been extracted and tabulated below.

Table 11: Equipment Summary of Sections 3.4-3.7

Process		Specifications/Operating Conditions
Thermochemical Cycle	Cycle type	4-step hybrid CuCl cycle
	Operating temperature	530℃
	Net efficiency	43%
Bioenergy	Process type	AD
	Digester temperature	55℃
	Feedstock	Waste crops, sweet sorghum & animal manure
	Biogas composition	60-70% methane, 30-40% CO_2 and trace hydrogen and hydrogen sulphide
Fuel Cell	Fuel Cell type	PEMFC
	Operating temperature	90℃
	Input	H_2, O_2
	Output	Heat, air, H_2O, electricity
	Electrical efficiency	54%
Solar Collector	Collector type	PTC
	Operating temperature	540℃
	Thermal efficiency	78%
	Working fluid	60/40 $NaNO_3/KNO_3$

3.9 Thermochemical Cycle Plant Preliminary Design & Description

This section includes a description of the thermochemical process adopted from Naterer *et al* (2011b) along with the process diagram. The biogas process remains the same as that presented in Section 3.5. Naterer *et al*'s (2011b) original schematic is presented in Appendix G. Furthermore, a conceptualized diagram of the thermochemical system is presented in this section and a detailed integrated PFD will be provided once heat pinch analysis has been applied.

Modified from Naterer *et al* (2011b), the thermochemical process presented in Figure 18 begins with $CuCl(aq)$ & $HCl(aq)$ in stream 1 being fed to the anode section of the electrolyzer, operating between 25-100℃ with a voltage of 0.8 V. The authors report stable electrolyzer performance using voltages from 0.477-0.7 V. A more detailed diagram of the electrolyzer is presented in Appendix B.

Recycled $HCl(aq)$ in stream 2 is fed to the cathode compartment thereby producing $CuCl_2$(aq) in stream 5 and $H_2(g)$ & $HCL(aq)$ in stream 4. The process assumes all the $CuCl(aq)$ is converted.

Stream 4 is fed to separator 1 to obtain $H_2(g)$, before being fed via stream 6 to an in-line hydrogen storage tank. In the same separator, $HCl(aq)$ is separated into stream 8 that is fed to mixer 1 and recycled to the electrolyzer via the anode feed tank.

For recycling, $CuCl_2$(aq) in stream 5 is fed to a spray dryer that operates between 25-100℃ to produce $CuCl_2$(s) in stream 9 which is then fed to a hydrolysis reactor. Liberated water from the dryer, enters stream 10 and is recycled back to mixer 1 after a fraction of the water is fed to mixer 2 via stream 27.

Water from mixer 2 coupled with $CuCl_2$(s) in stream 9 is fed to the hydrolysis reactor operating at 400℃. The products of the hydrolysis reaction include $Cu_2OCl_2(s)$ & $HCl(g)$ in stream 13.

These products are then fed to separator 2 where $HCl(g)$ is returned to the electrolyzer as an aqueous solution in stream 2. From separator 2, $Cu_2OCl_2(s)$ is fed via stream 14 to the decomposition reactor operating at 500℃.

Decomposition products, $CuCl(l)$ & $O_2(g)$ are fed to separator 3 to capture $O_2(g)$ whilst the $CuCl(l)$ is recycled to mixer 1 to form an aqueous solution after which, it is recycled back to the electrolyzer via the anode storage tank.

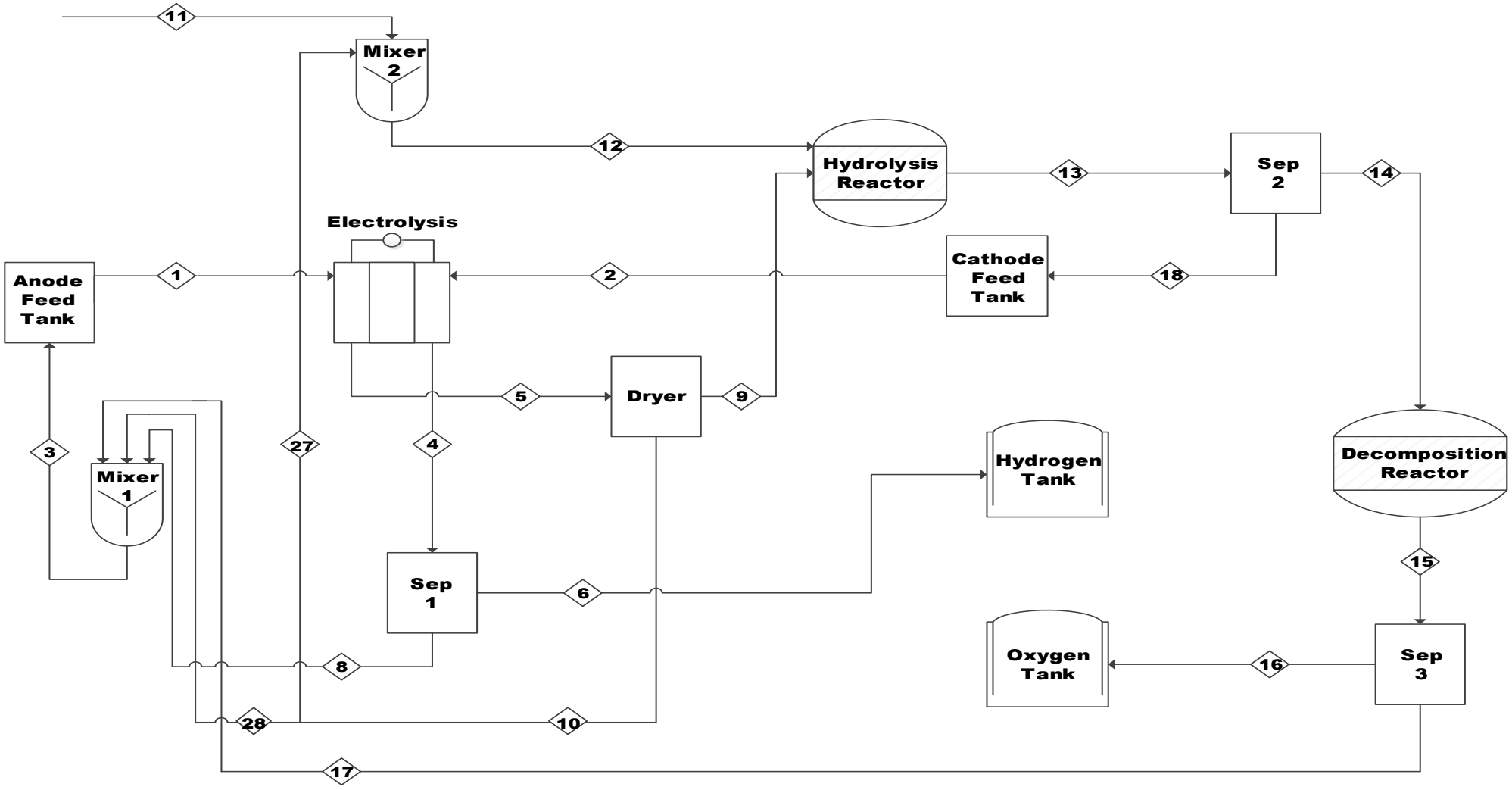

Figure 18: Thermochemical Process Section (**Naterer *et al*, 2011b)**

CHAPTER 4: METHODOLOGY

4.1 Chapter Outline

This section briefly describes the design methodology of the rural hybrid system. The methodology includes heat & power demand forecasting, estimating the plant capacity, material balances heat & power pinch analysis and concluded with an economic analysis.

4.2 Hourly Heat & Power Demand Forecasting

Authors Adeoye & Spartaru (2019) and Prinsloo *et al* (2016) agree that challenges exist in hourly electricity forecasting for rural homesteads due to the lack of quality data and modelling methodologies since smart-meters capable of recording user consumption are mainly available in grid-connected urban areas. Moreover, Prinsloo *et al* (2016) go on to note that it is equally challenging to find time-series datasets that represent heat and power load profiles for rural African villages.

Consequently, Prinsloo *et al* (2016) presented realistic hourly heat and power load profiles typical to small remote rural African villages capable of contributing to renewable hybrid electricity supply system design. Coupled with Lloyd & Cowan's (2004) average monthly energy consumption for newly electrified rural homesteads, the presented rural power load profiles will be used to estimate the electricity consumption and generate a power load profile for the proposed rural setting.

Furthermore, heat profiles were generated by Prinsloo *et al* (2016), to provide a convenient way to visualise thermal energy usage patterns in rural homesteads. Along with findings presented by Meyer & Tshimankinda (1996) on hot water usage in rural homesteads, the heat load profile and thermal usage for the proposed rural setting were determined.

Applicable load profiles are generated by using the assumed energy and hot water consumption and multiplying it with the fractional contribution of the original profiles presented by Prinsloo *et al* (2016) as shown in the equations below.

$$Hourly\ energy\ consumption = \bar{X}\ daily\ energy\ consumption \times hourly\ fraction \quad \text{Eq 4-1}$$

$$Hourly\ hot\ water\ consumption = \bar{X}\ daily\ hot\ water\ consumption \times hourly\ fraction \quad \text{Eq 4-2}$$

The hourly data is then tabulated and used to construct new daily village electricity and hot water load profiles.

4.3 Plant Capacity

Estimating the capacity of the hybrid energy system was initiated by determining the time that solar resources are available during the summer and winter months. This is important since the thermochemical plant is only capable of operating when daylight is available.

Once, the availability of solar resources was determined, the individual plants of the hybrid system were allocated time slots for optimum operation.

Individual plant capacities were estimated based on the amount of daylight available to ensure the operation of the thermochemical plant whilst the biogas plant will operate during times wherein the solar radiation is low.

Once the operating times were allocated, the hourly demand data from Section 5.2 was used to size each plant. Each plant was sized to ensure that it can cover the time interval with the largest demand wherein each plant exists.

4.4 Material Balances

The hybrid system was assumed to operate at steady state. This step is crucial in ensuring practically achievable energy targets for pinch analysis. Extensive material balance calculations and detailed explanation of assumptions for the hybrid system can be found in Appendix D whilst the summarised data is found in Section 5.4.

The fuel cell electrical efficiency of 54% as assumed in Section 3.6 was used to initiate the material balance for the thermochemical cycle process. Larminie & Dicks (2003) presented a set of equations as shown in appendix D that uses the assumed electrical efficiency and the electrical power of the FC stack to determine the Mean Voltage (V_c) of each cell and ultimately the hydrogen input for the FC. Hence, stoichiometric equations are used to estimate the oxygen and air requirement.

The calculated hydrogen usage is then used to back-calculate and complete a material balance around the electrolyzer. However, the balance is further simplified by assuming a binary system for the electrolyzer. Wang *et al* (2012) introduce applicable molar ratios necessary to determine all input and output flow by assuming a binary system.

Although unrealistic, all separators are balanced by assuming perfect separation to further simplify the material balance equations while the dryer balance assumes all input water is removed without leaving with the exhaust air. Wang *et al* (2012), considering a binary system, presents airflow rate ratios to determine its flowrate and hence completing the balance around the dryer. Furthermore, all mixers follow the typical steady-state conservation of mass approach.

Assuming a binary system mitigates potential risks such as insufficient contact between reactants, potential heat transfer resistance, and incomplete reaction within the hydrolysis reactor. Hence complete reaction with no side reactions is assumed in the hydrolysis reactor. The stoichiometric steam requirement is considered satisfactory by Wang *et al* (2012) to ensure complete conversion, however, excess steam is fed to ensure that $HCl\ (g)$ is converted to an aqueous solution since it is recycled to the recycler. Hence 89% excess steam is assumed as suggested by Weebly (2019). Additionally, the decomposition reactor assumes complete conversion thus the stoichiometric requirement is considered adequate to complete the balance.

All trace gases are neglected in the balance around the digester considering the biogas contents assumed in Section 3.5. Therefore, methane and carbon dioxide content were assumed to be 65 & 35%

respectively. Ghazi & Nazir (2017) note that the energy content of the biogas mixture is directly proportional to the methane content it contains. Hence, they suggest a volume to energy content conversion ratio as shown in appendix D. Coupled with yield results presented by Cavinito *et al* (2010) and biogas generation capacity found in Section 5.3, the production capacity can be estimated and hence the digester feed rate. A 12% solids are assumed in the feed based on results from Cavinito *et al* (2010) thus completing the digester balance.

4.5 Heat Pinch Analysis

Principally based on the laws of thermodynamics, pinch technology is one of the least complicated, most effective methods in optimising energy usage within a chemical process (John, 2014). Furthermore, the author states that the main aim of pinch analysis is to achieve maximum financial saving by maximising process to process heat recovery whilst simultaneously reducing utility usage. The systematic procedure provided in Section 2.3 was followed to ensure maximum energy recovery within the hybrid system.

Extracting the necessary data was the first step in the analysis. Data extraction was initiated by identifying the streams that need heating & cooling, followed by obtaining the mass flows of the extracted streams from the material balance. Included in data extraction, was obtaining the stream Heat Capacities (Cp) and selecting an appropriate ΔT_{min} which was found to be industry specific. Cps for each component were collected at the given temperature as shown in Appendix E whilst the Cp of mixtures was calculated as follows:

$$Cp_{(stream\ n)} = (wCp)_{Component\ A} + (wCp)_{Component\ B} \quad \text{Eq 4-3}$$

The Heat Capacity Flow Rate (CP) for each stream was calculated by multiplying the stream mass flow rate with its Cp and used in the HEN design.

The CCs & PTA were then constructed using Microsoft Excel to set the energy targets followed by the use of ASPEN Energy Analyzer to construct the HEN using the GD.

4.6 Hybrid System Final Design

The hybrid system was integrated by applying heat pinch analysis to the thermochemical cycle and biogas plant. Once integrated using Aspen Energy Analyzer to present the HEN, this information was extracted and used to construct the total site schematic using Visio. The plant PFD before integration can be found in Appendix I whilst Section 5.6 provides both the PFD and process description which includes the inlet and outlet temperatures of the hot and cold streams.

4.7 Power Pinch Analysis (PoPA)

The methodology presented in Section 2.4 was employed to construct both the PCT and SCT using Microsoft Excel and presented in Section 5.7. The original PCT parallel to the power allocation found in Section 5.3 can be found in Appendix J. The original PCT highlighted significant energy surplus, hence a modified version was presented. Modified operating times and cycling methods were chosen to provide the lowest AEEND before being less than MOES to prevent the use of outsourced electricity.

4.8 Economic Analysis

Ray & Johnston (1989) noted that, evaluating the economics of a process is initiated with capital costing followed by estimating the manufacturing costs. This section involves the estimation of the capital and manufacturing costs using factors to determine the production cost per kWh and is referred to by Turton *et al* (2013) as a study estimate. Ray & Johnston (1989) acknowledged that such an estimate has an accuracy of $\pm$ 20-30%, however, it is considered acceptable when evaluating multiple processes.

4.8.1 Estimation of Capital Costs

Capital costs of the hybrid system were estimated using the bare module costing technique. Programmed into Microsoft Excel, CAPCOST was used to estimate the bare module costs of the hybrid system. However, CAPCOST does not list equipment such as the FC, biogas generator, electrolyzer, and solar concentrator. Vendor purchased costs were found for the FC, biogas generator, electrolyzer, and their bare module factors were assumed to determine the bare module costs. As for the solar concentrator, it was estimated as a percentage of the bare module costs

Once the bare module costs were estimated, the Total Module Costs (TMC), Total Grass Roots Costs (TGRC), and fixed capital investment were computed to conclude the capital costs.

The costs for piping, instrumentation, pumps & plant layout were not considered. Raw materials costs were assumed as a capital cost since it is recycled and only requires a one-time cost at start-up.

Turton *et al* (2013) recommend using the bare module costing technique which sums the direct and indirect costs associated with purchasing equipment. The technique relates the purchased cost at some base conditions to the bare module costs using bare module factors. According to Turton *et al* (2013), the bare module factor considers equipment type, system pressure, capacity, and material of construction. The authors provided the following equation to estimate the bare module costs.

$$C_{BM} = C_P^0 F_{BM} \quad \text{Eq 4-4}$$

Where $C_{BM} =$ bare module equipment cost

$C_P^0 =$ purchased cost of equipment at base conditions

$F_{BM} =$ bare module factor

Moreover, inflation is accounted for using the Chemical Engineering Plant Cost Index (CEPCI). Cost data provided by Turton *et al* (2013) were that of the year 2006 when the CEPCI was 500. In this study, the annual CEPCI of 2018 which amounted to 603.1 (Scribd, 2019) was used in the following equation to correct the cost estimate.

$$Cost\ in\ year\ A = Cost\ in\ year\ B \times \frac{Cost\ index\ in\ year\ A}{Cost\ index\ in\ year\ B} \quad \text{Eq 4-5}$$

The subsequent equations as presented by Turton *et al* (2013) are used to compute the C_P^0 & F_{BM} which is required to estimate the plant bare module costs.

$$log_{10}C_P^0 = K_1 + K_2 log_{10}(A) + K_3[log_{10}(A)]^2 \quad \text{Eq 4-6}$$

$$F_{BM} = B_1 + B_2 F_m F_P \quad \text{Eq 4-7}$$

Where $A =$ Equipment capacity or size parameter

$K_n =$ Equipment correlation data

$F_m =$ Equipment material factor

$F_P =$ Equipment pressure factor

$B_n =$ Equipment constant

Fortunately, Turton *et al* (2013) recognized the tiresome nature of calculating the costs by hand and hence, developed CAPCOST. CAPCOST is programmed in Microsoft Excel, to allow for the easier and quicker computation of the bare module costs. Input data relating to the equipment such as equipment type, capacity, operating pressure, desired CEPCI, and materials of construction are required from the user. Considering the convenience of CAPCOST, the program was used to estimate the bare module costs of the hybrid system presented in this study. Capital costing results can be found in Table 30 whilst the CAPCOST input data can be found in Appendix O.

Grassroots costs were estimated in addition to the bare module costs since the rural hybrid system was a completely new facility. In doing so, additional costs were accounted for along with the bare module costs. These costs include contingency and fees which are estimated at 18% of the bare module costs (Turton *et al*, 2013). Including these costs in the bare module costs provide the TMC and are estimated by the equation below.

$$TMC = 1.18 C_{BMT} \quad \text{Eq 4-8}$$

Where $C_{BMT} =$ Total bare module costs

Once the TMC was determined, the grassroots costs were estimated by adding auxiliary facilities costs to the TMC. Auxiliary costs include site development, auxiliary buildings, off-sites, and utilities (Turton *et al*, 2013). According to the authors, these costs are assumed at 50% of the bare module costs at base case conditions. However, in this study, 25% of the bare module costs were assumed since bare module costs at base conditions are not available for all equipment. Furthermore, 25% instead of 50% was used since bare module costs are typically more costly than that at base conditions. The above assumption was further considered acceptable since Turton *et al* (2013) noted that these costs could range between 20-100% of the bare module costs.

The TGRC is given by the equation below. This cost is equivalent to the Fixed Capital Investment (FCI_L) excluding the cost of land.

$$TGRC = TMC + 0.25 C_{BMT} \quad \text{Eq 4-9}$$

The cost of land required for the hybrid system in the rural setting was assumed to be $60 000 which was added to the FCI_L to provide the Fixed Capital Investment (FCI).

4.8.2 Estimation of Manufacturing Costs

Manufacturing costs were estimated once the fixed capital investment including land, cost of operating labour, cost of utilities, cost of waste treatment, and cost of raw materials were computed. Fortunately, the manufacturing costs were reduced since no utility costs and waste treatment costs were included. Although included as a capital cost, reactants for make-up was introduced as a raw material cost. Lastly, the cost per kWh was determined to establish the affordability of the process.

According to Turton *et al* (2013), the Cost of Manufacture (COM) can be estimated once the Direct Manufacturing Costs (DMC), Fixed Manufacturing Costs (FMC), and the General Expenses (GE) are known. The COM is evaluated as the sum of these costs. However, the authors present an alternative equation once the following costs are known or can be estimated.

- FCI
- Cost of Operating Labour (C_{OL})
- Cost of Utilities (C_{UT})
- Cost of Waste Treatment (C_{WT})
- Cost of Raw Materials (C_{RM})

The subsequent equations are presented as an alternative to estimate the COM, where COM allows for depreciation amounting to 0.1FCI and COM_d excludes depreciation. In this section, both equations will be used to evaluate the cost of manufacturing.

$$COM = 0.280FCI + 2.73C_{OL} + 1.23(C_{UT} + C_{WT} + C_{RM}) \quad \text{Eq 4-10}$$

$$COM_d = 0.180FCI + 2.73C_{OL} + 1.23(C_{UT} + C_{WT} + C_{RM}) \quad \text{Eq 4-11}$$

Moreover, Turton *et al* (2013) recommend estimating the operating labour using the equation below:

$$N_{OL} = (6.29 + 31.7P^2 + 0.23N_{np})^{0.5} \quad \text{Eq 4-12}$$

Where $N_{OL} =$ Number of operators per shift

$P =$ Number of solid handling steps

$N_{np} =$ Number of non-solid handling steps

The cost of manufacturing along with the production cost can be found in Table 31.

4.9 Methodology Summary

The following flowchart provides shows the summarised flow of the design process initiated by the study of available resources and concluding with a cost analysis.

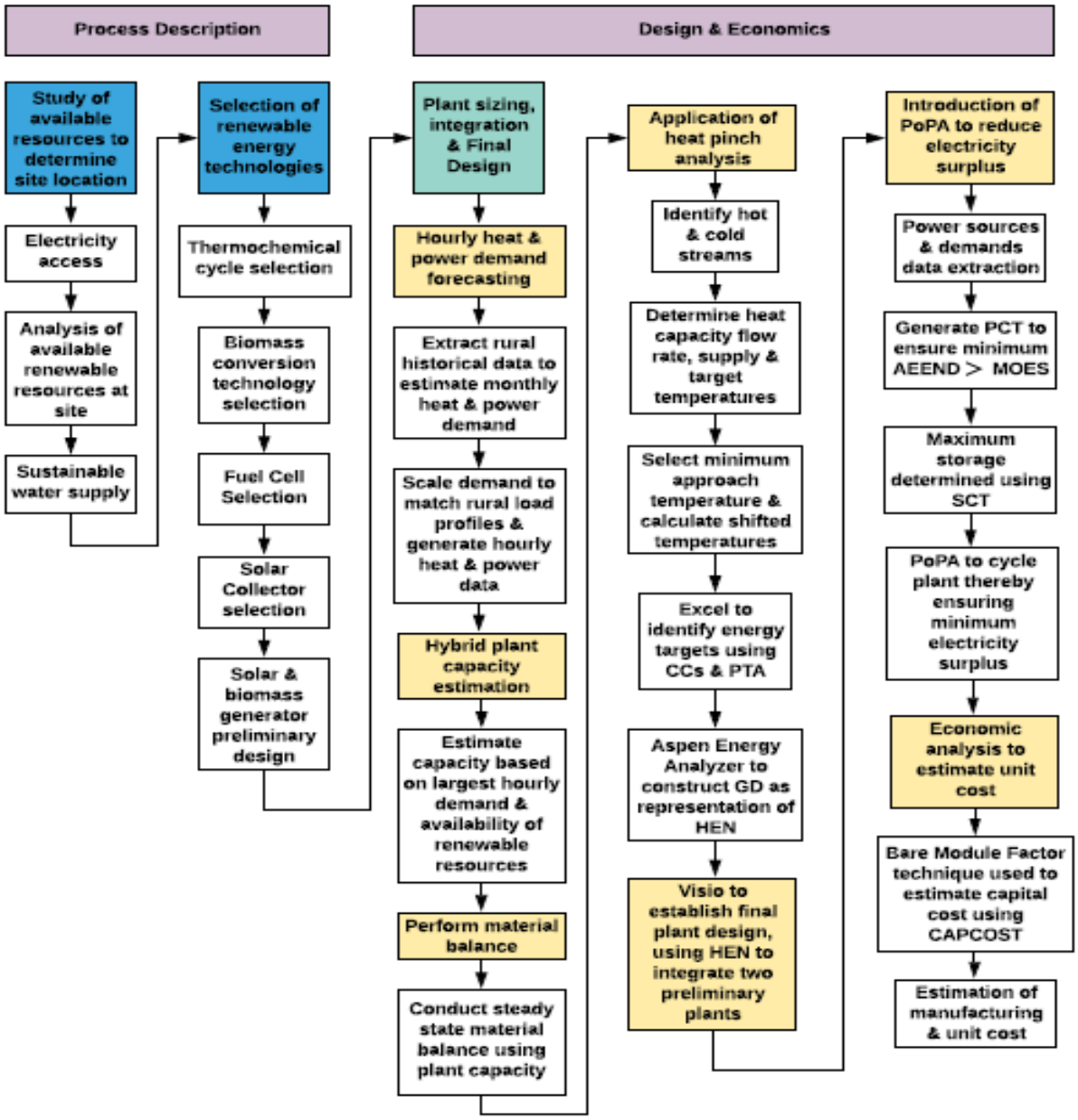

Figure 19: Summary of Design Process

CHAPTER 5: RESULTS & DISCUSSION

5.1 Chapter Outline

This section provides the results associated with the heat & power demand forecast, material balance, heat & power pinch analysis, and economic feasibility.

5.2 Hourly Heat & Power Demand Forecasting

5.2.1 Power Demand Forecasting

The necessary heat and power generation and consumption information need to be extracted in performing the systematic framework to use pinch analysis tools in an integrated manner presented by Aziz *et al* (2017). This step is necessary since it allows the designer to determine the heat and power plant size along with the accompanying storage capacity without which deficit electricity would otherwise be supplied by the central grid. However, since the proposed heat and power plant would be a stand-alone system, storage capacity is a necessity.

Typical monthly electricity usage amount to 210 kWh in households mainly cooking with electricity whilst households not using electricity for cooking averages around 150 kWh (Lloyd *et al*, 2004). However, to ensure robustness for the renewable hybrid system, 210 kWh per month per household will be assumed since there is potential that each household will use electricity for cooking with time.

Assuming a month of 30 days with an average monthly requirement per household of 210 kWh amounts to 8190 kWh for the entire village per month. The monthly village demand is found by multiplying the monthly household demand by the 39 households.

Furthermore, this load data can be scaled to match the hourly load profile represented by Figure 20. This is done by calculating the load as a fraction of the total load within each time interval using the old electricity load profile data in column 2 of Table 12. Once the usage per hour, represented by the fraction is calculated, it is then multiplied by the new daily village load of 273 kWh to determine the estimated load per hour. The new daily village load is found by dividing the monthly village demand by the assumed 30 days whereas the calculation of the new load within the different time intervals was calculated as follows;

$$New\ village\ load\ @\ time\ (t) = \frac{Old\ load\ @\ time\ (t)}{Old\ total\ daily\ load} \times New\ total\ daily\ village\ load \quad \text{.Eq 5-1}$$

Daily village power consumption values presented in Table 12 per household having a power requirement of 273 kWh is used to generate Figure 21 that depicts the daily village load profile.

Table 12: Daily Village Load Data

Time	Old Daily Village Load (kWh)	Fraction Prinsloo *et al* (2016)	New Daily Village Load (kWh)
01:00	0.65	0.031	8.44
02:00	0.965	0.046	12.53
03:00	1.17	0.056	15.19
04:00	1.023	0.049	13.28
05:00	0.629	0.030	8.17
06:00	0.418	0.020	5.43
07:00	0.439	0.021	5.70
08:00	0.56	0.027	7.27
09:00	0.586	0.028	7.61
10:00	0.481	0.023	6.24
11:00	0.381	0.018	4.95
12:00	0.376	0.018	4.88
13:00	0.392	0.019	5.09
14:00	0.408	0.019	5.30
15:00	0.665	0.032	8.63
16:00	1.301	0.062	16.89
17:00	2.095	0.100	27.20
18:00	2.337	0.111	30.34
19:00	2.037	0.097	26.45
20:00	1.47	0.070	19.08
21:00	0.96	0.046	12.46
22:00	0.707	0.034	9.18
23:00	0.518	0.025	6.73
00:00	0.46	0.022	5.97
Total	21.028	1	273

Prinsloo *et al* (2016) realized that it is difficult to obtain heat & power load profiles for rural African villages whilst an inconsistency exists between studies that scope rural household electricity usage patterns. However, the author's presented load profile should suffice for baseline studies. Prinsloo *et al* (2016) constructed Figure 20 using the village load values in column 2 of Table 12 to act as the representative load pattern for typical rural households or rural villages. The data in column 2 of Table 12 used to construct Figure 20, is therefore scaled to create the load profile and electricity forecast using 39 households representing the rural village, to provide an identical pattern as depicted in Figure 21 with different amplitudes.

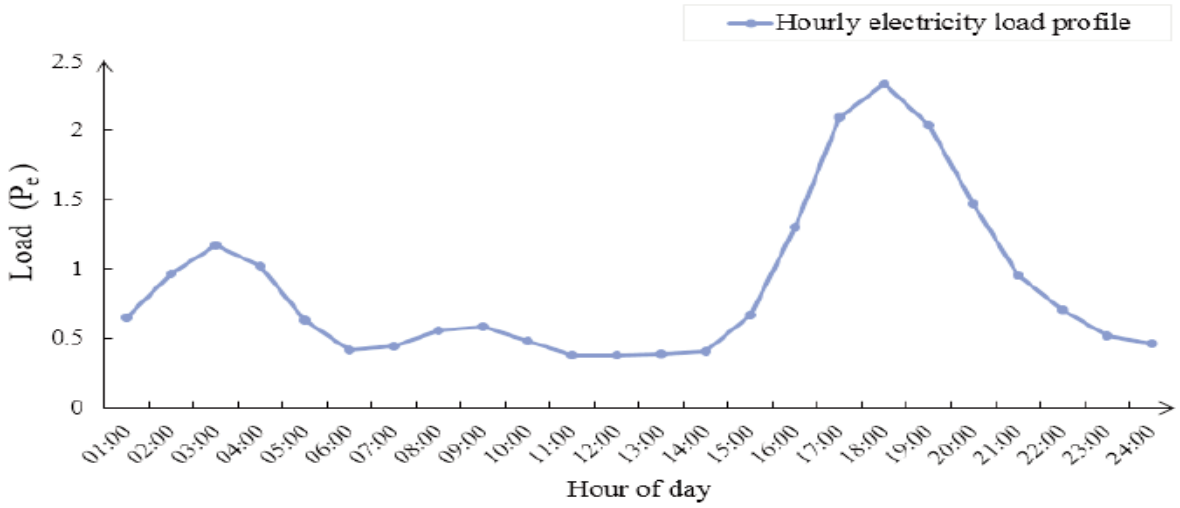

Figure 20: Typical Rural Load Profile (Prinsloo *et al*, 2016)

According to the authors, morning peaks are attributed to inhabitants using lights, kettles, and making breakfast whilst low midday peaks are associated with a semi farming community where not all workers return for lunchtime and use electricity. This behaviour is considered typical for a semi-farming village. Furthermore, as expected, the resulting large peak in the evening can be attributed to inhabitants returning home and using appliances for dinner, water heating, cleaning, and entertainment. Additionally, it is expected that morning peaks typically range between 5-7 am when people generally wake up instead of the morning peak ranging from 2-4 am, presented in Figure 20. The authors do not justify this peak however, it is accepted since it is assumed that village farmers are early risers so that they could get to work sooner to avoid working in the heat.

According to Lloyd *et al* (2004), there is slow uptake of thermal uses of electricity in newly electrified rural homesteads. A few reasons provided by the authors include;

- Availability of cooking or heating appliances using electricity versus already available appliances suited for solid or liquid fuel feeds.
- Affordability of electrical appliances as some inhabitants believe electrical appliances for heating or cooking incur higher running costs.
- Households are familiar with "traditional" fuels.

- Current solid or liquid-fuelled cookers or heaters can be used for multiple purposes whilst separate electrical appliances are needed for a specific purpose.

As such, this can be expected for the current rural setting once electrified. Consequently, the typical demand may be lower than estimated.

The presented load profile is expected to change as the seasons vary whilst profiles presented by Prinsloo *et al* (2016) are fixed and focusses on a universal shape & not the load. Therefore, as seasons vary, the shape remains constant whilst the peaks decrease, or increase based on demand. The shape given by Prinsloo *et al* (2016) does not differentiate between seasons hence, considering that traditional fuels for heating & cooking applications will likely still be used for newly electrified rural homesteads throughout the year, the presented load profiles are assumed acceptable as an annual average. Moreover, a monthly average of 210 kWh is used to avoid multiple load profiles for varying seasons.

Figure 21 depicts the village daily load profile, constructed using the new daily village load data tabulated in Table 12.

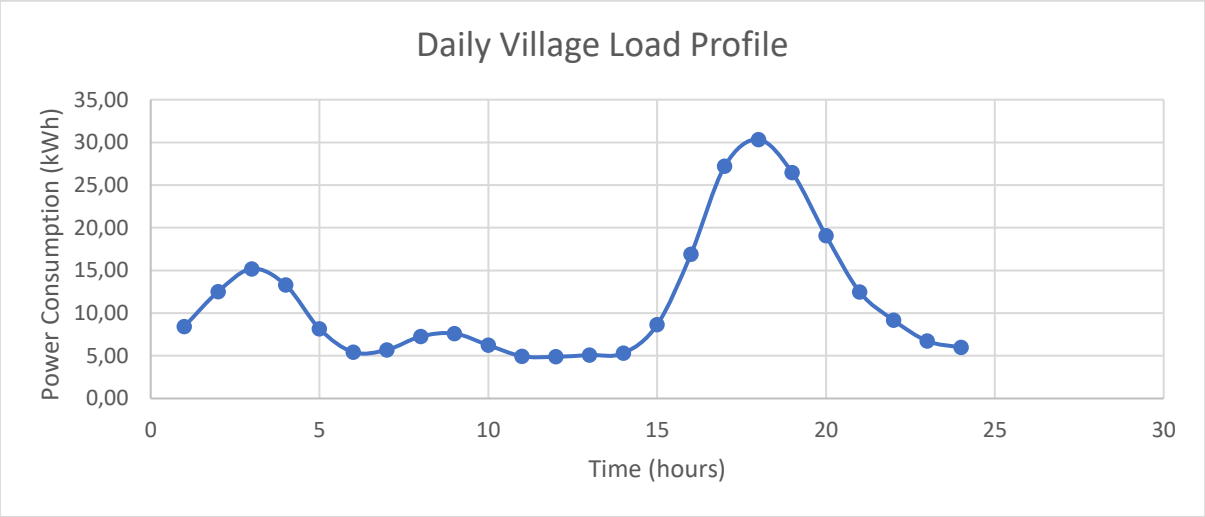

Figure 21: Village Daily Load Profile

It is clear that the new load profile presented in Figure 21 is similar but different in amplitude to the reference load profile in Figure 20 presented by Prinsloo *et al* (2016). Therefore, the same assumptions used to describe the peaks of Figure 20 hold for the new village load profile.

5.2.2 Heat Demand Forecasting

Meyer & Tshimankinda (1996), presented a paper wherein they measure over a year, the hot water consumption in traditional homesteads in Johannesburg, South Africa. According to the authors, low-density rural homes consists of 5.7 occupants using geysers with a set temperature of 65℃. However, a hot water stream at 80℃ will be fed to the village to account for heat losses during transport, winter, and storage if geysers are employed. Upon completing their measurements, they found that each person consumes 6.3 l of hot water per day for low-density households. These results along with the heat load

profile generated by Prinsloo *et al* (2016) is used to forecast the hot water requirement for the proposed village, using the same methodology as that used to forecast the power profile and consumption.

An average of 6.3 l of hot water is consumed per person, which amounts to 25.2 l of hot water at 80℃ per household per day since there is an average of 4 occupants per household. Multiplying the per-household consumption of 25.2 l by 39 households gives the village consumption of 982.8 l within a day. The total is smoothed in tandem with the hot water consumption profile provided by Prinsloo *et al* (2016) using their presented fractional contribution within each time allocation. Hence a new hot water consumption profile can be generated for the proposed village.

The village hourly consumption is calculated as follows.

$$Consumption\ @\ time\ (t) = \frac{Old\ consumption\ @\ time\ (t)}{Old\ total\ daily\ Consumption} \times New\ daily\ village\ consumption \quad \text{Eq 5-2}$$

Hourly consumption values are tabulated below and used to produce Figure 22.

Table 13: Hot Water Village Consumption Data

Time	Old Daily Village Consumption (Litres) Prinsloo *et al* (2016)	Fraction	New Daily Village Consumption (Litres)
01:00	0.063	0.009	8.88
02:00	0.065	0.009	9.17
03:00	0.081	0.012	11.42
04:00	0.148	0.021	20.87
05:00	0.404	0.058	56.97
06:00	0.479	0.069	67.55
07:00	0.434	0.062	61.20
08:00	0.376	0.054	53.03
09:00	0.324	0.046	45.69
10:00	0.269	0.039	37.94
11:00	0.214	0.031	30.18
12:00	0.182	0.026	25.67
13:00	0.172	0.025	24.26
14:00	0.166	0.024	23.41

15:00	0.199	0.029	28.06
16:00	0.319	0.046	44.99
17:00	0.474	0.068	66.85
18:00	0.535	0.077	75.45
19:00	0.528	0.076	74.46
20:00	0.498	0.071	70.23
21:00	0.426	0.061	60.08
22:00	0.34	0.049	47.95
23:00	0.158	0.023	22.28
00:00	0.115	0.017	16.22
Total	6.969	1	982.8

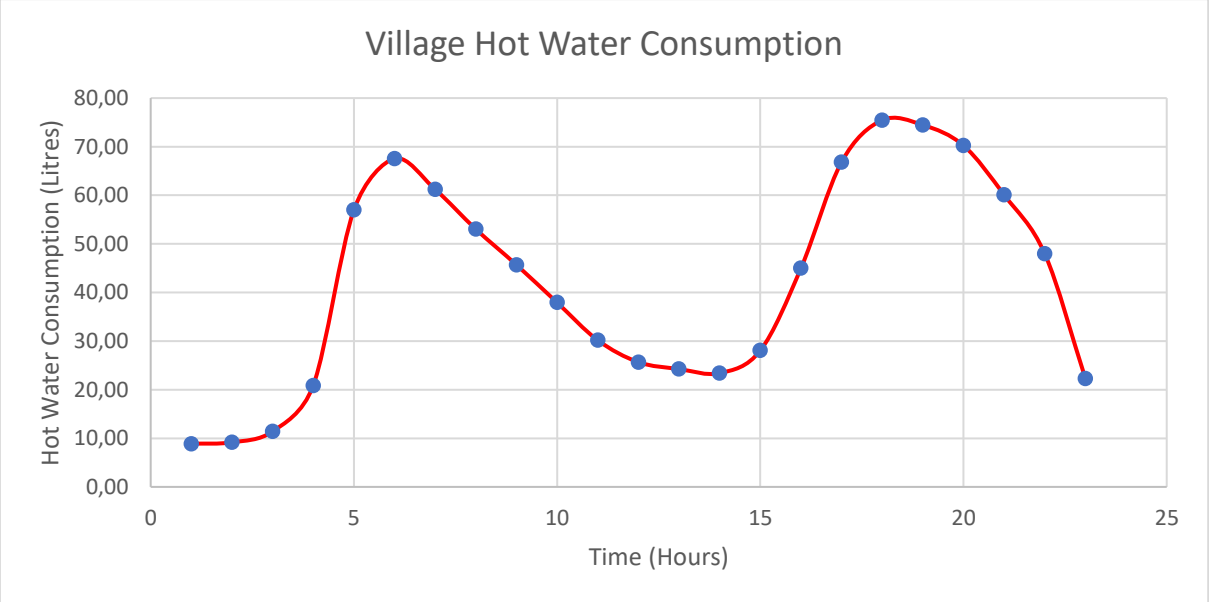

Figure 22: Village Hot Water Consumption Profile

Varying morning peaks are clear when comparing heat and power profiles. This was not justified by Prinsloo *et al* (2016). However, it is assumed that since farmworkers are early risers to avoid daylight, power will be more likely used for lighting whilst preparing for work during the morning 2-4 am power peak. The later hot water peak between 4-6 am is assumed to be attributed to children preparing for school whilst the at-home parent cleans. Higher hot water draws for children is expected since it is assumed that they are less wise with water than adults.

Morning and evening peaks of approximately 70 *l* & 75 *l* respectively seem slightly low and unreasonable for a village containing 39 households, housing a population of 156 people. It is worth noting that the reference profile is not accurate but suitable for baseline studies. Furthermore, it is considered acceptable since baths and showers are not expected to be present, hence a lower hot water consumption. The inhabitants are more likely to use buckets for washing purposes. Moreover, it cannot be assumed that the hot water line is the only source of hot water for these inhabitants. It is possible that, since these inhabitants traditionally use fire to heat their water that they will continue to do so to a certain extent, thus the low draw off from the hot water line.

5.3 Hybrid Power Plant Capacity

According to the Timeanddate (2019) website, the total daylight in the Eastern Cape exists between 5:02 am-7:14 pm during the summer months whilst the minimum during winter, exists between 7:17 am-5-23 pm. As a result, the power capacity of the biogas and thermochemical plant can be estimated using the forecasted electricity demand intervals provided in Table 12. The power capacity of each generator can be estimated by assuming the capacity is equivalent to the accumulative village load that exists in the intervals that each generator operates.

Ideally, the biogas plant will operate from 18:00 till 08:00 whilst the thermochemical cycle plant will operate from 08:00-18:00 as highlighted in green in Table 15. These time slots were chosen to ensure continuous operation during both low and high solar radiation months. The operating times are given in Table 15 with the solar plant given in green and the biogas plant in white.

Although these are the envisaged operating times, the plants will be sized in accordance with Table 14. The thermochemical plant will have an increased capacity capable of operating during the periods of total daylight with additional capacity to ensure robustness. Subsequently, the thermochemical plant covers intervals, the summation of which equals 202.51 kWh.

Furthermore, the biogas plant will operate between 00:00-08:00 and 18:00-00:00. However, the 17:00 time slot will be included in its capacity to ensure robustness. Hence, covering a power generation of 200 kWh.

Table 14: Power Sources & Demands

Power Source	Time (h)		Time Interval (h)	Electricity Generation (kWh)	Power Rating (kW)	Revised Power Rating (kW)
	From	To				
Biogas	17:00	08:00	15	200	13.3	35
Solar	04:00	21:00	17	203	12	30

The operating times of the thermochemical cycle plant highlighted in green in Table 15 assume consistent conditions to ensure continuous operation throughout all the months. The issue that arises is that the power ratings are not capable of covering the peak power demands. As an example, during the time interval of 03:00, the demand is 15.19 kWh. Hence the power rating of 13.3 kW of the biogas plant will not be able to cover the demand. Similarly, with the time interval of 18:00. As a result, the solution is to rate the FC and biogas plant at a capacity 10% greater than the maximum village demand, that exists in the time intervals wherein each of these plants operates alone. Hence, the revised power ratings in Table 14. However, the application of PoPA later revealed that the system using the revised power rating was significantly oversized.

Table 15: Power Allocation

Time	Daily Village Load (kWh)	Time	Daily Village Load (kWh)
01:00	8.44	13:00	5.09
02:00	12.53	14:00	5.30
03:00	15.19	15:00	8.63
04:00	13.28	16:00	16.89
05:00	8.17	17:00	27.20
06:00	5.43	18:00	30.34
07:00	5.70	19:00	26.45
08:00	7.27	20:00	19.08
09:00	7.61	21:00	12.46
10:00	6.24	22:00	9.18
11:00	4.95	23:00	6.73
12:00	4.88	00:00	5.97
Total kWh	273		

5.4 Plant Material Balance

5.4.1 Thermochemical Cycle Plant Material Balance

The results presented below summarizes the material balance for the thermochemical cycle and biogas plants as presented in Section 3.9 & 3.5 respectively, the values of which are required in pinch analysis. A detailed material balance along with all assumptions can be found in Appendix D. An ideal system was assumed therefore the balance conformed to the material balance equation below.

$$Mass\ into\ the\ system = Mass\ leaving\ the\ system \quad \text{Eq 5-3}$$

Table 16: Electrolyzer Material Balance

Stream No	Input Components	Flow Rate (mol/s)	Stream No	Output Components	Flow Rate (mol/s)
1	$CuCl$	0.39	5	$CuCL_2$	0.39
1	H_2O	2.93	5	H_2O	2.93
1	HCl	0.39	4	HCl	0.39
2	HCl	0.39	4	H_2	0.195
2	H_2O	1.56	4	H_2O	1.56

Table 17: Separator 1 Material Balance

Stream No	Input Components	Flow Rate (mol/s)	Stream No	Output Components	Flow Rate (mol/s)
4	HCl	0.39	8	HCl	0.39
4	H_2	0.195	6	H_2	0.195
4	H_2O	1.56	8	H_2O	1.56

Table 18: Dryer Material Balance

Stream No	Input Components	Flow Rate (mol/s)	Stream No	Output Components	Flow Rate (mol/s)
5	$CuCL_2$	0.39	9	$CuCL_2$	0.39
5	H_2O	2.93	10	H_2O	2.93
28	Air	14.57	28	Air	14.57

Table 19: Hydrolysis Reactor Material Balance

Stream No	Input Components	Flow Rate (mol/s)	Stream No	Output Components	Flow Rate (mol/s)
12	H_2O	1.755	13	Cu_2OCl_2	0.195
9	$CuCL_2$	0.39	13	HCl	0.39

			13	H_2O	1.56

Table 20: Separator 2 Material Balance

Stream No	Input Components	Flow Rate (mol/s)	Stream No	Output Components	Flow Rate (mol/s)
13	Cu_2OCl_2	0.195	14	Cu_2OCl_2	0.195
13	HCl	0.39	18	HCl	0.39
13	H_2O	1.56	18	H_2O	1.56

Table 21: Decomposition Reactor Material Balance

Stream No	Input Components	Flow Rate (mol/s)	Stream No	Output Components	Flow Rate (mol/s)
14	Cu_2OCl_2	0.195	15	$CuCl$	0.39
			15	O_2	0.098

Table 22: Separator 3 Material Balance

Stream No	Input Components	Flow Rate (mol/s)	Stream No	Output Components	Flow Rate (mol/s)
15	$CuCl$	0.39	17	$CuCl$	0.39
15	O_2	0.098	16	O_2	0.098

Table 23: Mixer 1 Material Balance

Stream No	Input Components	Flow Rate (mol/s)	Stream No	Output Components	Flow Rate (mol/s)
8	HCl	0.39	3	HCl	0.39
8	H_2O	1.56			
28	H_2O	1.37	3	H_2O	2.93
17	$CuCl$	0.39	3	$CuCl$	0.39

Table 24: Mixer 2 Material Balance

Stream No	Input Components	Flow Rate (mol/s)	Stream No	Output Components	Flow Rate (mol/s)
11	H_2O	0.195	12	H_2O	1.755
27	H_2O	1.56			

Table 25: Fuel Cell Material Balance

Stream No	Input Components	Flow Rate (mol/s)	Stream No	Output Components	Flow Rate (mol/s)
22	H_2	0.195	24	O_2	0.0975
23	O_2	0.195	24	N_2	0.735
23	N_2	0.735	24	H_2O	0.195

5.4.2 Biogas Plant Material Balance

The material balance for the biogas plant is considered important since stream 19 will need to be preheated and hence finds its place within the pinch analysis section. A biogas (65% methane, 35% carbon dioxide) production rate of 117 m^3/d in stream 7 was calculated and used to find the feed rate of 190 kg/d in stream 19. Stream 19 is made up of 12% solids with liquids making up the remainder. A detailed material balance along with all assumptions can be found in Appendix D.

5.5 Application of Heat Pinch Analysis

5.5.1 Data Extraction

5.5.1.1 Identifying Hot & Cold Streams

Identifying hot and cold streams is one of the first steps when applying pinch analysis. The hot and cold streams are identified once the supply and target temperatures are determined. According to Kemp (2007), streams that need to be heated are classified as cold streams whilst those that need cooling are classified as hot streams. Table 26 is constructed to identify the hot and cold streams and presents the basic data required for heat pinch analysis. Data in Table 26 was extracted from the table in Appendix E. The CP is calculated by multiplying the stream mass flow rate with its Cp.

It is worth noting that streams 12/12.1 & 18/18.1 as presented in Table 26 are one stream that is split into two for the analysis. Kemp (2007) advises that the stream Cp should be re-evaluated since the Cps change significantly when stream components have a change in phase.

Table 26: Hot & Cold Stream Classification

Stream No	Heat Capacity Flow Rate ($kW/℃$)	Supply Temperature (℃)	Target Temperature (℃)	Stream Description
5	0.2499	80	100	Cold
6	0.00572	80	20	Hot
12	0.0146	20	100	Cold
12.1	0.0066	100	400	Cold
14	0.0076	400	500	Cold
15	0.029	500	80	Hot
16	0.0029	80	20	Hot
18	0.0644	400	108.6	Hot
18.1	0.1617	108.6	80	Hot
19	0.3149	20	55	Cold
20	0.132	540	134	Hot
24	0.0312	90	20	Hot
25	0.4262	20	100	Cold
26	0.0502	20	80	Cold
27	0.1129	100	20	Hot

5.5.1.2 Minimum Approach & Shifted Temperatures

According to March (1998), initial ΔT_{min} values for the chemical industry are typically within the range of 10-20 ℃. As a result, 10 ℃ has been assumed. The hot and cold stream temperatures were converted to shifted temperatures using the formulas provided below, the results of which can be found in Table 27.

- $Shifted\ Hot\ Temperature = Normal\ Hot\ Temperature - \frac{\Delta Tmin}{2}$ Eq 5-4
- $Shifted\ Cold\ Temperature = Normal\ Cold\ Temperature + \frac{\Delta Tmin}{2}$ Eq 5-5

Both the CCs & PTA methods are used in Section 5.5.2 to set the energy targets. Kemp (2007) notes that the PTA is used for setting the targets algebraically. In doing so, within each interval, hot and cold streams will need to be at least ΔT_{min} apart. Hence the introduction of shifted temperatures.

Table 27: Shifted Stream Temperatures

Stream No	Shifted Supply Temperature (℃)	Shifted Target Temperature (℃)
5	85	105
6	75	15
12	25	105
12.1	105	405
14	405	505
15	495	75
16	75	15
18	395	103.6
18.1	103.6	75
19	25	60
20	535	129
24	85	15
25	25	105
26	25	85
27	95	15

5.5.2 Energy Targeting

The following figure constructed by adding the enthalpy changes of the streams in the respective temperature intervals using Microsoft Excel is a representation of the CCs used to set energy targets for the hybrid system. It can be observed that all cold streams can be satisfied using process heat whilst the hot composite curve requires roughly 43.86 kW external cooling. The PTA method found in Appendix F agrees with this external cooling requirement using a ΔT_{min} of 10 ℃.

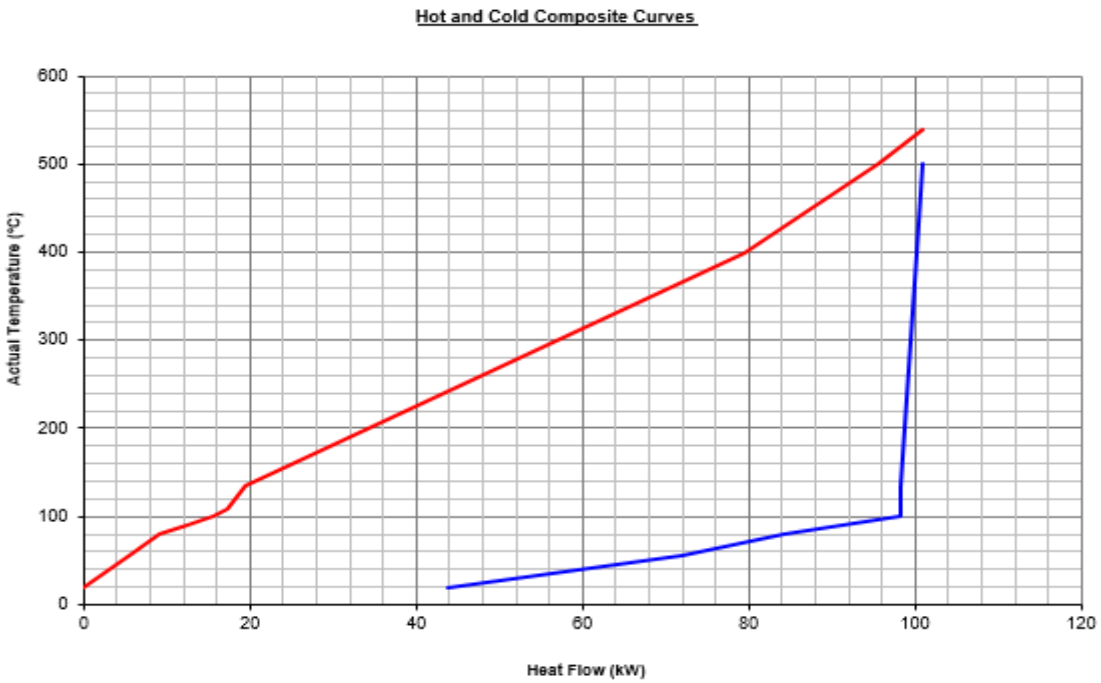

Figure 23: Composite Curve

5.5.3 Grid Diagram

Aspen Energy Analyzer was used to construct the GD, a representation of the HEN. On the *GD*, hot streams run horizontally from left to right decreasing in temperature whilst cold streams run horizontally below from right to left increasing in temperature. Heat transfer between matched streams is indicated using vertical lines joined by circles. The vertical lines indicate stream matching and are therefore a representation of the heat exchangers. Using a ΔT_{min} of 10 ℃, the resulting network is made up of 12 exchangers, having an unsatisfied cooling requirement of 43.86 kW with a hot and cold pinch located at 540 & 530℃ respectively.

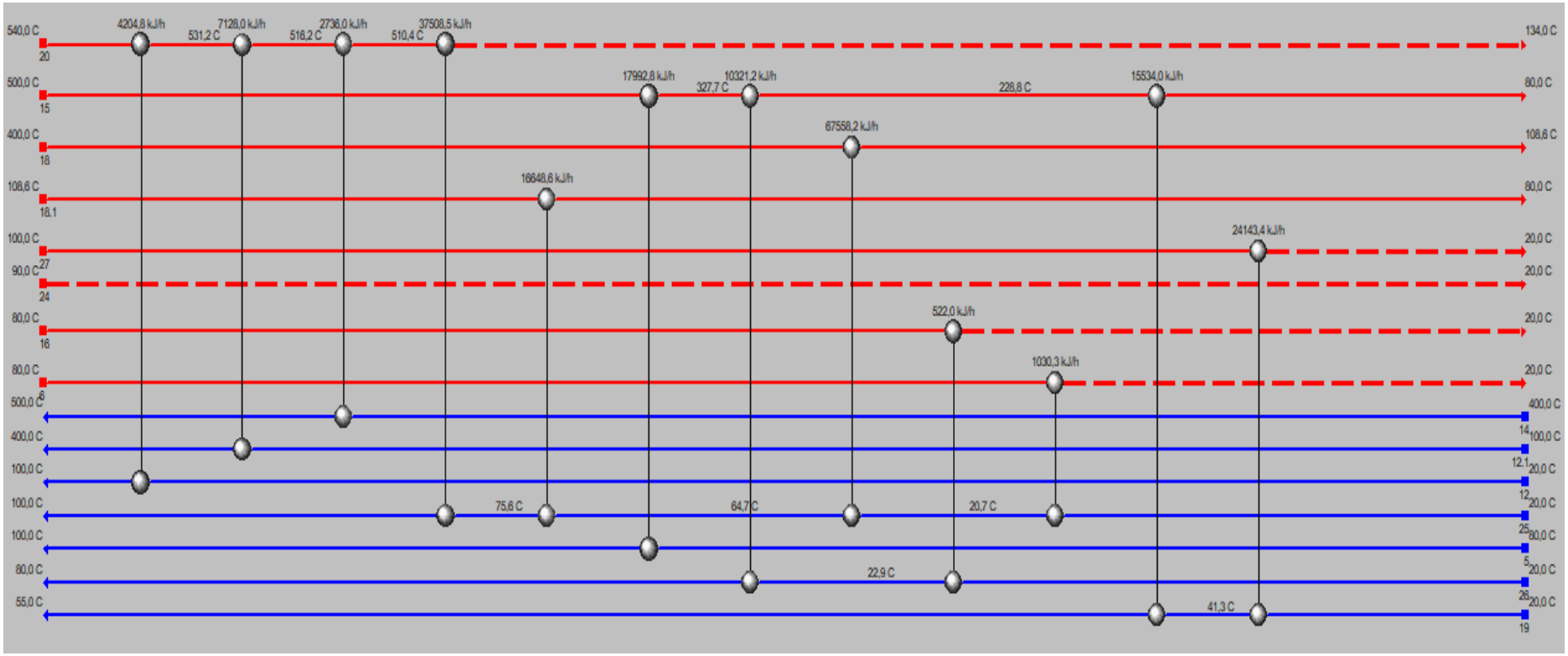

Figure 24: Final HEN

Only 12 heat exchangers were required to satisfy all the cold streams of the hybrid system using pinch analysis, whereas 19 exchangers were used for the original thermochemical process (no application of heat pinch analysis). The original process presented by Naterer *et al* (2011b) can be found in Appendix G. Hence, heat pinch analysis has shown its ability to reduce capital costs by reducing the number of units in the HEN.

The tables in Appendix H show that the unsatisfied cooling requirements amount to 43.86 kW which corresponds with the energy targets of the CCs and PTA; hence the GD presents the maximum energy recovery between streams.

No pinch lines are visible on the grid diagram since this is a threshold problem. Threshold problems occur if only one utility (heating or cooling) is required whilst the other utility is reduced to zero. Hence, this HEN is designed from the zero-utility end.

Cooling utilities were not included since this is an isolated hybrid system and any inclusion of external cooling will have significant cost implications.

Since many of the cold streams have an assumed temperature of 20℃, the lowest temperature any hot stream could reach is 30℃ thereby ensuring the minimum temperature difference. This holds true for streams 20, 27, 24, 16 & 6. This could be solved by reducing the minimum temperature difference or using an external cooling utility. However, reducing the temperature difference will increase the cost of the HEN, and introducing an external utility other than water will increase the costs significantly. Additionally, reducing those streams to 20℃ is not significant.

Unsatisfied streams were considered acceptable for the reasons listed below.

- Stream 20: The molten salt was not cooled any further since it will need to be heated by the solar collector to its supply temperature of 540℃ and hence will only need to be heated from 431.5℃ to 540℃.
- Stream 27: This stream will be heated to produce steam. Any additional cooling will require more heat for phase change and therefore was considered counter productive. It is assumed that by mixing stream 27 & 11, the output stream 12 will be at approximately 20℃.
- Stream 24: Exhaust air/water from the FC and therefore does not need any cooling since it will likely be expelled to the environment. However, since its flow is 0.195 mol/s which is equivalent to the freshwater feed in stream 11, therefore it could be used to supplement the feed. With stream 27 entering at 40.6℃ and stream 24 at 90℃, less heat will be required to convert stream 12 to steam. Alternatively, stream 24 can be used to supplement the 0.667 mol water/s in stream 26 feeding the village.
- Stream 16: Oxygen stream for storage. Its final temperature of 30 ℃ was not considered a hazard for storage. It could also be released to the atmosphere and hence does not need to be cooled any further.

- Stream 6: The hydrogen stream temperature of 30 ℃ was considered acceptable since the FC is maintained at 90 ℃.

A problem arises considering that the biogas plant should operate during off-peak periods. The biomass feed in stream 19 is heated to 55℃ using the solar thermochemical plant. Consequently, during the periods that the two plants are not operating simultaneously, the biomass feed in stream 19 cannot be heated. The implication being that the biogas plant will operate using a mesophilic temperature range and hence the yield will be reduced, and more biomass will need to be fed to maintain a constant output. One option is to use the stored biogas to heat the feed. However, producing biogas in excess to heat the feed will still require more biomass feed.

Several storage options are available which include storing molten salts, hydrogen, biogas, and electricity. Either of these storage options excluding biogas for the reason discussed above, if employed, can be used to heat the feed of the process. During winter periods, when solar is limited, the biogas plant will need to run at lower yield should the solar plant not be operating. Storage, if employed can be used to heat the biogas feed, but unlikely since stored energy will need to be used during emergencies and very low solar radiation. Molten salts could potentially be stored considering that the temperature of the stream is only reduced to 431.5℃. Hence, this stream can be used to heat the biogas plant during off-peak periods.

Appendix I provides the schematic of the hybrid plant before pinch analysis was applied. The plant before heat pinch analysis found in Appendix I can now be integrated using the GD as shown in Section 5.6.

5.6 Final Plant PFD & Description

Integrating the process provided in Appendix I by applying heat pinch analysis brings about the modified process as presented by Figure 25 below.

The process is initiated by feeding $CuCl\ (aq)$ & $HCl\ (aq)$ via stream 1 to the anode compartment of the electrolyzer, operating between 25-100℃. Coupled with this feed is additional, albeit recycled $HCl\ (aq)$ in stream 2 that is fed at 80℃ to the cathode compartment.

Electrolysis products $H_2(g)$ & $HCl(aq)$ flows in stream 4 before being fed to separator 1 wherein the liquid-gas mixture is separated into streams 6 & 8 respectively. $HCl(aq)$ in stream 8 is returned to mixer 1 whilst stream 6 contributes to the heating of stream 25 before feeding the in-line hydrogen storage tank. Note; this is not hydrogen storage capable of overcoming solar intermittency but is used to ensure constant hydrogen flow to the FC and is also capable of housing unreacted recycled hydrogen. Hydrogen is then fed to the FC in stream 22 along with air in stream 23.

Additionally, product $CuCl_2\ (aq)$ leaves the electrolyzer at 80℃ and fed to the dryer after it has been preheated to 100℃ using stream 15. Air in stream 25 at 20℃ is heated to 100℃ and fed to the dryer to liberate all water from $CuCl_2(aq)$ thereby converting it to $CuCl_2(s)$ which is fed via stream 9 to the hydrolysis reactor.

Hot air is vented, whilst the evaporated water exits into stream 10 wherein it is assumed to be converted to mainly water. Stream 10 is split into streams 27 & 28. Once split, stream 27 assists in heating the biomass feed in stream 19 before being pumped to mixer 2 at 40.6℃ whilst stream 28 is recycled to mixer 1.

Freshwater is fed to mixer 2 along with recycled water from stream 27 is heated in stream 12 & 12.1 from 20 to 400℃ to form steam via stream 20 leaving the solar concentrator at 540℃, before feeding the hydrolysis reactor along with $CuCl_2(s)$ in stream 9. Hydrolysis products $Cu_2OCl_2(s)$, $HCl(g)$ and excess steam in stream 13 is fed to separator 2 with output streams 14 and 18. $Cu_2OCl_2(s)$ in stream 14 is heated to 500℃ using the molten salts stream 20 whilst $HCl(g)$ and excess steam is cooled using stream 25 before being returned to the cathode compartment at 80℃ in stream 2.

Once heated, stream 14 is fed to the decomposition reactor to produce $CuCl(l)$ & $O_2(g)$ at 500℃ in stream 15. Decomposition products are then used to heat stream 5, 26 and 19 before being fed at 80℃ to separator 3 to produce $O_2(g)$ in stream 16 and $CuCl(l)$ in stream 17. Stream 17, containing $CuCl(l)$ is recycled back to mixer 1 whilst stream 16 assists in heating the hot water stream 26 before being stored or vented.

Stream 26 is a freshwater line that is heated using stream 15 & 16 from 20 to 80℃ to be used as hot water by the villagers.

The biogas plant starts with grinding of the solid biomass feedstock and then fed to a mixer which is also fed with manure, waste crops, and sweet sorghum. The mixture leaves the mixer in stream 19 at 20℃ and is heated using streams 15 & 27 to its target temperature of 55℃ before feeding the digester. The resultant digestate can be used as fertilizer whilst the biogas is fed to gas treatment via stream 7 and then to an electric generator that, along with the FC feeds electricity into the electricity header that supplies electricity to the village. Furthermore, a stream legend for all numbered streams is included in Appendix N.

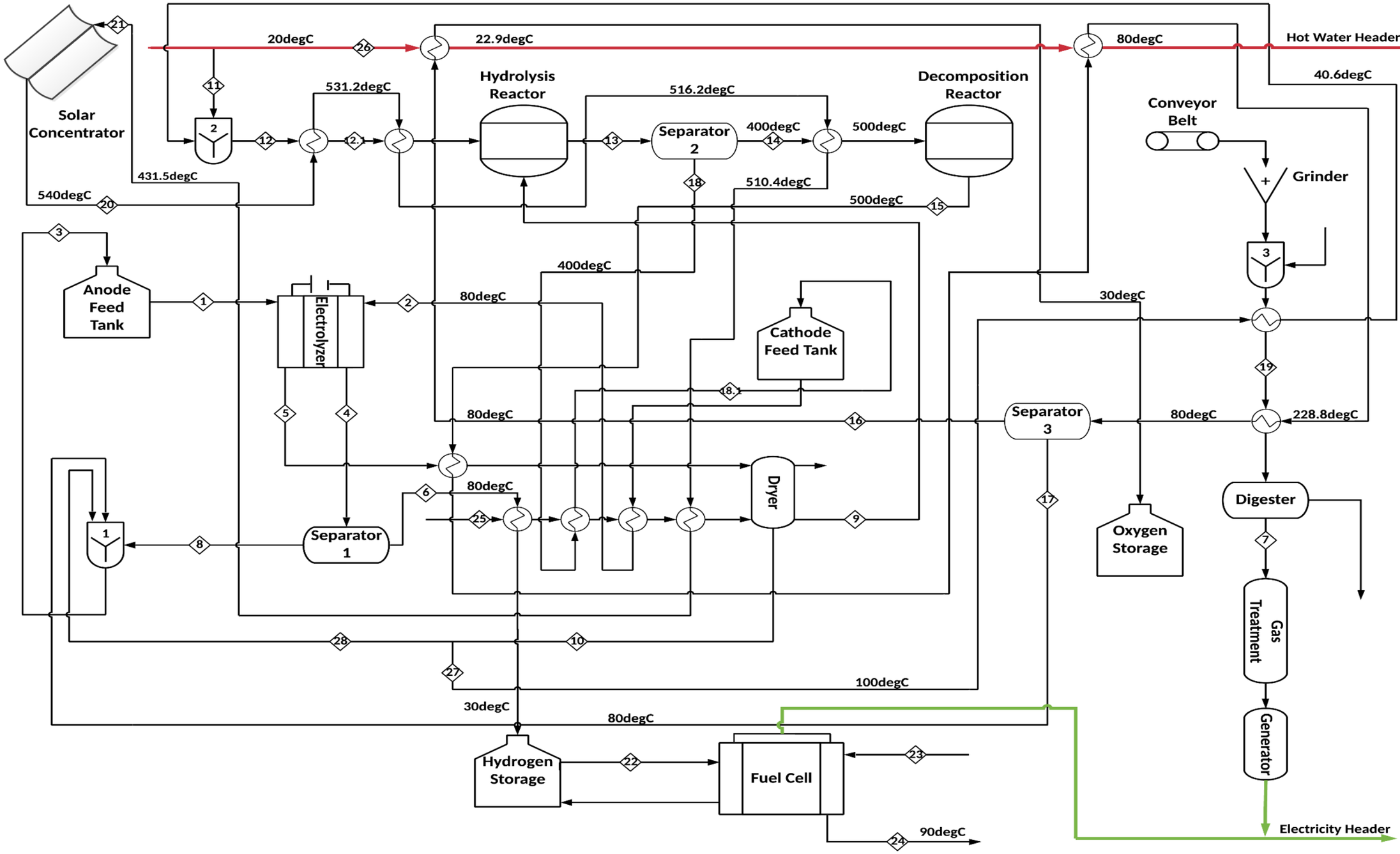

Figure 25: Final Integrated Plant Schematic

5.7 Application of Power Pinch Analysis (PoPA)

The PCT with modified operating times is presented below whilst the original can be found in Appendix J. The MOES & AEEND was found to be 94.8 & 107 kWh respectively as highlighted in yellow with surplus energy amounting to 12 kWh.

Table 28: Modified PCT

1	2	3	4	5		6	7	8	9	10	11	12
Time (h)	Time Interval Duration (h)	Source		Power Rating (kW)					Start up		Operation	
		Biogas (35kW)	Solar (30kW)	Source kW	Demand kW	Source kWh	Demand kWh	Net Electricity (kWh)	Infeasible Cascade (kWh)	Feasible Cascade (kWh)	Infeasible Cascade (kWh)	Feasible Cascade (kWh)
0									0	94.81	94.81	94.81
	1			0		0	8.44	-8.44				
1									-8.44	86.37	86.37	86.37
	1			0		0	12.53	-12.53				
2									-20.97	73.84	73.84	73.84
	1			0		0	15.19	-15.19				
3									-36.16	58.65	58.65	58.65
	1			0		0	13.28	-13.28				
4									-49.44	45.37	45.37	45.37
	1			0		0	8.17	-8.17				
5									-57.61	37.2	37.2	37.2
	1			0		0	5.43	-5.43				
6									-63.04	31.77	31.77	31.77
	1			0		0	5.7	-5.7				
7									-68.74	26.07	26.07	26.07
	1			0		0	7.27	-7.27				
8									-76.01	18.8	18.8	18.8
	1			0		0	7.61	-7.61				
9									-83.62	11.19	11.19	11.19
	1			0		0	6.24	-6.24				
10									-89.86	4.95	4.95	4.95
	1			0		0	4.95	-4.95				
11									-94.81	0	0	0
	1			30		30	4.88	25.12				
12									-69.69	25.12	60.12	60.12
	1			30		30	5.09	24.91				
13									-44.78	50.03	85.03	85.03
	1			30		30	5.3	24.7				
14									-20.08	74.73	109.73	109.73
	1			65		65	8.63	56.37				
15									36.29	131.1	131.1	131.1
	1			65		65	16.89	48.11				
16									84.4	179.21	179.21	179.21
	1			65		65	27.2	37.8				
17									122.2	217.01	217.01	217.01
	1			0		0	30.34	-30.34				
18									91.86	186.67	186.67	186.67
	1			0		0	26.45	-26.45				
19									65.41	160.22	160.22	160.22
	1			0		0	19.08	-19.08				
20									46.33	141.14	141.14	141.14
	1			0		0	12.46	-12.46				
21									33.87	128.68	128.68	128.68
	1			0		0	9.18	-9.18				
22									24.69	119.5	119.5	119.5
	1			0		0	6.73	-6.73				
23									17.96	112.77	112.77	112.77
	1			0		0	5.97	-5.97				
24									11.99	106.8	106.8	106.8

In constructing the SCT below, the maximum transferrable energy in each time slot was found whilst no energy can be stored during 4-5 pm with maximum storage for start-up and operation of 217 kWh.

Table 29: SCT

1	2	3	4	5	6	7	8	9	10	11	12	13
Time (h)	Time Interval Duration (h)				Start Up				Operation			
		Source (kWh)	Demand (kWh)	Amount of electricity Transfer (kWh)	Net Electricity (kWh)	Storage Capacity (kWh)	Outsourced Electricity Needed (kWh)	Outsourced Power Rating (kW)	Net Electricity (kWh)	Storage Capacity before limit (kWh)	Storage Capacity with limit (kWh)	Excess Power source wasted (kWh)
0										106.8	106.8	
	1	0	8.44	0	-8.44		-8.44	8.44	-8.44	98.36	98.36	
1												
	1	0	12.53	0	-12.53		-12.53	12.53	-12.53	85.83	85.83	
2												
	1	0	15.19	0	-15.19		-15.19	15.19	-15.19	70.64	70.64	
3												
	1	0	13.28	0	-13.28		-13.28	13.28	-13.28	57.36	57.36	
4												
	1	0	8.17	0	-8.17		-8.17	8.17	-8.17	49.19	49.19	
5												
	1	0	5.43	0	-5.43		-5.43	5.43	-5.43	43.76	43.76	
6												
	1	0	5.7	0	-5.7		-5.7	5.7	-5.7	38.06	38.06	
7												
	1	0	7.27	0	-7.27		-7.27	7.27	-7.27	30.79	30.79	
8												
	1	0	7.61	0	-7.61		-7.61	7.61	-7.61	23.18	23.18	
9												
	1	0	6.24	0	-6.24		-6.24	6.24	-6.24	16.94	16.94	
10												
	1	0	4.95	0	-4.95		-4.95	4.95	-4.95	11.99	11.99	
11												
	1	30	4.88	4.88	25.12	25.12			25.12	37.11	37.11	
12												
	1	30	5.09	5.09	24.91	50.03			24.91	62.02	62.02	
13												
	1	30	5.3	5.3	24.7	74.73			24.7	86.72	86.72	
14												
	1	65	8.63	8.63	56.37	131.1			56.37	143.09	143.09	
15												
	1	65	16.89	16.89	48.11	179.21			48.11	191.2	191.2	
16												
	1	65	27.2	27.2	37.8	217.01			37.8	229	217.01	11.99
17												
	1	0	30.34	0	-30.34	186.67			-30.34	198.66	186.67	
18												
	1	0	26.45	0	-26.45	160.22			-26.45	172.21	160.22	
19												
	1	0	19.08	0	-19.08	141.14			-19.08	153.13	141.14	
20												
	1	0	12.46	0	-12.46	128.68			-12.46	140.67	128.68	
21												
	1	0	9.18	0	-9.18	119.5			-9.18	131.49	119.5	
22												
	1	0	6.73	0	-6.73	112.77			-6.73	124.76	112.77	
23												
	1	0	5.97	0	-5.97	106.8			-5.97	118.79	106.8	
24												
						Total External Requirment during Start Up	-94.81					

It is worth noting that the operating times were chosen to ensure the lowest AEEND>MOES is achieved before grid electricity is required. This was done since there is no electrical grid in the chosen location. Once MOES<AEEND, external power sources will be required.

Introducing the PCT, highlighted the fact that the initial operating hours as assumed in Section 5.3 has a significant energy surplus. Although, the assumption in Section 5.3 to use supply capacities greater than the peak energy demands in each interval is still considered a reasonable one. Constructing a PCT based on the original operating times resulted in an energy surplus of 586.99 kWh as shown in Appendix J whereas the modified PCT as presented by Table 28 only had a surplus of 12 kWh. This demonstrates the significance of applying PoPA in power systems.

As is, the hybrid plant is oversized considering that the operating times for the solar and biogas plant were significantly reduced to only 6 and 3 hours a day respectively, once PoPA was applied. Srinvas & Reddy (2014) recommends against on/off cycling of the biogas plant since it requires a longer period to start. Instead, part-load operating conditions should be employed to ensure 24-hour operation of the biogas plant. Furthermore, on/off cycling will require a larger sized biogas plant whilst 24-hour operation will require a smaller sized plant without significantly affecting the availability of feedstock.

However, the hybrid system may not be oversized and can potentially subscribe to having a biogas plant operating 24-hours with its current assumed capacity. Firstly, the PoPA tool assumes 100% efficiency for power transfer and storage with an error of 15-25% to account for losses. Moreover, electrical components such as the electrolyzer, pumps, valves, flow meters, etc, will need to use power and hence may require additional operating times compared to the current PoPA proposed operating times. Furthermore, the introduction of a power source may attract neighbouring villagers which would increase demand.

Many power capacity iterations were performed to ensure that the biogas plant operates continuously assuming 100% efficiency whilst maintaining equal plant capacities. In doing so, it was found that dual 10 kW plants were the minimum capacities achievable to allow continuous operation of the biogas plant whilst maintaining AEEND>MOES. The PCT can be found in Appendix K with excess energy of 26.99 kWh.

However, assuming the solar plant is not operating due to weather constrictions or maintenance, the biogas plant will need to run continuously to satiate the demand. Constructing the PCT in Appendix L highlights the minimum rated capacity at 12 kW for the biogas plant whilst maintaining the minimum AEEND>MOES. Therefore the 10 kW biogas plant will not suffice. As a result, the solar plant can be rated at a minimum of 1 kW to satisfy the needs of the village. However, this is considered a waste of resources and capital.

Therefore, as suggested in Appendix M, the biogas plant is rated at 12 kW to ensure sustainable electricity during periods when the solar plant experiences downtime and the solar plant at 10 kW.

However, the biogas plant output can be manipulated via cycling to operate at a minimum of 1 kW during periods of high solar radiation thus achieving continuous operation. This generates a surplus of 8.99 kWh. It is worth noting that PoPA assumes 100% efficiency whilst disregarding energy requirements within the plant thus is still considered preferable to oversize the plant. Therefore, the original plant capacity can hold, and the plant can be cycled to assume the operating profile of the PCT in Appendix M with the capability of varying supply pending the demand. Alternatively, as with Appendix K, both plants can be cycled (not sized) to 10 kW each and hence achieve the minimum capacities required.

Alternatively, instead of cycling excess energy can be sold. It is assumed that there are no transmission lines in the area. However, car batteries used for cell phone charging and lighting is typical of rural homesteads. Therefore, excess electricity can be sold by charging car batteries of neighbouring villages. Any additional surplus will need to be limited by ramping down biogas input and output or vented in the form of hydrogen.

Although not included in this study, storage options will need to be included to account for the MOES during start-up and operation. The specified storage capacity of 217 kWh will hold for all cycling scenarios.

Furthermore, all Appendix PCTs are constructed with no cascade for operation since this will remain the same as the feasible cascade for start-up if AEEND>MOES.

5.8 Evaluation of Process Economics

5.8.1 Estimation of Capital Costs

The following section provides an estimate of the capital costs associated with the hybrid system. CAPCOST was used to apply the bare module costing technique to compute the TMC, TGRC and fixed capital costs in this section, whilst the detailed results can be found in Appendix O. It is worth noting that the costs for piping instrumentation, pumps and plant layout were not considered while the raw material costs were assumed as a capital cost since it is recycled and only requires a one-time start-up cost.

Table 30: Hybrid System Capital Costs

Equipment Type	Equipment Identification	Purchased Cost ($)	Bare Module Cost ($)
Reactor	Hydrolysis Reactor	69 227	276 908
	Decomposition Reactor	27 983	111 932
	Digester	54 454	217 816
Holding/Storage Tank	Anode Feed Tank	8 480	164 156
	Cathode Feed Tank	8 480	164 156
	Hot Molten Salt Tank	8 480	67 078
	Cold Molten Salt Tank	8 480	67 078
	Hydrogen Storage	8 480	67 078
	Oxygen Storage	8 480	67 078
	Gas Treatment Tank	8 480	67 078
Fuel Cell	PEM Fuel Cell	106 110	306 658
Generator	Biogas Generator	14 000	41 580
Electrolyzer	Electrolyzer	9 000	26 730
Mixing Tank	Mixer 1	165 121	227 867
	Mixer 2	132 532	182 894
	Mixer 3	40 055	55 276
Separator	Separator 1	9 824	200 673
	Separator 2	2 247	6 428
	Separator 3	4 775	37 771
Dryer	Dryer	45 575	72 920
Heat Exchanger (12)	Heat Exchanger	40 284	260 326
CSP	Parabolic Trough Concentrator	365 322	456 653
Total Purchased Cost (P_c)		1 145 869	
Total Bare Module (C_{BMT})			3 146 134
Total Module Cost (TMC)=1.18C_{BMT}			3 712 438
Total Grass Roots Cost (TGRC)= TMC+0.25C_{BMT}			4 498 972
Initial CuCl Cost			93 593
Initial HCl Cost			6 008
Total Initial Raw Material Cost			99 601
Fixed Capital Investment Excluding Land (FCI_L)			4 598 573
Fixed Capital Investment Including Land (FCI)			4 658 573

Additional inaccuracy was introduced into the capital cost estimate since CAPCOST restricted the capital costing to a minimum allowable sizing parameter. Consequently, units with a sizing parameter less than the minimum were oversized and hence costed more. All heat exchangers were sized with an area of 1 m^2 since this was the minimum allowable area whilst the actual heat transfer areas were less than 1 m^2. The double pipe heat exchanger was chosen over the shell & tube since the latter has a

minimum area of 10 m^2 and therefore would have cost significantly more. The oversizing of the double pipe heat exchangers was considered acceptable since it could account for potential fouling. Two of the exchangers were designed using titanium since it is in contact with HCl. Sandler & Luckiewicz (1987) as cited in Turton *et al* (2013) recommend the use of titanium when in contact with HCl.

Similarly, the anode feed tank, cathode feed tank, and separator 1 were costed using titanium. The storage tank option in CAPCOST was not chosen to size the above storage tanks since it does not consider the materials it is in contact with. Hence, the vessel option in CAPCOST was used as a storage tank to better account for the chemicals it houses. Additionally, storage tanks were not chosen since it had a minimum allowable volume of 100 m^3 which would take up significantly more space than the tanks sized at 3 m^3.

Purchase costs per kW for the FC, electrolyzer & biogas generator was obtained from the vendor cost since CAPCOST did not have costing data for this equipment. Battelle Memorial Institute (2017) reported an FC cost of $3537/kW whilst the Office of Energy Efficiency & Renewable Energy (2019) reported an electrolyzer cost of $300/kW. An electrolyzer output of 30 kW was assumed to correspond with that of the FC. AP Electric & Generators (2019) advertised a 35 kW biogas generator for $14 000 which was used for the purchased prices. The purchased costs of this equipment were potentially not at base conditions; however, it was considered insignificant. Hence, it was used as the purchased cost at base conditions, thus the need for a bare module factor. The bare module factor was assumed for this equipment taking into account the cost multipliers for equipment, materials, labour, freight, overhead, and engineering. Bare module factors can be found in Appendix O.

The drum dryer area of 0.5 m^2 was assumed based on the vendor's, Feeco International (2019) area/output specifications. Initially, a spray dryer was chosen to be used in this study however, CAPCOST only allowed for the drum dryer to account for liquid-like slurries and suspensions. Consequently, the drum dryer was used.

According to Energy.Gov (2019), CSP is usually 40-50% of the total bare module costs of a CSP plant. However, this consists of a concentrator, two working fluid tanks, a water feed tank, and a turbine. This study contains more major equipment therefore, the solar concentrator is estimated at 15% of the total bare module costs. Rahbari *et al* (2018) listed a parabolic trough solar bare module factor of 1.25 which was used to calculate the purchased cost. The US Department of Energy (2012) reported the cost of a solar concentrator at \$75/ m^2. Land requirement for the solar concentrator was estimated at 0.16 m^2 resulting in a concentrator cost of \$46. This cost was considered unreasonable hence it was estimated at 15% of the bare module costs.

The cost of oxygen storage was included, although it may not be necessary. It could be sold; however, it was assumed infeasible due to the distribution costs. Stored oxygen could be fed to the FC which

could increase its lifespan and reduce maintenance costs since the particulates in the air could foul the FC.

Raw material costs were included in the capital costs since raw materials are recycled and only a one-time cost is required for start-up. Only the cost of make-up is included in the manufacturing costs. Ghandehariun *et al* (2010) stated that the nitrate mixture used as the heating fluid is inexpensive and hence was neglected since it was considered insignificant relative to the large capital cost. Again, it was considered a capital cost since it is a recycled mixture.

Capital costs could potentially be lowered since certain units had to be oversized to be accommodated on CAPCOST. However, to get a more accurate estimate, the plant should be scaled to a capacity wherein all sizing parameters are included in CAPCOST and all units at its relative sizes are available from vendors.

Holding tanks for the hot and cold molten salts as shown in Figure 17 were included in the cost estimate, although it is not included in the final PFD. It was not included since the holding tanks & concentrator were considered as one unit on the PFD. Hot molten salts from these tanks can feed the biogas heat exchangers during times when the solar plant is not operating.

5.8.2 Estimation of Manufacturing Costs

An estimate of the manufacturing costs is provided below by employing the equations given by Turton *et al* (2013) as presented in Section 4.8.2. Consequently, the affordability of the process was identified by determining the cost per kWh.

Table 31: Hybrid System Manufacturing Costs

Cost Type	Symbol	Unit Cost	Amount ($/y)
Cost of Operating Labour	C_{OL}	$\$338/month.operator$	64 896
Cost of Utilities	C_{UT}	0	0
Cost of Waste Treatment	C_{WT}	0	0
Cost of Raw Materials (Make-Up)	C_{RM}	\$84.2 $CuCl/kg$	5 736
		\$17.6 HCl/l	360
FCI (\$)			4 658 600
$COM = 0.280FCI + 2.73C_{OL} + 1.23(C_{UT} + C_{WT} + C_{RM})$			1 489 000
$COM_d = 0.180FCI + 2.73C_{OL} + 1.23(C_{UT} + C_{WT} + C_{RM})$			1 023 000
$\$/kWh = COM/kWh/y$			3
$\$/kWh = COM_d/kWh/y$			2

According to Turton *et al* (2013), the equation used for estimating operating labour should not be used when dealing with more than 2 solid processing steps. Furthermore, 4.5 operators are hired for every 1 operator per shift.

Assuming at most 2 processing steps set the number of operators to 53. However, the hybrid system has 5 solid handling steps which would result in significantly more operators. Therefore, for this estimate, the solid processing steps were assumed to be zero. Consequently, the operating labour was set at 16 which appeared more reasonable. Especially, since about only 2 operators are needed at night to feed the biomass whilst the solar plant is shut down.

A typical monthly salary for an operator in the Eastern Cape is R5000 (Jobcrystal, 2019). This monthly figure was considered acceptable for unskilled labour. As of November 2019, the Rand/Dollar exchange rate was found to be R14.81/$1, hence the monthly salary per operator is $338.

Utility costs were set to zero since no utilities are used. Water from the Mzimvubu river is pumped to the plant. Assuming potable water was used at $0.26/1000 kg (Turton *et al,* 2013), the cost would amount to $127/y which is considered negligible and was not included in the analysis.

Since reactants are recycled in the thermochemical plant, the only waste that is generated is produced as fertilizer in the biogas plant. Generated fertilizer will be used in the village and will not be discarded. Logan & Visvanathan (2019) notes that AD can be used without the need for waste management controls, especially when made for farm use. Hence, waste treatment was set to zero.

The initial cost of raw materials was included in the capital cost estimate since it is being recycled. However, 1% of the make-up was introduced once every 2 months. It was assumed that minimum make-up for reactants was needed since significant leaking was not expected for this completely new plant.

The cost of CuCl per kg & HCl per litre was found to be $84.2 (MERCK, 2019) & $17.6 (SCIENCECompany, 2019) respectively. Raw material costs could have been cheaper if bulk prices were used such as per tonne or cubic metre.

Previously, it has been assumed that a month is 30 days, hence a year for the purposes of calculating the unit cost below is considered as 360 days. It is assumed that the hybrid system operates continuously at its rated capacity whilst the biogas plant operates for 24 hours.

Table 32: Hybrid System Capacity & Generation

Plant	Rated Capacity (kW)	Time Interval (hours)	Electricity Generation (kWh)
Biogas	35	24	840
Solar thermochemical	30	17	510
Total			1350

- $1350\ \frac{kWh}{d} \times \frac{360\ d}{1\ year} = 486\ 000\ kWh/y$ Eq 5-6
- $Cost/kWh(COM) = 1\ 489\ 000/486\ 000 = \$3.06/kWh$ Eq 5-7
- $Cost/kWh(COM_d) = 1\ 023\ 000/486\ 000 = \$2.1/kWh$ Eq 5-8

BusinessTech (2019) reported that the cost of electricity in South Africa amounts to 106.8 cents/kWh which is equivalent to $0.07/kWh. Moreover, the production costs calculated above does not consider any profits. It is clear that the presented hybrid system is costly. However, this outcome was expected since producing electricity via fossil fuels is more affordable than using renewables. Furthermore, current centralized fossil fuel systems have a significant output hence they can be more affordable compared with the plant presented in this study. Many of the units were oversized since small capacities as required by this study do not exist which may have contributed to the significant cost/kWh.

The thermochemical system has demonstrated its benefit in reducing its manufacturing costs by recycling its reactants, using only water and heat as inputs whilst limiting any waste products. Biomass feedstock was not included in the costs since it is assumed to be waste that is collected from the farms and the surrounding area. Additionally, it is clear that the fixed capital investment term in the manufacturing costs has a significant role in determining the unit cost of production since it contributes to more than 80% of the COM& COM_d. Unit costs could potentially be reduced by scaling up production whilst taking advantage of economy of scale. These costs can be further reduced once the cost of FCs and solar collectors are reduced since these two units make up 25% of the bare module costs. These costs are expected to reduce as the production scale of these units increases with the affinity for renewable energy technologies. Moreover, Khan & Arsalan (2016) stated that CSP is more suited for large scale plants. Introducing CSP into this study raised the unit costs since it becomes less economical with lower capacities.

Storage capacity of 217 kWh as specified by the SCT in Section 5.7 has not been included in the capital cost which if included would further increase the unit cost.

It was suggested that the plant be cycled, however, as the output is reduced the product cost per kWh increases. This is more likely to be economic once the system is scaled up to allow for greater output.

PoPA revealed that the process is oversized. Therefore, reducing the plant size to its proper size will reduce the unit cost. Although, there will be an additional error in the estimate considering the limitations of CAPCOST.

CHAPTER 6: CONCLUSION & RECOMMENDATIONS

The conceptual design was initiated by locating a non-grid connected rural setting in South Africa with sufficient renewable energy sources. Government statistics directed the study to Ward 22 as part of the Matatiele local municipality in the Eastern Cape Province which was chosen as the representative rural setting. Biomass and solar-driven renewable power generators were chosen to supply electricity to this rural setting considering the site's biomass and solar resources.

Coupled with AD as the biomass generator, a 4-step hybrid CuCl thermochemical cycle was chosen to operate as the solar generator. The 4-step hybrid CuCl was chosen mainly for its greater thermal efficiency and practical viability when compared with alternative cycles. A PTC was chosen to harness solar energy since it was the most proven, affordable, and capable of achieving the cycle operating temperatures. Moreover, a PEMFC was chosen to convert hydrogen from the thermochemical process into electricity since it was found to be the most promising and advanced FC technology.

An average monthly household power usage of 210 kWh for newly electrified rural homesteads was used to estimate the monthly village requirement of 8190 kWh. The requirement was then used to construct a power load profile which assisted in the initial plant capacity estimation. Consequently, the AD and solar plant capacity were estimated at 35 and 30 kW respectively.

Applying heat pinch analysis using an assumed ΔT_{min} of 10℃ achieved a cooling utility requirement of 43.86 kW and no heating requirement. The cooling requirement was considered insignificant; hence 5 streams were accepted as unsatisfied. Most importantly, the total number of heat exchangers from the original process diagram was reduced from 19 to 12 once heat pinch analysis was applied whilst pinch analysis integrated the two power generators for improved heat distribution.

Introducing PoPA highlighted the importance of proper plant sizing, plant operating times, and consequent associated electricity surplus. PoPA revealed an energy surplus of 587 kWh using the envisioned plant capacity and operating times given. Consequently, plant cycling was adopted and used alongside the PoPA tool, resulting in a minimum energy surplus of about 9 kWh. The iterative application of PoPA ensured that the hybrid hub can supply sustainable electricity to the village during periods of low solar radiation.

The study was limited by maintaining constant solar radiation, hence varying solar radiation levels based on the weather patterns of the chosen location would provide greater insights into the applicability of the hybrid system. Furthermore, ideally, PoPA had to be applied when initially determining the initial of the plant. In doing so, component flows would have been reduced and heat pinch analysis may have been improved. However, its application at the end has emphasized its importance in plant cycling, whilst the additional plant capacity was accepted to accommodate additional demand and energy losses.

The cost analysis revealed a unit cost of $3/kWh & $2/kWh with and without depreciation, respectively. Hence, the system cannot be considered as cost-effective. However, as a recommendation for future

studies, scaling up the capacity could reduce errors in the estimate. Furthermore, increasing the capacity of the system will take advantage of economy of scale which will reduce the unit cost.

Further studies, using PoPA, could address the energy losses during transport and storage to improve the accuracy of electricity distribution. Despite the practical feasibility of applying heat pinch, an ASPEN simulation could further demonstrate the technical feasibility of the HEN. To further augment the implications of the results, the cost improvements in reducing the plant size using PoPA and reducing the number of heat exchangers via heat pinch analysis can be illustrated by performing comparative cost analysis. Further research into storage options is also needed since PoPA highlights the need for storage as given by the MOES. Simulating the plant under varying weather patterns will provide more insights into the robustness of the current design.

REFERENCES

1 Abanades, S., Charvin, P., Flamant, G. & Neveu, P. 2006. Screening of water-splitting thermochemical cycles potentially attractive for hydrogen production by concentrated solar energy. *Solar Energy*, 31(2006): 2805-2822

2 Abbasi, T., Premalatha, M., Abbasi, T. & Abbasi, S.A. 2014. Wind energy: Increasing deployment, rising environmental concerns. *Renewable and Sustainable Energy Reviews,31(2014): 270-288*

3 Abdeshahian, P., Lim, J.S., Ho, W.S., Hashim, H. & Lee, C.T. 2016. Potential of biogas production from farm animal waste in Malaysia. *Renewable and Sustainable Energy Reviews 60(2016); 714-723*

4 Abdin, Z. Webb, C.J. & Gray, E.M. 2015. Solar hydrogen hybrid energy systems for off-grid electricity supply: A critical review. *Renewable and Sustainable Energy Reviews, 52(2015): 1791-1808*

5 Acar, C. & Dincer, I. 2019. Review and Evaluation of Hydrogen Production Options for Better Environment. *Journal of Cleaner Production*

6 Adeoye, O. & Spataru, C. 2019. Modelling and forecasting hourly electricity demand in West African countries. *Applied Energy, 242(2019): 311-333*

7 Akikur, R.K., Saidur, R., Ping, H.W. & Ullah, K.R. 2013. Comparative study of stand-alone and hybrid solar energy systems suitable for off-grid rural electrification: A review. *Renewable and Sustainable Energy Reviews*, 27(2013): 738–752

8 Aliyu, A.K., Modu, B. & Tan, C.W. 2018. A review of renewable energy development in Africa: A focus in South Africa, Egypt and Nigeria. *Renewable and Sutainable Energy Reviews, 81(2018): 2502-2518*

9 Andress, R.J., Huang, X., Bequette, B.W. & Martin, L.L. 2009. A systematic methodology for the evaluation of alternative thermochemical cycles for hydrogen production. *International Journal of Hydrogen Energy, 34(2009) 4146-4154*

10 Andwari, A.M., Pesiridis, A., Rajoo, S., Martinez-Botas, R. & Esfahanian, V. 2017. A review of Battery Electric Vehicle technology and readiness levels. *Renewable and Sustainable Energy Reviews*, 78(2017): 414-430

11 AP Electric & Generators. 2019. *30 kW- 38 kW Generators*. https://apelectric.com/liquid-cooled-generator-kw-ratings/30kw-generators-38kw-generators. [18 November 2019]

12 Arnason, B. & Sigfusson, T.I. 2000. Iceland-a future hydrogen economy. *International Journal of Hydrogen Energy*, 25(2000): 389-394

13 Arsalis, A. 2019. A comprehensive review of fuel cell-based micro-combined-heat-and-power systems. *Renewable and Sustainable Reviews, 105(2019): 391-414*

14 Aziz, E.A., Wan Alwi, S.R., Lim, J.S., Manan, Z.A. & Klemes, J.J. 2017. An integrated Pinch Analysis framework for low CO_2 emissions industrial site planning. *Journal of Cleaner Production, 146(2017): 125-138*

15 Balat, M. 2008. Potential importance of hydroge as a future solution to environmental and transportation problems. *International Journal of Hydrogen Energy*, 33(2008): 4013-4029

16 Ball, M. & Weeda, M. 2015. The hydrogen economy-Vision or Reality?. *International Journal of Hydrogen Energy*, 40(2015): 7903-7919

17 Banks, D. & Schaffler, J. 2006. *The potential contribution of renewable energy in South Africa*. Sustainable Energy Climate Project (SECCP)

18 Barnea, J. 1972. Geothermal Power. *Scientific American Vol. 226, No 1 (1972): 70-77*

19 Battelle Memorial Institute. 2017. *Manufacturing Cost Analysis of 100 and 250 kW Fuel Cell Systems for Primary Power and Combined Heat and Power Applications.* https://www.energy.gov/sites/prod/files/2018/02/f49/fcto_battelle_mfg_cost_analysis_100_250kw_pp_chp_fc_systems_jan2017.pdf. [17 November 2019]

20 Bigili, M., Bilirgen, H., Ozbek, A., Ekinci, F. & Demirdelen, T. 2018. The role of hydropower installations for sustainable energy development in Turkey and the world. *Renewable Energy, 126(2018): 755-764*

21 Bioenergy Atlas for South Africa. 2016. *Feasibility.* https://www.dst.gov.za/images/2017/2017_pdfs/Bio-Energy-Atlas_DevV15.pdf. [16 April 2019]

22 Bockris, J. O'M. 2002. The origin of ideas on a Hydrogen Economy and its solution to the decay of the environment. *International Journal of Hydrogen Energy*, 27(2002): 731-740

23 BP. 2018. BP Statistical Review of world Energy. https://www.bp.com/content/dam/bp/business-sites/en/global/corporate/pdfs/energy-economics/statistical-review/bp-stats-review-2018-full-report.pdf. [11 October 2018]

24 BusinessTech. 2019. *South Africa's petrol and electricity prices vs the world.* https://businesstech.co.za/news/energy/306592/south-africas-petrol-and-electricity-prices-vs-the-world/. [25 November 2019]

25 Cavinato, C., Fatone, F., Bolzonella, D. & Pavan, P. 2010. Thermphilic anaerobic co-degestion of catlle manure with agro-wastes and energy crops: Comparison of pilot and full scale experiences. *Bioresource Technology, 101(2010): 545-550*

26 Chan, C.C. 2007. The State of the Art of Electric, Hybrid and Fuel Cell Vehicles. *Proceedings of the IEE*, 95(4): 704-718

27 Chang, R. 2010. *Chemistry*. Tenth Edition. New York: McGraw-Hill.

28 Chew, K.H., Klemes, J.J., Wan Alwi, S.R., Manan, Z.A. & Reverberi, A.P. 2015. Total Site Heat Integration Considering Pressure Drops. *Energies, 8(2015): 1114-1137*

29 Chi, J. & Yu, H. 2018. Water electrolysis based on renewable energy for hydrogen production. Chinese Journal of Catalysis, 39(2018): 390-394

30 Cipollina, A., Di Silvestre, M.I., Giacalone, F., Micale, G.M., Sanseverino, E.R., Sangiorgio, R., Tran, Q.T.T., Vaccaro, V. & Zizzo, G. 2018. A methodology for assessing the impact of salinity gradient power generation in urban contexts. *Sustainable Cities and Society, 38 (2018): 156-173*

31 Cippollina, A., Di Silvestre, M.L., Giacalone, F., Micale, G.M., Riva Sanseverino, E., Sangiorgio, R., Tran, Q.T.T., Vaccaro, V. & Zizzo, G. 2018. A methodology for assessing the impact of salinity gradient power generation in urban contexts. *Sustainable Cities and Society. 38(2017): 158-173*

32 Community Survey. 2016. *Statistical Release*. http://cs2016.statssa.gov.za/wp-content/uploads/2016/07/NT-30-06-2016-RELEASE-for-CS-2016-_Statistical-releas_1-July-2016.pdf. [15 August 2016]

33 Community Survey. 2016. *Statistical Release*. http://cs2016.statssa.gov.za/wp-content/uploads/2016/07/NT-30-06-2016-RELEASE-for-CS-2016-_Statistical-releas_1-July-2016.pdf. [15 April 2018]

34 *Conference*, 31st Aug-3rd September. 2010. United Kingdom.

35 Coscia, K., Nelle, S., Elliot, T., Mohapatra, S., Oztekin, A. & Neti, S. 2013. Thermphysical Properties of $LiNO_3 - NaNO_3 - KNO_3$ Mixtures for Use in Concentrated Solar Power. *Journal of Solar Energy Engineering, 135(2013): 034506-1*

36 Daud, W.R.W., Rosli, R.E., Majlan, E.H., Hamid, S.A.A., Mohamed, R. & Husaini, T. 2017. PEM fuel cell system control: *A review. Renewable Energy, 113(2017): 620-638*

37 Davidson, O. & Mwakasonda, S.A. 2004. Electricity access for the poor: a study of South Africa and Zimbabwe. *Energy for Sustainable Development*. 8(4): 26-24.

38 Department of Energy. 2019. *hydro-power*. http://www.energy.gov.za/files/esources/renewables/r_hydro.html. [15 March 2019]

39 Dincer, I. & Rosen, M.A. 1999. Energy, environment and sustainable development. *Applied Energy*, 64(1999): 427-440.

40 Dodds, P.E., Staffel, I., Hawkes, A.D., Li, F., Grunewald, P., McDowall, W. & Ekins, P. 2015. Hydrogen and fuel cell technologies for heating: A review. *International Journal of Hydrogen Energy, 40(2015): 2065-2083*

41 Douglas, T. 2016. Dynamic modelling and simulation of a solar-PV hybrid battery and hydrogen energy storage system. *Journal of Energy Storage, 7(2016):104-114*

42 Dunpont, V. 2007. Steam Reforming of Sunflower Oil For Hydrogen Gas Production. *Helia*, 30(46): 103-132

43 Eastern Cape Socio Economic Consultative Council. 2017. *Alfred Nzo District Municipality Economic Review & outlook 2017*. https://www.ecsecc.org/documentrepository/informationcentre/alfred-nzo-district-municipality_80763.pdf. [18 April 2018]

44 Eastern Cape Socio Economic Consultative Council. 2017. *Amathole District Municipality Economic Review & outlook 2017*. https://www.ecsecc.org/documentrepository/informationcentre/amathole-district-municipality_74397.pdf. [18 April 2018]

45 Eastern Cape Socio Economic Consultative Council. 2017. *Chris Hani District Municipality Economic Review & outlook 2017*. https://www.ecsecc.org/documentrepository/informationcentre/chris-hani-district-municipality_88299.pdf. [18 April 2018]

46 Eastern Cape Socio Economic Consultative Council. 2017. *Joe Gqabi District Municipality Economic Review & outlook 2017*. https://www.ecsecc.org/documentrepository/informationcentre/joe-gqabi-district-municipality_18472.pdf. [18 April 2018]

47 Eastern Cape Socio Economic Consultative Council. 2017. *OR Tambo District Municipality Economic Review & outlook 2017*. https://www.ecsecc.org/documentrepository/informationcentre/o-r-tambo-district-municipality_34313.pdf. [18 April 2018]

48 Eastern Cape Socio Economic Consultative Council. 2017. *Sarah Baartman District Municipality Economic Review & outlook 2017*. https://www.ecsecc.org/documentrepository/informationcentre/sarah-baartman-district-municipality_63083.pdf. [18 April 2018]

49 Elam, C.C., Padro, C.E.G., Sandrock, G., Luzzi, A., Lindblad, P. & Hagen, E.F. 2003. Realizing the hydrogen future: The International Energy Agency's efforts to advance hydrogen energy technologies. *International Journal of Hydrogen*, 28(2003): 601-607

50 El-Shatter. T.F. Eskandar, M.N. & El-Hagry, M.T. 2002. *Renewable Energy, 27(2002): 479-485*

51 Embadi, A., Gikas, P., Farazaki, M. & Emami, Y. 2016. Salinity gradient energy potential at the hyper saline Urmia Lake-ZarrinehRud River system in Iran. *Renewable Enrgy, 86(2016): 154-162*

52 Energy.GOV. 2019. *Project Profile Low Cost Lightweight Solar Concentrator*. https://www.energy.gov/eere/solar/project-profile-low-cost-lightweight-solar-concentrator. [15 November 2019]

53 Engineering ToolBox. 2003. *Specific Heat and Individual Gas Constant of Gases*. https://www.engineeringtoolbox.com/specific-heat-capacity-gases-d_159.html. [11 July 2019]

54 Engineering ToolBox. 2003. *Specific Heat of Liquids and Fluids*. https://www.engineeringtoolbox.com/specific-heat-fluids-d_151.html. [11 July 2019]

55 Engineering ToolBox. 2004. *Water-Heat Capacity (Specific Heat).* https://www.engineeringtoolbox.com/specific-heat-capacity-water-d_660.html?vA=375&units=C#. [11 July 2019]

56 Engineering ToolBox. 2005. *Hydrogen-Specific Heat.* https://www.engineeringtoolbox.com/hydrogen-d_976.html. [10 July 2019]

57 Engineering ToolBox. 2005. *Nitrogen-Specific Heat*. https://www.engineeringtoolbox.com/nitrogen-d_977.html. [11 July 2019]

58 Engineering ToolBox. 2005. *Oxygen Gas-Specific Heat*. https://www.engineeringtoolbox.com/oxygen-d_978.html. [11 July 2019]

59 Engineering ToolBox. 2005. *Water Vapor-Specific Heat*. https://www.engineeringtoolbox.com/water-vapor-d_979.html. [11 July 2019]

60 Erdinc, O. & Uzunoglu, M. 2012. Optimum design of hybrid renewable energy systems: Overview of different approaches. *Renewable and Sustainable Energy Reviews, 16(2012): 1412-1425*

61 Eskom. 2017. Coal Power. http://www.eskom.co.za/AboutElectricity/ElectricityTechnologies/Pages/Coal_Power.aspx [15 August 2017]

62 Eskom. 2019. *Biomass Power*. http://www.eskom.co.za/AboutElectricity/ElectricityTechnologies/Pages/Biomass_Power.aspx. [13 March 2019]

63 Esposito, G., Frunzo, L., Giordano, A., Liotta, F., Panico, A. & Pirozzi, F. 2012. Anaerobic co-digestion of organic wastes. Rev Environ Sci Biotechnol, 11(2012): 325-341

64 Esteban, M. & Leary, D. 2012. Current developments and future prospects of offshore wind and ocean energy. *Applied Energy, 90(2012): 128-136*

65 Esteban, M. & Leary, D. 2012. Current developments and future prospects of offshore wind and ocean energy. *Applied Energy, 90(2012): 128-136*

66 Feeco International. 2019. *Rotary Dryers*. https://feeco.com/rotary-dryers/. [16 November 2019]

67 Fennel, L.P. & Boldor, D. 2014. Dielectric and Thermal Properties of Sweet Sorghum Biomass. *Journal o Microwave Power and Electromagnetic Energy, 48(4): 244-260*

68 Funk, J. 2001. Thermochemical hydrogen production: past and present. *Hydrogen Energy*, 26(2001): 185-190

69 Ghandehariun, S., Naterer, G.F., Dincer, I. & Rosen, M.A. 2010. Solar thermochemical plant analysis for hydrogen production with copper-chlorine cycle. *International Journal of Hydrogen Energy*, 35(2010): 8511-8520

70 Ghazi, T.I.M. & Nasir, I.M. 2017. Maximising Potential of Methane Production from Biogas for Power Generation. *Pertanika J. Science & Technology, 25 (1): 153–160 (2017)*

71 Global Wind Report. 2017. *Global Statuus of Wind Power in 2017*. https://www.researchgate.net/publication/324966225_GLOBAL_WIND_REPORT_-_Annual_Market_Update_2017. [13 March 2017]

72 Graf, D., Monnerie, N., Roeb, M., Schmitz, M. & Sattler, C. 2008. Economic comparison of solar hydrogen generation by means of thermocemical cycles and electrolysis. *International Journal of Hydrogen Energy*, 33(2008): 4511-4519

73 Guney, M.S. 2016. Solar power and application methods. *Renewable and Sustainable Energy Reviews*, 57(2016): 776-785

74 Hefler, F., Lemckert, C & Anissimov, Y.G. 2014. Osmotic power with Pressure Retarded Osmosis: Theory, performance and trends-A review. *Journal of Membrance Science, 453(2014): 337-358*

75 Holladay, J.D., Hu, J., King, D.I. & Wang, Y. 2009. An overviuew of hydrogen production technologies. *Catalysis Today*, 139(2009): 244-260

76 Holladay, J.D., Hu, J., King, D.I. & Wang, Y. 2009. An overviuew of hydrogen production technologies. *Catalysis Today*, 139(2009): 244-260

77 Inci, M. & Turksoy, O. 2019. Review of fuel cells to grid interface: Configurations, technical challenges and trends. *Journal of Cleaner Production, 213(2019): 1353-1370*

78 Intergovernmental Panel on Climate Change. 2018. IPCC Press Release. 13-18

79 International Renewable Energy Agency. 2014.*Tidal Energy Technology Brief.* www.irena.org [24 July 2018]

80 Jia, Z., Wang, B., Song, S. & Fan, Y. 2014. Blue energy: Current technologies for sustainable power generatuion from water salinity gradient. *Renewable and Sustainable Energy Reviews, 31(2014): 91-100*

81 Jobcrystal. 2019. *Salary Survey*. https://jobcrystal.co.za/salary-survey/. [21 November 2019]

82 Kabir, E., Kumar, P. Kumar, S., Adelodun, A.A. & Kim, K. 2018. Solar energy: Potential and future prospects. *Renewable and Sustainable Energy Reviews, 82 (2018): 894-900*

83 Kanan, N. & Vakeesan, D. 2016. Solar energy for future world: - A review. *Renewable and Sustainable Energy Reviews, 62 (2016): 1092-1105*

84 Kaundinya, D.P., Balachandra, P. & Ravindranath, N.H. 2009. Grid-connected versus stand-alone energy systems for decentralized power-A review of literature. *Renewable and Sustainable Energy Reviews*, 13(2009): 2041–2050

85 Kaygusuz, K. 2011. Prospect of concentrating solar power in Turkey: The sustainable future. *Renewable and Sustainable Energy Reviews, 15(2011): 808-814*

86 Kemp, I.C. 2007. *Pinch Analysis and Process Integration-A User Guide on Process Integration for the Efficient Use of Energy*. Second Edition. Oxford: Butterworth-Heinemann

87 Khalid, A., Arshad, M., Anjum, M., Mahmood, T. & Dawson, L. 2011. The anaerobic digestion of solid organic waste. *Waste Management, 31(2011): 1737-1744*

88 Khan, J. & Arsalan, M.H. 2016. Solar power technologies for sustainable electricity generation-A review. *Renewable and Sustainable Energy Reviews*, 55(2016): 414-425

89 Khan, J. & Arsalan, M.H. 2016. Solar power technologies for sustainable electricity generation – A review. *Renewable and Sustainable Energy Reviews, 55 (2016): 414-425*

90 Khan, N., Kalair, A., Abas, N. & Haider, A. 2017. Review of ocean tidal, wave and thermal energy technologies. *Renewable and Sustainable Energy Reviews, 72(2017): 590-604*

91 Khan, N., Kalair, A., Abas, N. & Haider, A. 2017. Review of ocean tidal, wave and thermal energy technologies. *Renewable and Sustainable Energy Reviews, 72(2017): 590-604*

92 King, J. 2008. The king review of low-carbon cars Part II: Recommendations for action. http://www.climatesolver.org/sites/default/files/pdf/bud08_king_1080.pdf. [3 January 2019]

93 Klemes, J.J. & Kravanja, Z. 2013. Forty years of Heat Integration: Pinch Analysis (PA) and Mathematical Programming (MP). *Current Opinion in Chemical Engineering, 2(2013): 461-474*

94 Klemes, J.J., Varbanov, P.S. & Kravanja, Z. 2013. Recent developments in Process Integration. *Chemical Engineering Research and Design, 91(2013): 2037-2053*

95 Klemes, J.J., Varbanov, P.S., Walmsley, T.G. & Jia, X. 2018. New directions in the implementation of Pinch Methodology (PM). *Renewabke and Sustainable Energy Reviews, 98(2018): 439-468*

96 Klemes, J.J., Wang, Q.W., Varbanov, P.S., Zeng, M., Chin, H.H., Lal, N.S., Li, N.Q., Wang, B., Wang, X.C. & Walmsley, T.G. 2020. Heat transfer enhancement, intensification and optimisation in heat exchanger network retrofit and operation. *Renewable and Sustainable Energy Reviews, 120(2020): 109644*

97 Lewis, M.A., Masin, J.G. & O'Hare, P.A. 2009. Evaluation of alternative thermochemical cycles, Part I: The methodology. *International Journal of Hydrogen Energy, 34(2009): 4115-4124*

98 Lloyd, P., Cowan, B. & Mohlakoana, N. 2004. *Improving access to electricity and stimulation of economic growth and social upliftment.*

http://www.erc.uct.ac.za/sites/default/files/image_tool/images/119/Papers-2004/04Lloyd-Cowan-Mohloakana_Improving_access.pdf. [1 April 2019]

99 Logan, M. & Visvanathan, C. 2019. Management strategies for anaerobic digestate of organic fraction of municipal solid waste: Current status and future prospects. *Waste Management & Research, 37(1): 27-39*

100 Loots, I., Van Dijk, M., Barta, B., Van Vuuuren, S.J. & Bhagwan, J.N. 2015. A review of low head hydropower technologies and applications in a South African context. *Renewable and Suustainable Reviews, 50(2015): 1254-1268*

101 Lopez, I., Andreu, J., Ceballos, S., Alegria, I. & Kortabarria, I. 2013. Review of wave energy technologies and the necessary power-equipment. *Renewable and Sustainable Energy Reviews, 27(2013): 413-434*

102 Lovins, A.B. 2005. Twenty Hydrogen Myths. https://d231jw5ce53gcq.cloudfront.net/wp-content/uploads/2017/05/RMI_Document_Repository_Public-Reprts_E03-05_20HydrogenMyths.pdf. [19 February 2019]

103 Mamphweli, N. & Meyer, E.L. 2009. Implementation of the biomass gasification project for community empowerment at Melani village, Eastern Cape, South Africa. *Renewable Energy, 34(2009): 2923-2927*

104 Manwell, J. 2004. Hybrid Energy Systems. *Encyclopedia of Energy*. 3(2004): 215-229

105 March, L. 1998. *Introduction to Pinch Technology*. Northwich: Targeting House

106 Masin, J.G. & Lewis, M.A. 2006. *Development of the Low Temperature Hybrid Cu-Cl Thermochemical Cycle*. Argonne National Laboratory

107 Matatiele Local Municipality. (2018). *Research and analysis of ward profiling: Ward based Plans-Ward 22*. http://matatiele.gov.za/documents/strategic-documents/idp/1121-ward-based-plans-ward-16-to-ward-23. [23 April 2019]

108 Mekhilef, S., Saidur, R. & Safari, A. 2012. Comparative study of different fuel cell technologies. *Renewable and Sustainable Energy Reviews, 16(2012): 981-989*

109 Melikoglu, M. 2018. Current status and future of ocean energy sources: A global review. *Ocean Engineering, 148(2018): 563-573*

110 MERCK. 2019. *Copper (1) Chloride.* https://www.sigmaaldrich.com/catalog/product/sigald/212946?lang=en&region=ZA. [20 November 2019]

111 Meyer, J.P. & Tshimankinda, M. 1996. Domestic Hot Water Consumption By Developing Communities in South African Traditional Houses. *Energy, 21(12): 1101-1106*

112 Modi, A., Buhler, F., Andreasen, J.G. & Haglind, F. 2017. A review of solar energy based heat and power generation systems. *Renewable and Sustainable Energy Reviews, 67 (2017): 1047-1064*

113 Mohammed, Y.S., Mustafa, M.W. & Bashir, N. 2014. Hybrid renewable energy systems for off-grid electric power: Review of substantial issues. *Renewable and Sustainable Energy Reviews,* 35(2014): 527-539

114 Morrison, G., Stevens, J. & Joseck, F. 2018. Relative economic competitiveness of light-duty battery electric and fuel cell electric vehicles. *Transportation Research Part C,* 87(2018): 183-196

115 Muneer, T. Asif, M. & Munawwar, S. 2005. Sustainable production of solar energy with particular reference to the Indian economy. *Renewable & Sustainable Energy Reviews,* 9(2005): 444-473

116 Municipalities of South Africa. 2019. *Eastern Cape Municipalities*. https://municipalities.co.za/provinces/view/1/eastern-cape. [14 April 2018]

117 Nasruddin, M., Alhamid, I., Daud, Y., Surachman, A., Sugiyono, A., Aditya, H.M. & Mahlia, T.M.I. 2016. Potential of geothermal energy for electricity generation in Indonesia: A review. *Renewable and Sustainable Energy Reviews, 53(2016): 733-740*

118 Naterer, G.F., Suppiah, S., Stolberg, L., Lewis, M., Ferrandon, M., Wang, Z., Dincer, I., Gabriel, K., Rosen, M.A., Secnik, E., Easton, E.B., Trevani, L., Pioro, I., Tremaine, P., Lvov, S., Jiang, J., Rizvi, G., Ikeda, B.M., Lu, L., Kaye, M., Smith, W.R., Mostaghimi, J., Spekkens, P., Fowler, M. & Avsec, J. 2011b. Clean hydrogen production with Cu-Cl cycle-Progress of international consortium, II: Simulations, thermochemical data and materials. *International Journal of Hydrogen Energy,* 36(2011b): 15486-15501

119 Naterer, G.F., Suppiah, S., Stolberg, L., Lewis, M., Ferrandon, M., Wang, Z., Dincer, I., Gabriel, K., Rosen, M.A., secnik, E., Easton, E.B., Tevani, L., Pioro, i., Tremaine, p., lvov, S., Jiang, J., Rizvi, G., Ikeda, B.M., Lu, L., Kaye, M., Smith, W.R., Mostaghimi, J., Spekkens, P., Fowler, M. & Avsec, J. 2011a. Clean hydrogen production with the Cu-Cl cycle-Progress of international consortium, I: Experimental unit operations. *International Journal of Hydrogen Energy, 36(2011): 15472-15485*

120 National Climate Change Response: White Paper. 2011. https://www.environment.gov.za/sites/default/files/legislations/national_climatechange_response_whitepaper.pdf. [25 October 2018]

121 Nayyeri, M.A., Kianmehr, M.H., Arabhosseini, A. & Hassan-Beygi, S.R. 2009. Thermal properties of diary cattle manure. *International Agrophysics, 23(2009): 359-366*

122 Nema, P., Nema, R.K. & Rangnekar, S. 2009. A current and future state of art development of hybrid system using wind and PV-solar: A review. *Renewable and Sustainable Energy Reviews*, 13(2009): 2096–2103

123 Ngoh, S.K. & Njomo, D. 2012. An overview of hydrogen gas production from solar energy. *Renewable and Sustainable Energy Reviews*, 16(2012): 6782-6792

124 Nicodemus, J.H. 2018. Technologial learning and the future of solar H2: A component learning comparison of solar thermochemical cycles and electrolysis with solar PV. Energy Policy, 120(2018): 100-109

125 Nikolaidis, P. & Poullikkas, A. 2017. A comparative overview of hydrogen production processes. *Renewable and Sustainable Energy Reviews*, 67(2017): 597-611

126 Offer, G.J., Howey, D., Contestabile, M. Clague, R. & Brandon, N.P. 2010. Comparative analysis of battery electric, hydrogen fuel cell and hybrid vehicles in a future sustainable road transport system. *Energy Policy*, 38(2010): 24-29

127 Office of Energy Efficiency & Renewable Energy. 2019. *DOE Targets for Hydrogen Production from Electrolysis*. https://www.energy.gov/eere/fuelcells/doe-technical-targets-hydrogen-production-electrolysis. [17 November 2019]

128 Ogungbemi, E., Ijaodola, O., Khatib, F.N., Wilberforce, T., Hassan, Z.E., Thompson, J., Ramadan, M. & Olabi, A.G. 2019. Fuel cell membranes-Pros and cons. *Energy, 172(2019): 155-172*

129 Ogunmodimu, O. & Okoroigwe, E.C. 2018. Concentrating solar power technologies for solar thermal grid electricity in Nigeria: A review. *Renewable and Sustainable Energy Reviews, 90(2018): 104-119*

130 Ozbilen, A., Dincer, I. & Rosen, M.A. 2016. Development of a four-step Cu-Cl cycle for hydrogen production-Part I: Exergoeconomic and exergoenvironmental analysis. International Journal of Hydrogen Energy, 41(2016: 7814-7825

131 Ozbilen, A., Dincer, I. & Rosen, M.A. 2016. Development of a four-step Cu-Cl cycle for hydrogen production-Part II: Multi-objective optimization. International Journal of Hydrogen Energy, 41(2016: 7826-7834

132 Parra, D., Valverde, L., Pino, F.J. & Patel, M.K. 2019. A review on the role, cost and value of hydrogen energy systems for deep decarbonisation. *Renewable and Sustainable Energy Reviews, 101(2019): 279-294*

133 Pegels, A. 2010. Renewable energy in South Africa: Potentials, barriers and options for support. *Energy Policy*, 38(2010): 4945-4954

134 Pele, R. & Fujita, R.M. 2002. Renewable energy from the ocean. *Marine Policy, 26(2002): 471-479*

135 Pollet, B.G., Staffel, L. & Shang, J.L. 2012. Current status of hybrid, battery and fuel cell electric vehicles: From electrochemistry to market prospects. *Electrochimica Acta*, 84(2012): 235-249

136 Power Africa. 2019. *South Africa Power Africa Fact Sheet*. https://www.usaid.gov/powerafrica/south-africa. [13 March 2019]

137 Pregger, T., Graf, D., Krewitt, W., Sattler, C., Roeb, M. & Moller, S. 2009. Prospects of solar thermal hydrogen production processes. *International Journal of Hydrogen Energy*, 34(2009): 4256-4267

138 Pretorius, I., Piketh, S.J., Burger, R.P. & Neomagus, H. 2015. A perspective of South African coal-fired power station emissions. *Journal of Energy in South Africa,* 26(2015): 27-40

139 Prinsloo, G., Dobson, R. & Brent, A. 2016. Scoping exercise to determine load profile archetype reference shapes for solar co-generation models in isolated of-grid rural African villages. *Journal of Energy in Southern Africa, 27(3): 11-27*

140 Rahbari, A., Shirazi, A., Mahesh, B.V. & Pye, J. 2018. *A solar fuel plant via supercritical water gasification integrated with Fischer-Tropsch synthesis: steady-state modelling and techno-economic assessment.* https://www.researchgate.net/publication/329840552_A_solar_fuel_plant_via_supercritical_water_gasification_integrated_with_Fischer-Tropsch_synthesis_steady-state_modelling_and_techno-economic_assessment. [20 November 2019]

141 Ramachandran, R. & Menon, R.K. 1998. An Overview of Industrial Uses of Hydrogen. *International Journal of Hydrogen Energy*, 23(7): 593-598

142 Ramon, G.Z., Feinberg, B,J, & Hoek, E.M.V. 2011. Membrane-based production of salinity-gradient power. *Energy and Environmental Science, 4(11): 4423-4434*

143 Ray, M.S. & Johnston, D.W. 1989. *Chemical Engineering Design Project A Case Study Approach.* Volume 6. New York: Gordon and Breach Science Publishers.

144 Romm, J. 2006. The car and fuel of the future. *Energy Policy*, 34(2006): 2609-2614

145 Rosen, M.A. 2010. Advances in hydrogen produuction by thermochemical water decomposition: A review. *Energy*, 35(2010): 1068-1076

146 Rourke, F.O., Boyle, F. & Reynolds, A. 2010. Tidal energy update 2009. *Applied Energy, 87(2010) 398-409*

147 Rozali, N.E.M., Wan Alwi, S.R., Manan, Z.A., Klemes, J.J. & Hassan, M.Y. 2013.Process Integration techniques for optimal design of hybrid power systems. *Applied Thermal Engineering, 61 (2013): 26-35*

148 Sainz, D., Dieguez, P.M., Sopena, C., Urroz, J.C. & Gandia, L.M. 2012. Conversion of a commerical gasoline vehicle to run on bi-fuel (hydrogen-gasoline). *International Journal of Hydrogen Energy*, 37(2012): 1781-1789

149 Sayyaadi, H. & Boroujeni, M.S. 2017. Conceptual design, process integration and optimization of a solar Cu-Cl thermochemical hydrogen production plant. *International Journal of Hydrogen Energy*, 42 (2017): 2771-2789

150 Schaetzle, O. & Buisman, C. 2015. Salinity Graduient Energy: Current State and New Trends. *Engineering, 1(2): 164-166*

151 SCIENCECompany. *Hydrochloric Acid, Concentratred, 3.8L*. https://www.sciencecompany.com/Hydrochloric-Acid-Concentrated-38L-P16672.aspx. [21 November 2019]

152 Scribd. 2019. *Economic Indicators*. https://www.scribd.com/document/410567937/cepci-2019. [17 November 2019]

153 Shafiee, S. & Topal, E. 2009. When will fossil fuel reserves be diminished?. *Energy Policy*, 37(2009): 181-189

154 Sharma, S. & Ghoshal, S.K. 2015. Hydrogen the future transportation fuel: From production to applications. *Renewable and Sustainable Energy Reviews*, 43(2015): 1151-1158

155 Silva, O.A., Osorio, A.F. & Winter, C. 2016. Practical global salinity gradient energy potential. *Renewable and Sustainable Energy Reviews, 60(2016): 1387-1395*

156 Silva, S., Lowry, M., Macaya-Solis, C., Byatt, B. & Lucas, M.C. 2017. Can navigation locks be used to help migratory fishes with poor swimming performance pass tidal barrages? A test with lampreys. *Ecological Engineering, 102(2017): 291-302*

157 Smith, R. 2005. Chemical Process Design and Integration. Second Edition. West Sussex: John Wiley & Sons, Ltd

158 South Africa's Intended Nationally Determined Contribution. 2015. *Introduction: Context and National Priorities*. https://www.environment.gov.za/sites/default/files/docs/sanational_determinedcontribution.pdf. [26 October 2018]

159 Spiegel, C. 2019. *Fuel Cell Operating Conditions*. https://www.fuelcellstore.com/blog-section/fuel-cell-operating-conditions. [7 June 2019]

160 Statistics South Africa. 2017. *General Household Survey*. http://www.statssa.gov.za/publications/P0318/P03182017.pdf. [11 April 2019]

161 Steinfeld, A. & Palumbo, R. 2001. Solar Thermochemical Process Technology. *Encyclopedia of Physical Science & Technology*, 15: 237-256

162 Stern, N. 2006. What is the Economics of Climate Change?. *World Economics*, 7 (2), April-June

163 Suri, M., Cebecauer, T. Meyer, A.J. & van Niekerk, J.L. (2015). *Accuracy-Enhanced Solar Resource Maps of South Africa*.

https://repository.up.ac.za/bitstream/handle/2263/49525/Suri_Accuracy_2015.pdf?sequence=1&isAllowed=y. [15 April 2019]

164 Tantimuratha, L. Kokossis, A.C. & Muller. 2000. The heat exchanger network design as a paradigm of technology integration. *Applied Thermal Engineering*, 20(2000): 1589-1605

165 The Carbon Report. 2015. How will the draft carbon tax bill affect your business?. http://www.thecarbonreport.co.za/the-proposed-south-african-carbon-tax/. [14 August 2017]

166 The NEED Project. 2012. *The Intermediate Energy Infobook*. www.Need.org. [25 June 2018]

167 Thomas, C.E. 2009. Fuel cell and battery electric vehicles compared. *International Journal of Hydrogen Energy*, 34(2009): 6005-6020

168 Timeanddate. 2019. Eastern Cape, Eastern Cape, South Africa-Sunrise, Sunset, and Daylength, June 2019. https://www.timeanddate.com/sun/@1085593. [28 June 2019]

169 Turkay, B.E. & Telli, A.Y. 2011. Econoic analysis of standalone and grid connected hybrid energy systems. *Renewable Energy, 36(2011): 1931-1943*

170 Turton, R., Bailie, R.C., Whiting, W.B., Shaeiwitz, J.A. & Bhattacharyya, D. 2013. *Analysis, Synthesis, and Dseign of Chemical Processes.* Fourth Edition. Upper Saddle River: Pearson Education International.

171 U.S. Energy Information Administration. 2013. EIA projects world energy consumption will increase 56% by 2040. https://www.eia.gov/todayinenergy/detail.php?id=12251#. [9 October 2018]

172 U.S. Energy Information Administration. 2016. *International Energy Outlook 2016*. https://www.eia.gov/outlooks/ieo/pdf/0484(2016).pdf. [15 August 2017]

173 U.S. Energy Information Administration. 2016. *International Energy Outlook 2016*. https://www.eia.gov/outlooks/ieo/pdf/0484(2016).pdf. [15 August 2017]

174 Uihlein, A. & Magagna, D. 2016. Wave and tidal current energy-A review of the current state of research beyond technology. Renewable and Sustainable Energy Reviews, 58(2016): 1070-1081

175 US Department of Energy. 2012. *Low Cost, Lightweight Solar Concentrator*. https://www.nrel.gov/docs/fy12osti/55451.pdf [16 November 2019]

176 VanZwieten, J., Rauchenstein, L. & Lee, L. 2017. An assessment of Florida's ocean thermal energy converstion (OTEC) resource. *Renewable and Sustainable Energy Reviews, 75(2017): 663-691*

177 Vassilev, S.V., Vassileva, C.G. & Vassilev, V.S. 2015. Advantages and disadvantages of composition and properties of biomass in comparison with coal: An overview. *Fuel, 158(2015): 330-350*

178 Verhelst, S. & Wallner, T. 2009. Hydrogen-fueled internal combustion engines. *Progress in Energy and Combustion Science*, 35(2009): 490-527

179 Verhelst, S. 2014. Recent progress in the use of hydrogen as a fuel for internal combustion engines. *International Journal of Hydrogen Energy*, 39(2014): 1071-1085

180 Visser, H., Thopil, G.A. & Brent, A. 2019. Life cycle cost profitability of biomass power plants in South Africa within the international context. *Renewable Energy, 139(2019):9-21*

181 Wade, K. & Jennings, M. 2016. *The impact of climate change on the global economy*. http://www.schroders.com/en/sysglobalassets/digital/us/pdfs/the-impact-of-climate-change.pdf. [19 August 2017]

182 Wan Alwi, S.R., Rozali, N.E.M., Abdul-Manan, Z. & Klemes, J.J. 2012. A process integration targeting method for hybrid power systems. *Energy, 44 (2012): 6-10*

183 Wang, J., Wang, H. & Fan, Y. 2018. Techno-Economic Challenges of Fuel Cell Commercialization. *Engineering, 4(2018): 352-360*

184 Wang, S. & Wang, S. 2015. Impacts of wind energy on environment: A review. *Renewable and Sustainable Energy Reviews, 49(2015): 437-443*

185 Wang, Z., Roberts, R.R., Naterer, G.F. & Gabriel, K.S. 2012. Comparison of thermochemical, electrolytic, photoelectric and photochemical solar-to-hydrogen production technologies. *International Journal of Hydrogen Energy*, 37(2012): 16287-16301

186 WASA. 2019. *Wind Atlas for South Africa*. http://www.wasaproject.info/. [16 April 2019]

187 Wazimap. 2019. *Alfred Nzo*. https://wazimap.co.za/profiles/district-DC44-alfred-nzo//. [12 April 2019]

188 Wazimap. 2019. *Amathole*. https://wazimap.co.za/profiles/district-DC12-amathole/. [12 April 2019]

189 Wazimap. 2019. *Chris Hani*. https://wazimap.co.za/profiles/district-DC13-chris-hani/. [12 April 2019]

190 Wazimap. 2019. *Joe Gqabi*. https://wazimap.co.za/profiles/district-DC14-joe-gqabi/. [12 April 2019]

191 Wazimap. 2019. *Matatiele Ward 22 (24401022)*. https://wazimap.co.za/profiles/ward-24401022-matatiele-ward-22-24401022/. [22 April 2019]

192 Wazimap. 2019. *O.R.Tambo*. https://wazimap.co.za/profiles/district-DC15-ortambo/. [12 April 2019]

193 Wazimap. 2019. *Sarah Baartman*. https://wazimap.co.za/profiles/district-DC10-sarah-baartman/. [12 April 2019]

194 WBA Global Bioenergy Statistics. 2017. *Global Overview*. https://worldbioenergy.org/uploads/WBA%20GBS%202017_hq.pdf. [13 March 2019]

195 Weebly. 2019. *Hydrochloric acid*. https://psa-hydrochloric-acid.weebly.com/physical--chemical-properties.html. [17 July 2019]

196 White, C.M., Steeper, R.R. & Lutz, A.E. 2006. The hydrogen-fueled internal combustion engine: a technical review. *International Journal of Hydrogen Energy*, 31(2006): 1292-1305

197 White, S. & Koopman, S. 2011. *Off-grid electrification in rural areas of South Africa*. http://www.ee.co.za/wp-content/uploads/legacy/Energize_2011_/09_SeT_01_Eskom_off-grid.pdf. [29 August 2017]

198 Wilberforce, T., Alaswad, A., Palumbo, A., Dassisti, M. & Olabi, A.G. 2016. Advances in stationary portable fuel cell applications. *International Journal of Hydrogen Energy, 41(2016): 16509-16522*

199 Winkler, H. & Marquand, A. 2009. Changing development paths: From an energy-intensive to low-carbon economy in South Africa. Climate and Development, 1(1): 47-65

200 Winkler, H. 2005. Renewable energy policy in South Africa: policy options for renewable energy. *Energy Policy*, 33(2005): 27-38

201 Winkler, H., Simoes, A.F., Rovere, E.L.L., Rahman, M.A.A. & Mwakasonda, S. 2011. Access and Affordability of Electricity in Developing Countries. *World Development*, 39(6): 1037-1050.

202 World Energy Council. 2016. Marine Energy. https://www.marineenergywales.co.uk/wp-content/uploads/2016/01/World-Energy-Council-Marine-Energy-Resources-2016.pdf. [8 March 2019]

203 World Energy Council. 2019. *Hydropower*. https://www.worldenergy.org/data/resources/resource/hydropower/. [15 March 2019]

204 World Health Organisation. 2017. *Climate change and health*. www.who.int/mediacentre/factsheets/fs266/en/. [15 August 2017]

205 World Resources Institute. 2018. South Africa. https://www.climatewatchdata.org/countries/ZAF. [8 October 2018]

206 WWF. 2012. *Solar PV Atlus: Solar Power In Harmony With Nature*. http://awsassets.panda.org/downloads/solar_pv_atlas_final_screen_version_feb_2013.pdf. [15 August 2017]

207 Xu, F., Li, Y., Ge, X., Yang, L. & Li, Y. 2018. Anaerobic digestion of food waste-Challenges and opportunities. *Bioresource Technology, 247(2018): 1047-1058*

208 Yadav, D. & Banerjee, R. 2016. A review of solar thermochemical processes. *Renewable and Sustainable Energy Reviews*, 54(2016): 497-532

209 Yilanci, A., Dincer, I. & Ozturk, H.K. 2009. A review on solar-hydrogen/fuel cell hybrid energy systems for stationary applications. *Progress in Energy and Combustion Science*, 35(2009): 231-244

210 Yilanci, A., Dincer, I. & Ozturk, H.K. 2009. A review on solar-hydrogen/fuel cell hybrid energy systems for stationary applications. *Progress in Energy and Combustion Science*, 35(2009): 231-244

211 Yilmaz, F., Balta, M.T. & Sebas, R. 2016. A review of solar based hydrogen production methods. *Renewable and Sustainable Energy Reviews*, 56(2016): 171-178

212 Yilmaz, F., Balta, M.T. & Selbas, R. 2016. A review of solar based hydrogen production methods. *Renewable and Sustainable Energy Reviews*, 56(2016): 171-178

213 Zamfirescu, C., Dincer, I. & Naterer, G.F. 2010. Thermophysical properties of copper compounds in copper-chlorine thermochemical water splitting cycles. *International Journal of Hydrogen Energy, 35(2010): 4839-4852*

214 Zhang, C., Su, H., Baeyens, J. & Tan, T. 2014. Reviewing the anaerobic digestion of food waste for biogas production. *Renewable and Sustainable Energy Reviews, 38(2014): 383-392*

215 Zhang, W., Li, Y., Wu, X. & Guo, S. 2018. Review of the applied mechanical problems in ocean thermal energy conversion. *Renewable and Sustainable Energy Reviews, 93(2018): 231-244*

216 Zhou, W., Lou, C., Li, Z., Lu, L. & Yang, H. 2010. Current status of research on optimum sizing of stand-alone hybrid solar-wind power generation systems. *Applied Energy*, 87(2010): 380–389

APPENDICES

Appendix A

Table 33: CuCl Process Steps

Reaction Steps	Temp Range (℃)	Input	Output
$2CuCl(aq) + 2HCl(aq) \rightarrow H_2(g) + 2CuCl_2(aq)$	< 100	Aqueous CuCl & HCl + V+Q	$H_2(g) + 2CuCl_2(aq)$
$CuCl_2(aq) \rightarrow CuCl_2(s)$	< 100	Slurry containing HCl & $CuCl_2$+ Q	Granular $CuCl_2 + H_2O/HCl$ vapors
$2CuCl_2(s) + H_2O(g) \rightarrow Cu_2OCl_2(s) + 2HCl(g)$	400	Powder/granular $CuCl_2 + H_2O(g) + Q$	Powder/granular $Cu_2OCl_2 + 2HCl(g)$
$Cu_2OCl_2(s) \rightarrow 2CuCl(l) + \frac{1}{2}O_2(g)$	500	Powder/granular $Cu_2OCl_2(s) + Q$	Molten $CuCl$ salt + oxygen

Appendix B

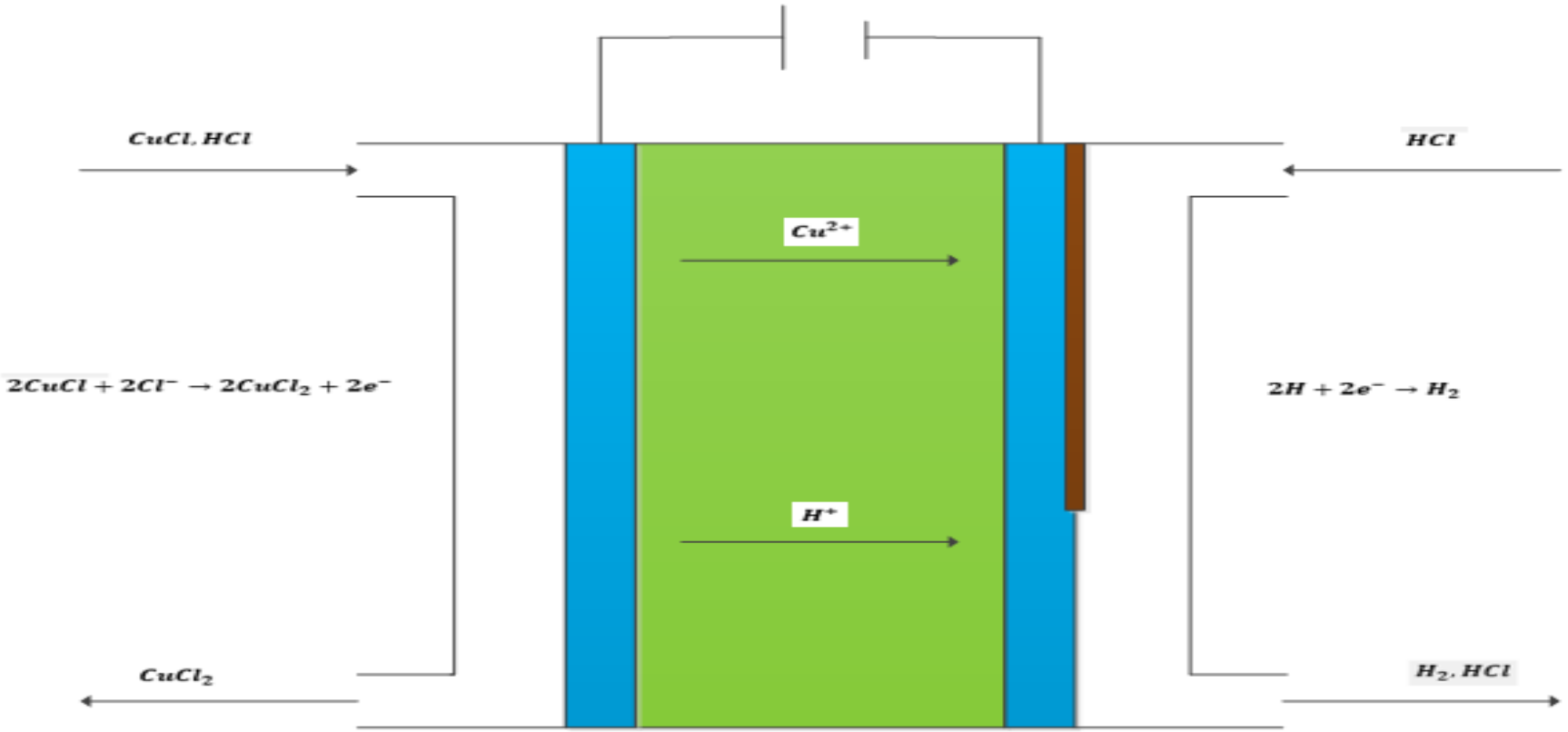

Figure 26: Electrolyzer

Appendix C

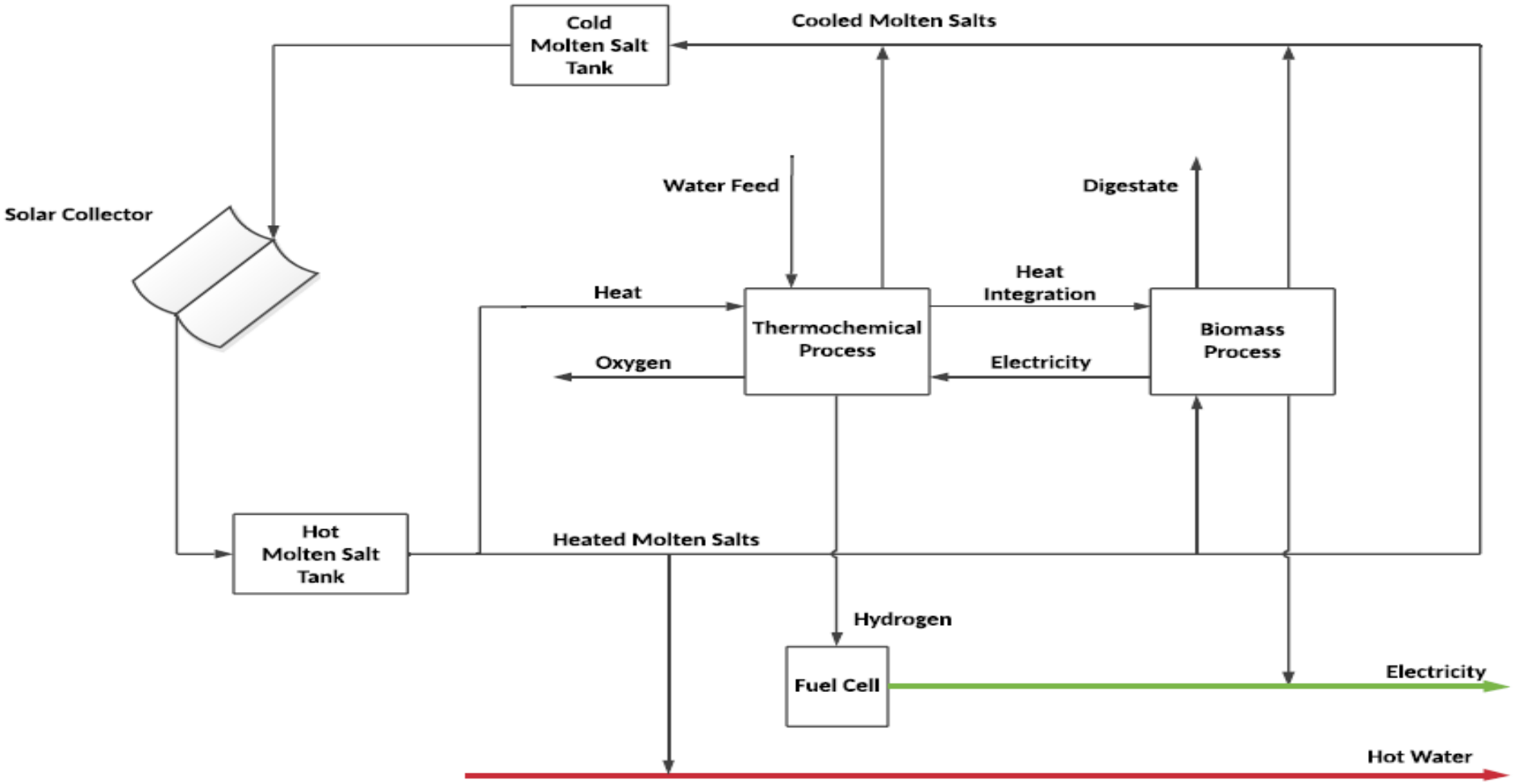

Figure 27: Modified Conceptual Diagram

Appendix D

Thermochemical Cycle Plant Material Balance

Fuel Cell Balance

Larminie & Dicks (2003) presents some useful equations when performing material balance equations for hydrogen fed fuel cells. The V_c of each cell is calculated using one of their derived expressions as shown below.

- $Fuel\ Cell\ Efficiency = \frac{V_c}{1.48}$ Eq D-1

It has been previously noted that electrical efficiency of 54% will be assumed.

- $0.54 = \frac{V_c}{1.48} \therefore V_c = 0.799 \sim 0.8\ V$

An additional derivation presented by Larminie & Dicks (2003) is shown below to calculate the hydrogen usage.

- $H_2\ usage\ (kg/s) = 1.05 \times 10^{-8} \times \frac{P_e}{V_c}$ Eq D-2

wherein P_e is the electrical power of the whole fuel cell stack equating to 30 kW.

- $H_2\ usage = 1.05 \times 10^{-8} = \frac{30 \times 10^3}{0.8} = 3.94 \times 10^{-4} kg/s$
- $Mr[H_2] = 2.02\ kg/kmol = 2.02 \times 10^{-3} kg/mol$
- $\therefore N_{H_2} = \frac{m}{Mr} = \frac{3.94 \times 10^{-4} kg/s}{2.02 \times 10^{-3} kg/mol} = 0.195\ mol/s$ *(stream 4)* Eq D-3

Note: Fuel cell calculations continue below.

Electrolyzer Balance

Wang *et al* (2012) note that there are several potential output streams from the electrolyzer. The authors highlight the minimum molar ratio outputs for various scenarios, from binary to quaternary outputs. Ideally, in a binary system, all $CuCl$ is oxidized to $CuCl_2$ at the anode side whilst all available protons (H^+) move to the cathode side. However, the authors acknowledge that practically, it is very challenging to have all the protons move to the cathode side, whilst the anode side will still consist of HCl. They add that, the anode side output stream is more likely to be a quaternary system since all the *CuCl* is unlikely to convert. Furthermore, the electrolyzer will need to operate at 80℃ given the binary system scenario.

However, a binary system is assumed since it will simplify the entire material balance. Additionally, it is assumed that all HCl is consumed and that stoichiometric proportion is considered adequate for full conversion in an ideal context.

- $2CuCl\ (aq) + 2HCl\ (aq) \rightarrow H_2\ (g) + 2CuCl_2\ (aq)$

- $\frac{0.195\ mol/s\ H_2 \times 2\ mol/s\ CuCl}{1\ mol/s\ H_2} = 0.39\ mol/s\ CuCl\ in\ feed$ Eq D-4

$\therefore 0.39\ mol/s\ CuCl_2\ produced$

According to Wang *et al* (2012), a minimum water to cupric chloride ($CuCl_2$) molar ratio of 7.5 occurs in the electrolytic cell for the binary system. Hence, this system will be used to estimate the flow rate of water in stream 5.

- $7.5 = \frac{H_2O}{CuCl_2} = \frac{H_2O}{0.39\ mol/s} \therefore H_2O\ (stream\ 5) = 2.93\ mol/s$ Eq D-5

The flow rate of water in stream 5 is assumed to be equivalent to that in stream 1 since water is used only to dissolve the $CuCl$ & HCl in the anode side. Furthermore, stream 2 has an HCl and H_2O flow rate of 0.39 & 1.56 mol/s, the computation of which will be shown later.

Separator 1 Balance

Perfect separation is assumed especially since the feed is a liquid-gas mixture, hence $0.195\ mol/s\ H_2$ leaves in stream 6 whilst 0.39 & 1.56 $mol/s\ HCl$ and H_2O leaves in stream 8 to mixer 1.

Dryer Balance

Although all the water cannot be removed, it is assumed that all water fed to the dryer is removed, any remaining water is considered insignificant and no water leaves with the exhaust air.

- $CuCl_2(aq) \rightarrow CuCl_2(s)$

As a result, the $2.93\ mol/s\ H_2O$ that is fed via stream 5 to the Dryer is removed via stream 10 whilst $0.39\ mol/s\ CuCl_2(s)$ is fed to the hydrolysis reactor in stream 9.

According to experimental results presented by Wang *et al* (2012), the mass ratio of air to water is usually 8 or higher to completely evaporate water with air below 120 ℃. The molar flow rate of air can be calculated using equation D-3 once its mass flow rate has been calculated.

- $8 = \frac{Air}{Water} \therefore m_{air} = 8m_{H_2O} = 8(nMr)_{H_2O} = 8(2.93 \times 18) = 422\ g/s = 0.422\ kg/s$ Eq D-6

- $Mr[Air] = 28.97\ g/mol \therefore n_{air} = \frac{422}{28.97} = 14.57\ mol/s$

Note: the exhaust air will be released into the atmosphere. Any additional pressure required to transport the exhaust gas for heating applications is considered a waste.

Hydrolysis Balance

Assuming a binary system is especially advantageous in the context of the hydrolysis reactor. According to Wang *et al* (2012), HCl from the electrolytic cell that is fed to the hydrolysis reactor may prevent the hydrolysis reaction from occurring. The authors add that, unreacted $CuCl$ may reduce the contact

between the steam and $CuCl_2$ particles and increase the heat transfer resistance. Furthermore, it is assumed that no side reactions are competing with the hydrolysis with a complete conversion.

- $2CuCl_2(s) + H_2O(g) \rightarrow Cu_2OCl_2(s) + 2HCl(g)$

As mentioned before, in assuming a binary mixture Wang *et al* (2012) report that, steam fed to the hydrolysis reactor in its stoichiometric proportion is the minimum requirement for complete conversion. Hence, the stoichiometric ratio like equation D-4 is used to find the water requirement.

- $H_2O(g)\ requirement = \frac{0.39\ mol/s\ CuCl_2 \times 1\ mol/s\ H_2O}{2\ mol/s\ CuCl_2} = 0.195\ mol/s\ H_2O\ (stream\ 12)$
- $\therefore Cu_2OCl_2(s) = 0.195\ mol/s\ (stream\ 13)$
- $\therefore HCl\ (g) = 0.39\ mol/s\ (stream\ 13)$

Excess steam will be fed despite, only requiring the stoichiometric proportion to ensure complete conversion. This is done so that the output $HCl\ (g)$ can be converted to an aqueous solution with the excess steam. Excess steam of 89% will be assumed to ensure a solution with a 20.22 HCl mol%. According to Weebly (2019), this will allow the gas mixture to be condensed at 108.58℃ before being fed to the electrolyzer.

- $n_{HCl(18)} = x_{HCl} n_{18} \therefore n_{18} = 0.39/0.2 = 1.95\ mol/s$ Eq D-7
- $\therefore n_{H_2O(18)} = n_{18} - n_{HCl(18)} = (1.95 - 0.39) mol/s = 1.56\ mol/s$ following the material balance equation given by Eq 5-3
- $\therefore excess\ \% = \frac{n_{H_2O(18)}}{n_{H_2O(18)} + n_{H_2O(11)}} \times 100 = \frac{1.56}{1.56 + 0.195} \times 100 = 89\%$ Eq D-8

Separator 2 Balance

Perfect separation is once again assumed. Stream 13 is separated into stream 14 and 18. $0.195\ mol/s\ Cu_2OCl_2(s)$ flows through stream 14 whilst $0.39\ mol/s\ HCl\ (g)$ & $1.56\ mol/s\ H_2O$ flow through stream 18. Stream 18 first undergoes many cooling operations being fed to the cathode feed tank and then via stream 2 it returns to the cathode compartment of the electrolytic cell.

Decomposition Reactor

Complete conversion is assumed. Hence stoichiometric ratios similar to Eq D-4 will be used to calculate molar flow rates. Wang *et al* (2012) mention that $CuCl$ produced in the decomposition reactor exists as molten salt and will, therefore, need to be solidified and dissolved in an aqueous solution of HCl before being fed to the electrolytic cell.

- $Cu_2OCl_2(s) \rightarrow 2CuCl(l) + \frac{1}{2}O_2(g)$
- $CuCl\ produced = \frac{0.195\ mol/s\ Cu_2OCl_2 \times 2\ mol/s\ CuCl}{1\ mol/s\ Cu_2OCl_2} = 0.39\ mol/s\ CuCl\ (stream\ 15)$
- $O_2\ produced = \frac{0.195\ mol/s\ Cu_2OCl_2 \times 0.5\ mol/s\ O_2}{1\ mol/s\ Cu_2OCl_2} = 0.098\ mol/s\ O_2 (stream\ 15)$

Separator 3

Again, perfect separation is assumed, therefore, $0.39\ mol/s\ CuCl$ is separated into stream 17 whilst $0.098\ mol/s\ O_2$ is separated into stream 16 and captured.

Mixer 1

Stream 17, 28 & 8 is fed to this mixer before feeding to the anode feed tank. Before feeding into the mixer, stream 10 is split into streams 28 and 27. Stream 27 contains $1.56\ mol/s\ H_2O$ which is fed to mixer 2 to account for the excess steam fed to the hydrolysis reactor whilst the balance of $1.37\ mol/s\ H_2O$ flow in stream 28 to mixer 1. Additional input streams to mixer 1 include $0.39\ mol/s\ CuCl$ in stream 17 and stream 8 is made up of $0.39\ mol/s\ HCl$ and $1.56\ mol/s\ H_2O$.

Fuel Cell Balance Continued

The fuel cell will be maintained at 90℃ and therefore it is assumed that the output stream will leave at the same temperature. Hence, this stream (24) can be used as a hot stream for the pinch application. The balance is started by calculating the air requirement in stream 23 using stoichiometric ratios similar to Eq D-4.

- $H_2(g) + 0.5O_2 \rightarrow H_2O\ (l)$
- $O_2\ requirement = \frac{0.195\ mol\ H_2/s \times 0.5\ mol\ O_2}{1\ mol\ H_2} = 0.0975\ mol/s$
- $Air\ Requirement = \frac{O_2\ requirement}{0.21} = \frac{0.0975\ mol/s}{0.21} = 0.464\ mol/s$

However, Larminie & Dicks (2003) add that, feeding air by its stoichiometric requirement is impractical and air is typically fed double its stoichiometric requirement.

- $\therefore Air\ feed = 0.464\ mol/s \times 2 = 0.93\ mol/s$ (stream 23)
- $\therefore O_2\ feed = 2 \times 0.0975\ mol/s = 0.195\ mol/s$
- $\therefore N_2\ feed = (0.93 - 0.195) mol/s = 0.735\ mol/s$

The flow of exit stream 24 can now be calculated assuming the all H_2 is converted in stoichiometric proportion following the equation given by Eq D-4.

- $N_2\ flow = 0.735\ mol/s$
- $O_2\ flow = (0.195 - 0.0975) mol/s = 0.0975\ mol/s$ following the Eq 5-3
- $H_2O\ flow = \frac{0.195\ mol/s\ H_2 \times 1 mol\ H_2O}{1\ molH_2} = 0.195\ mol/s$

Biogas Plant Material Balance

The product biogas of AD consists of 60-70% methane, 30-40% carbon dioxide, and traces of other gases such as hydrogen and hydrogen sulphide (Xu *et al*, 2018). The traces of other gases will be neglected for the material balance whilst the methane content will be assumed to be 65% with a corresponding 35% carbon dioxide content.

- Methane $(CH_4) = 0.65$
- Carbon dioxide $(CO_2) = 0.35$

According to Ghazi & Nasir (2017), the energy content of the biogas mixture is directly proportional to the methane content in it, which amounts to about 6 kWh per cubic metre of biogas. However, the authors add that one cubic metre of biogas (65% methane) can only be converted to approximately 1.7 kWh of useable electric energy due to conversion losses.

- $1m^3 = 1.7\ kWh$

Cavinito *et al* (2010) provides experimental results that show an improvement from 0.45 to 0.62 $m^3/kg\ VS$ with a digester operating at thermophilic conditions (55℃).

- Therefore, a yield of $0.62\ m^3/kg\ VS$ will be assumed.

The production rate can be calculated since the biogas plant will cover a generation capacity of 200 kWh. Note, considering the load, this output can be ramped up or down by manipulating the feed rate.

- $Production\ capacity = \frac{200\ kWh \times 1m^3}{1.7\ kWh} = 117.6\ m^3\ biogas$ Eq- D-9

Since the production rate is calculated from the daily generation capacity, the ratio is changed from $117.6\ m^3\ biogas$ to $117.6\ m^3\ biogas/d$. Note: this is the biogas produced in stream 7 and it is assumed that the gas treatment and conversion to electricity in the generator account for the losses that reduce the energy content of 6 kWh to 1.7 kWh. It is not necessary to perform the balance beyond stream 7.

The feed rate can be calculated using the yield and biogas output.

- $117.6\ m^3 \frac{biogas}{d} \times \frac{1kg}{0.62\ m^3} = 190\ kg/d$ *(stream 19)* Eq D-10

The plant in Figure 15, adapted from Cavinito *et al* (2010) has a digester feed with ranging from 10-12% solids, hence it will be assumed that the solid content of the feed is 12%.

Appendix E

Pinch Cp Data Extraction

Data extraction is a crucial element of pinch analysis and incorrect extraction can lead to impossible targets (Kemp, 2007). The author adds that temperature changes in the context of extracting Cps, can lead to inaccurate extraction considering that the Cp varies with temperature changes. More so when there is a phase change. Kemp (2007) notes that there are cases in which the Cp can be considered constant whereas, in others, significant changes in Cp should be considered in the analysis. The subsequent list provides the Cps of the different process chemicals as required by heat pinch analysis.

- $Cp_{H_2O} = 75.3\ kJ/\ kmol$ ℃ @ 20℃ (Engineering ToolBox, 2004)
- $Mr[H_2O] = 18\ kg/kmol \therefore Cp_{H_2O} =$ 75.3 $kJ/\ kmol$ ℃ × $kmol/18\ kg = 4.18\ kJ/kg$℃

Eq E-1

A different Cp will be used when water is converted to steam

- $\therefore Cp_{H_2O(steam)} = 1.890\ kJ/kg$℃ @ ~100℃ (Engineering ToolBox, 2005)

The Cp changes insignificantly for $H_{2(g)}$ over a large temperature interval, hence a constant figure will be used. This will apply to all the chemical compounds subsequently listed.

- $Cp_{H_2(g)} = 14.31\ kJ/kg$℃ @ ~20℃ (Engineering ToolBox, 2005)
- $Cp_{O_2(g)} = 0.918\ kJ/kg$℃ @ ~20℃ (Engineering ToolBox, 2005)
- $Cp_{N_2(g)} = 1.04\ kJ/kg$℃ @ ~20℃ (Engineering ToolBox, 2005)
- $Cp_{HCl(g)} = 0.795\ kJ/kg$℃ @ ~20℃ (Engineering ToolBox, 2003)
- $Cp_{HCl(l)} = 3.14\ kJ/kg$℃ (Engineering ToolBox, 2003)

Coscia *et al* (2013) cites Cps for $NaNO_3$ ranging from 1.67 kJ/kg℃ to 1.82 kJ/kg℃ at 400℃. According to their experimental results, Cps for $NaNO_3$ ranging from 1.12 kJ/kg℃ to 1.51 kJ/kg℃ at 100℃ and 400℃ respectively. Considering the insignificant difference between the Cps for that large interval, it is assumed that the Cp won't change significantly from 400℃ to 550℃. The same assumption holds for KNO_3 as reported in their paper.

- $Cp_{NaNO_3} = 1.82\ kJ/kg$℃ @ 540℃
- $Cp_{KNO_3} = 1.39\ kJ/kg$℃ @ 540℃

According to Zamfirescu *et al* (2010) the Cp of liquid $CuCl$ remains constant.

- $Cp_{CuCl} = 66.9\ J/mol$℃
- $Mr[CuCl] = 99\ kg/kmol \therefore Cp_{CuCl} =$ 66.9 $kJ/\ kmol$ ℃ × $kmol/99\ kg = 0.68\ kJ/kg$℃

As calculated in Eq E-1.

Below, Zamfirescu *et al* (2010) provide a correlation to estimate the Cp of Cu_2OCl_2 for temperatures ranging from 25 to 402℃.

- $Cp(kJ/kmolK) = a + bT + cT^2 + dT^3 where\ a = 53.72, b = 0.33, c = -5.22 \times 10^{-4}, d = 2.99 \times 10^{-7}$ Eq E-2
- $\therefore Cp_{Cu_2OCl_2} = 39.52\ kJ/kmol$ ℃ @ 400℃
- $Mr[Cu_2OCl_2] = 214\ kg/kmol \therefore Cp_{Cu_2OCl_2} =$ 39.5 $kJ/\ kmol$ ℃ $\times\ kmol/214\ kg =$ 0.18 kJ/kg℃ as calculated in Eq E-1.

$CuCl_2$ is an additional chemical compound with a Cp that does not change significantly over a large temperature range as shown by Zamfirescu *et al* (2010).

- $\therefore Cp_{CuCl_2} = 78.28\ J/mol$ ℃
- $Mr[CuCl_2] = 134.5\ kg/kmol \therefore Cp_{CuCl_2} =$ 78.3 $kJ/\ kmol$ ℃ $\times\ kmol/134.5\ kg =$ 0.58 kJ/kg℃ as calculated in Eq E-1.

- $Cp_{Sweet\ Sirghum} = 2321.2\ J/kg$ ℃ (Fennel & Bolder, 2014)
- $Cp_{Cow\ Manure} = 3.61\ kJ/kg$ ℃ (Nayyeri *et al*, 2009)

The following table provides the hot and cold streams data required in the data extraction Section 5.5.1. Sections within the table are left blank since only the mass flowrates and stream heat capacities are important. Sample calculations are provided.

Table 34: Hot & Cold Stream Data

Stream No	Components	Mol Flow (mol/s)	Molar Mass (g/mol)	Mass Flow (g/s)	Mass Flow (kg/s)	Mass Fraction	Component Cp $(kj/kg$ ℃)	Stream Cp $(kj/kg$ ℃)
Stream 5	$CuCl_2(l)$	0.39	134.5	52.46	0.052	0.5	0.58	2.38
	$H_2O(l)$	2.93	18	52.74	0.053	0.5	4.18	
Stream 6	$H_2(g)$	0.195	2	0.4	0.0004	1	14.31	14.31
Stream 12	$H_2O(l)$	0.195	18	3.5	0.0035	1	4.18	4.18
Stream 12.1	$H_2O(g)$	0.195	18	3.5	0.0035	1	1.89	1.89
Stream 14	Cu_2OCl_2	0.195	214	41.7	0.042	1	0.18	0.18
Stream 15	$CuCl(l)$	0.39	99	38.6	0.039	0.93	0.68	0.69
	$O_2(g)$	0.098	32	3.1	0.0031	0.07	0.918	
Stream 16	$O_2(g)$	0.098	32	3.1	0.0031	1	0.918	0.92
Stream 18	$HCl(g)$	0.39	36.5	14.2	0.014	0.33	0.795	1.53
	$H_2O(g)$	1.56	18	28.1	0.0281	0.67	1.89	
Stream 18.1	$HCl(l)$	0.39	36.5	14.2	0.014	0.33	3.14	3.84

	$H_2O(l)$	1.56	18	28.1	0.0281	0.67	4.18	
Stream 19	$H_2O(l)$				0.0019	0.88	4.18	143.17
	Sweet sorghum				0.00013	0.06	2321.2	
	Manure				0.00013	0.06	3.61	
Stream 20	$NaNO_3$		85		0.048	0.6	1.82	1.65
	KNO_3		101		0.032	0.4	1.39	
Stream 24	$N_2(g)$	0.735	28	20.58	0.021	0.76	1.04	1.13
	$O_2(g)$	0.0975	32	3.12	0.0031	0.11	0.918	
	$H_2O(l)$	0.195	18	3.51	0.0035	0.13	4.18	
Stream 25	$N_2(g)$		28		0.33	0.79	1.04	1.01
	$O_2(g)$		32		0.092	0.21	0.918	
Stream 26	$H_2O(l)$		18		0.012	1	4.18	4.18
Stream 27	$H_2O(l)$	1.56	18	27	0.027	1	4.18	4.18

Stream 19 component mass flow

The total mass flow of stream 19 was calculated to be 190 kg/d as shown in Appendix D. Furthermore, it was assumed that the solids accounted for 12% of the mixture, with the solids equivalent in weight.

- $190\ kg/d \times 1\ d/86400\ s = 0.0022\ kg/s$
- $\therefore w_{H_2O} = 0.88 \times 0.0022 = 0.00194\ kg/s$
- $w_{Manure} = w_{sweet\ sorghum} = 0.06 \times 0.0022\ kg/s = 0.00013\ kg/s$ as shown in Eq D-7.

Stream 26 mass flow

It was found in the heat demand Section 5.2.2 that the total village hot water consumption amounted to 982.8 l/d. The total flow will be adjusted to $1000\ l/d$ to account for potential leaks, wastage, and overuse.

- $\rho_{H_2O} = 1000\ kg/m^3$ & $1000\ l/d = 1m^3\ /d \therefore 1000\ kg/m^3 \times 1m^3/d = 1000\ kg/d = 0.012\ kg/s$ Eq E-3

Stream 5 sample Cp calculation following Eq 4-3

- $Cp_{(stream\ 5)} = (wCp)_{CuCl_2} + (wCp)_{H_2O} = (0.5 \times 0.58) + (0.5 \times 4.18) = 2.38\ kj/kg$ ℃

Stream 25 mass flow rates following Eq D-7

- $m_{N_2} = x_{N_2} \times m_{25} = 0.79 \times 0.422\ kg/s = 0.33 \therefore m_{O_2} = (0.422 - 0.33) kg/s = 0.092\ kg/s$

Appendix F

Table 35: PTA Energy Targeting

Shift Temperature	Interval	$T_{(i+1)}$-T_i	mCp_{net}	dH		Infeasible Cascade	Feasible Cascade
°C		°C	kW/K	kW			
535						PINCH ▼ 0	▼ 0
	1	30	0.132	3.96	surplus	3.96	3.96
505						▼ 3.96	▼ 3.96
	2	10	0.1244	1.244	surplus	1.244	1.244
495						▼ 5.204	▼ 5.204
	3	90	0.1534	13.806	surplus	13.806	13.806
405						▼ 19.01	▼ 19.01
	4	10	0.1544	1.544	surplus	1.544	1.544
395						▼ 20.554	▼ 20.554
	5	266	0.2188	58.2008	surplus	58.2008	58.2008
129						▼ 78.755	▼ 78.755
	6	24	0.0868	2.0832	surplus	2.0832	2.0832
105						▼ 80.838	▼ 80.838
	7	1.4	-0.5973	-0.8362	demand	-0.83622	-0.83622
103.6						▼ 80.002	▼ 80.002
	8	8.6	-0.5	-4.3	demand	-4.3	-4.3
95						▼ 75.702	▼ 75.702
	9	10	-0.3871	-3.871	demand	-3.871	-3.871
85						▼ 71.831	▼ 71.831
	10	10	-0.1562	-1.5616	demand	-1.5616	-1.5616
75						▼ 70.269	▼ 70.269
	11	15	-0.3382	-5.0735	demand	-5.07354	-5.07354
60						▼ 65.196	▼ 65.196
	12	35	-0.6531	-22.8598	demand	-22.8598	-22.85976
25						▼ 42.336	▼ 42.336
	13	10	0.1527	1.5272	surplus	1.52724	1.52724
15						▼ 43.863	▼ 43.863

Hot Pinch	540	°C
Cold Pinch	530	°C
Min Hot Utility	0.0	kW
Min Cold Utility	43.86	kW

SINGLE PINCH PROBLEM

THRESHOLD PROBLEM

Appendix G

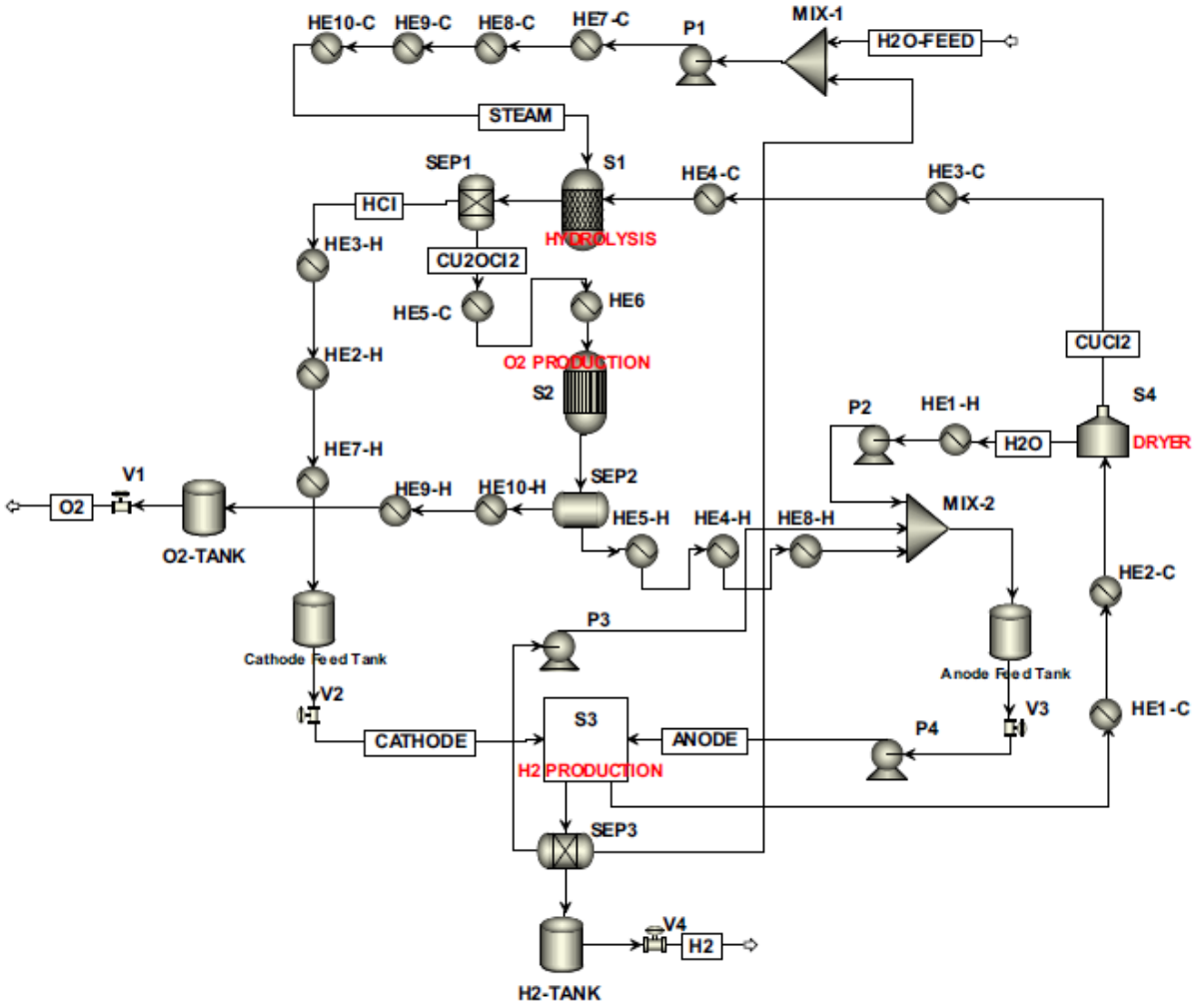

Figure 28: Original Thermochemical Process (Naterer *et al*, 2011b)

Appendix H

Table 36: Total Heat Transferred by Unsatisfied Streams

Stream No	Heat Transferred (kJ/h)	Total Heat Transferred (kJ/h)
20	4204.8+7128+2736+37508.5	51577.3
27	24143.4	24143.4
24	0	0
16	522	522
6	1030.3	1030.3

Table 37: Heat Required to Satisfy Unsatisfied Streams

Stream No	$CP(T_s - T_T)$	Required Q (kJ/h)
20	475.2(540-134)	192931.2
27	406.44(100-20)	32515.2
24	112.32(80-20)	7862.4
16	10.44(80-20)	626.4
6	20.61(80-20)	1236.38

Eq H-1

Table 38: Total Unsatisfied Heat

Stream No	Required-Heat Transferred (kJ/h)	Unsatisfied (kJ/h)
20	192931.2-51577.3	141353.9
27	32515.2-24143.4	8371.8
24	7862.4-0	7862.4
16	626.4-522	104.4
6	1236.38-1030.3	206.08
Total		157898.58
Unsatisfied (kW)	157898.58/3600	43.86

Appendix I

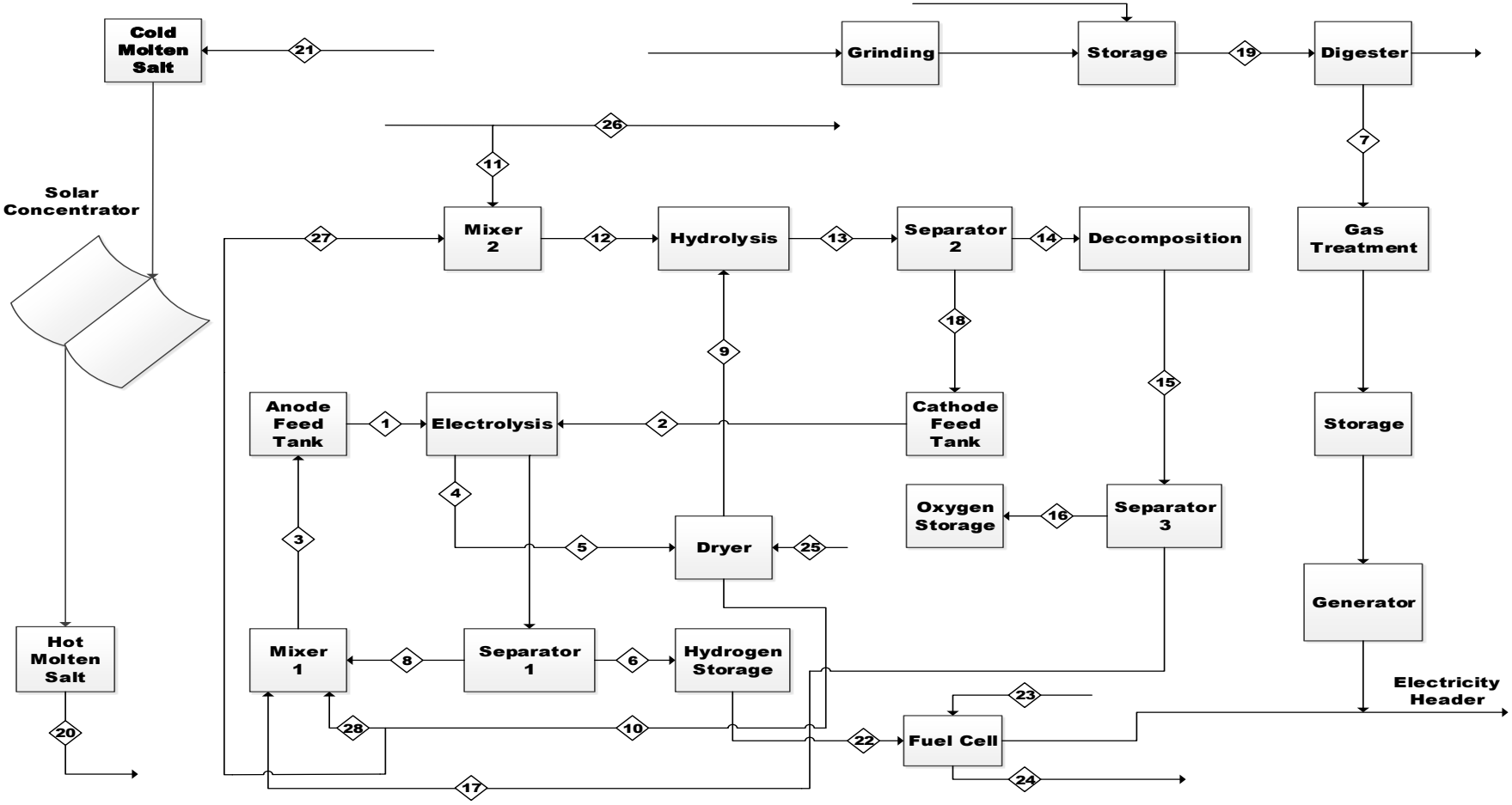

Figure 29: Hybrid Plant Before Integration

Appendix J

Table 39: Original PCT

Time (h)	Time Interval Duration (h)	Source		Power Rating (kW)				
		Biogas (35kW)	Solar (30kW)	Source kW	Demand kW	Source kWh	Demand kWh	Net Electricity (kWh)
0								
	1			35		35	8.44	26.56
1								
	1			35		35	12.53	22.47
2								
	1			35		35	15.19	19.81
3								
	1			35		35	13.28	21.72
4								
	1			35		35	8.17	26.83
5								
	1			35		35	5.43	29.57
6								
	1			35		35	5.7	29.3
7								
	1			35		35	7.27	27.73
8								
	1			65		65	7.61	57.39
9								
	1			30		30	6.24	23.76
10								
	1			30		30	4.95	25.05
11								
	1			30		30	4.88	25.12
12								
	1			30		30	5.09	24.91
13								
	1			30		30	5.3	24.7
14								
	1			30		30	8.63	21.37
15								
	1			30		30	16.89	13.11
16								
	1			30		30	27.2	2.8
17								
	1			65		65	30.34	34.66
18								
	1			35		35	26.45	8.55
19								
	1			35		35	19.08	15.92
20								
	1			35		35	12.46	22.54
21								
	1			35		35	9.18	25.82
22								
	1			35		35	6.73	28.27
23								
	1			35		35	5.97	29.03
24							Total Wasted	586.99

Appendix K

Table 40: Dual 10 kW Hybrid with Continuous Biogas Operation

1	2	3	4	5		6	7	8	9	10
Time (h)	Time Interval Duration (h)	Source		Power Rating (kW)					Start up	
		Biogas (10kW)	Solar (10kW)	Source kW	Demand kW	Source kWh	Demand kWh	Net Electricity (kWh)	Infeasible Cascade (kWh)	Feasible Cascade (kWh)
0									0	9.44
	1			10		10	8.44	1.56		
1									1.56	11
	1			10		10	12.53	-2.53		
2									-0.97	8.47
	1			10		10	15.19	-5.19		
3									-6.16	3.28
	1			10		10	13.28	-3.28		
4									-9.44	0
	1			10		10	8.17	1.83		
5									-7.61	1.83
	1			10		10	5.43	4.57		
6									-3.04	6.4
	1			10		10	5.7	4.3		
7									1.26	10.7
	1			10		10	7.27	2.73		
8									3.99	13.43
	1			10		10	7.61	2.39		
9									6.38	15.82
	1			10		10	6.24	3.76		
10									10.14	19.58
	1			10		10	4.95	5.05		
11									15.19	24.63
	1			20		20	4.88	15.12		
12									30.31	39.75
	1			20		20	5.09	14.91		
13									45.22	54.66
	1			20		20	5.3	14.7		
14									59.92	69.36
	1			20		20	8.63	11.37		
15									71.29	80.73
	1			20		20	16.89	3.11		
16									74.4	83.84
	1			20		20	27.2	-7.2		
17									67.2	76.64
	1			10		10	30.34	-20.34		
18									46.86	56.3
	1			10		10	26.45	-16.45		
19									30.41	39.85
	1			10		10	19.08	-9.08		
20									21.33	30.77
	1			10		10	12.46	-2.46		
21									18.87	28.31
	1			10		10	9.18	0.82		
22									19.69	29.13
	1			10		10	6.73	3.27		
23									22.96	32.4
	1			10		10	5.97	4.03		
24									26.99	36.43

Appendix L

Table 41: Continuous 12 kW Biogas Operation Excluding Solar

1	2	3	4	5	6	7	8	9	10
Time (h)	Time Interval Duration (h)	Source		Power Rating (kW)				Start up & Operation	
		Biogas (12kW)	Solar (0kW)	Source kW	Source kWh	Demand kWh	Net Electricity (kWh)	Infeasible Cascade (kWh)	Feasible Cascade (kWh)
0								0	1.44
	1			12	12	8.44	3.56		
1								3.56	5
	1			12	12	12.53	-0.53		
2								3.03	4.47
	1			12	12	15.19	-3.19		
3								-0.16	1.28
	1			12	12	13.28	-1.28		
4								-1.44	0
	1			12	12	8.17	3.83		
5								2.39	3.83
	1			12	12	5.43	6.57		
6								8.96	10.4
	1			12	12	5.7	6.3		
7								15.26	16.7
	1			12	12	7.27	4.73		
8								19.99	21.43
	1			12	12	7.61	4.39		
9								24.38	25.82
	1			12	12	6.24	5.76		
10								30.14	31.58
	1			12	12	4.95	7.05		
11								37.19	38.63
	1			12	12	4.88	7.12		
12								44.31	45.75
	1			12	12	5.09	6.91		
13								51.22	52.66
	1			12	12	5.3	6.7		
14								57.92	59.36
	1			12	12	8.63	3.37		
15								61.29	62.73
	1			12	12	16.89	-4.89		
16								56.4	57.84
	1			12	12	27.2	-15.2		
17								41.2	42.64
	1			12	12	30.34	-18.34		
18								22.86	24.3
	1			12	12	26.45	-14.45		
19								8.41	9.85
	1			12	12	19.08	-7.08		
20								1.33	2.77
	1			12	12	12.46	-0.46		
21								0.87	2.31
	1			12	12	9.18	2.82		
22								3.69	5.13
	1			12	12	6.73	5.27		
23								8.96	10.4
	1			12	12	5.97	6.03		
24								14.99	16.43

Appendix M

Table 42: 22 kW Hybrid with Biogas Plant Cycling

1	2	3	4	5		6	7	8	9	10
Time (h)	Time Interval Duration (h)	Source		Power Rating (kW)					Start up	
		Biogas (12kW)	Solar (10kW)	Source kW	Demand kW	Source kWh	Demand kWh	Net Electricity (kWh)	Infeasible Cascade (kWh)	Feasible Cascade (kWh)
0									0	5.13
	1			12		12	8.44	3.56		
1									3.56	8.69
	1			12		12	12.53	-0.53		
2									3.03	8.16
	1			12		12	15.19	-3.19		
3									-0.16	4.97
	1			12		12	13.28	-1.28		
4									-1.44	3.69
	1			12		12	8.17	3.83		
5									2.39	7.52
	1			12		12	5.43	6.57		
6									8.96	14.09
	1			12		12	5.7	6.3		
7									15.26	20.39
	1			12		12	7.27	4.73		
8									19.99	25.12
	1			12		12	7.61	4.39		
9									24.38	29.51
	1			12		12	6.24	5.76		
10									30.14	35.27
	1			12		12	4.95	7.05		
11									37.19	42.32
	1			11		11	4.88	6.12		
12									43.31	48.44
	1			11		11	5.09	5.91		
13									49.22	54.35
	1			11		11	5.3	5.7		
14									54.92	60.05
	1			11		11	8.63	2.37		
15									57.29	62.42
	1			11		11	16.89	-5.89		
16									51.4	56.53
	1			11		11	27.2	-16.2		
17									35.2	40.33
	1			12		12	30.34	-18.34		
18									16.86	21.99
	1			12		12	26.45	-14.45		
19									2.41	7.54
	1			12		12	19.08	-7.08		
20									-4.67	0.46
	1			12		12	12.46	-0.46		
21									-5.13	0
	1			12		12	9.18	2.82		
22									-2.31	2.82
	1			12		12	6.73	5.27		
23									2.96	8.09
	1			12		12	5.97	6.03		
24									8.99	14.12

Appendix N

Table 43: Stream Legend

Stream No	Components	Description
1	$CuCl(aq), HCl(aq)$	Electrolyzer Anode Feed
2	$HCl(aq)$	Electrolyzer Cathode Feed
3	$CuCl(aq), HCl(aq)$	Anode Tank Feed
4	$H_2(g), HCl(aq)$	Electrolyzer Product/Separator 1 Feed
5	$CuCl_2(aq)$	Electrolyzer Product/Dryer Feed
6	$H_2(g)$	Hydrogen Storage Feed
7	$Biogas$	Digester Product
8	$HCl(aq)$	Mixer 1 Feed
9	$CuCl_2(s)$	Hydrolysis Feed
10	$H_2O(l)$	Dryer Product
11	$H_2O(l)$	Fresh Water Feed
12	$H_2O(l)$	Hydrolysis Feed
12.1	$H_2O(g)$	Hydrolysis Feed
13	$Cu_2OCl_2(s), HCl(g)$	Hydrolysis Product
14	$Cu_2OCl_2(s),$	Decomposition Reactor Feed
15	$CuCl(aq), O_2(g)$	Separator 3 Feed
16	$O_2(g)$	Oxygen Storage Tank Feed
17	$CuCl(l)$	Mixer 1 Feed
18	$HCl(g)$	Cathode Tank Feed
18.1	$HCl(aq)$	Cathode Tank Feed
19	$Biomass$	Digester Feed
20	$Molten\ Salt$	Process Heating Stream
21	$Molten\ Salt$	Molten Salts Recycle Stream
22	$H_2(g)$	Fuel Cell Feed
23	$Air\ (g)$	Fuel Cell Feed
24	$H_2O(l)$	Fuel Cell Product
25	$Air\ (g)$	Dryer Heating Fluid
26	$H_2O(l)$	Village Hot Water Stream
27	$H_2O(l)$	Dryer Product/Mixer 2 Feed
28	$H_2O(l)$	Mixer 1 Feed

Appendix O

Table 44: CAPCOST Data

CEPCI: 603.1								
Reactors	**Type**	**Volume (m^3)**					**Purchased Cost ($)**	**Bare Module Cost ($)**
Hydrolysis	Jacketed Agitated	11					69 227	276 908
Decomposition	Jacketed Agitated	2					27 983	111 932
Biogas	Jacketed Agitated	7					54 454	217816
Holding/Storage Tanks	MOC	**Height (m)**	**Diameter (m)**	**Volume (m^3)**	**Pressure (barg)**		**Purchased Cost ($)**	**Bare Module Cost ($)**
Anode Feed Tank	Titanium	4	1	3.1	3		8 480	164 156
Cathode Feed Tank	Titanium	4	1	3.1	3		8 480	164 156
Hot Molten Salt Tank	Stainless Steel	4	1	3.1	3		8 480	67 078
Cold Molten Salt Tank	Stainless Steel	4	1	3.1	3		8 480	67 078
Hydrogen Tank	Stainless Steel	4	1	3.1	3		8 480	67 078
Oxygen Tank	Stainless Steel	4	1	3.1	3		8 480	67 078
Gas Treatment Tank	Stainless Steel	4	1	3.1	3		8 480	67 078
Mixers	**Type**	**Power (kW)**					**Purchased Cost ($)**	**Bare Module Cost ($)**
Mixer 1	Propeller	150					165 121	227 867
Mixer 2	Propeller	104					132 532	182 894
Mixer 3	Propeller	5.5					40 055	55 276
Separators	**MOC/Type**	**Height (m)**	**Diameter (m)**	**Volume (m^3)**	**Pressure (barg)**	**Volumetric Flowrate (m^3/s)**	**Purchased Cost ($)**	**Bare Module Cost ($)**
Separator 1	Titanium	3.6	1.2	4	4		9 824	200 673
Separator 2	Dust Collector /Cyclone Scrubber					0.1	2 247	6 428
Separator 3	Stainless Steel	2.6	0.7	1	4		4 775	37 771
Dryers	**Type**	**Area (m^2)**					**Purchased Cost ($)**	**Bare Module Cost ($)**
Dryer	Rotary Dryer	0.5					45 575	72 920
Heat & Power		**Power (kW)**				**$Cost/kW**	**F_{BM}**	**Purchased Cost ($)**	**Bare Module Cost ($)**
Fuel Cell		30				3 537	2.89	106 110	306 658
Biogas Generator		35					2.97	14 000	41 580
Electrolyzer		30				300	2.97	9 000	26 730
Solar Concentrator							1.25	365 322	456 653
Exchangers	**Type**	**Shell Pressure (barg)**	**Tube Pressure (barg)**		**MOC**		**Area (m^2)**	**Purchased Cost ($)**	**Bare Module Cost ($)**
HX1	Double Pipe	4	4		Stainless Steel/Stainless Steel		1	3 357	20 046
HX2	Double Pipe	4	4		Stainless Steel/Stainless Steel		1	3 357	20 046
HX3	Double Pipe	4	4		Stainless Steel/Stainless Steel		1	3 357	20 046
HX4	Double Pipe	4	4		Stainless Steel/Stainless Steel		1	3 357	20 046
HX5	Double Pipe	4	4		Titanium/Carbon Steel		1	3 357	29 933
HX6	Double Pipe	4	4		Stainless Steel/Stainless Steel		1	3 357	20 046
HX7	Double Pipe	4	4		Stainless Steel/Stainless Steel		1	3 357	20 046
HX8	Double Pipe	4	4		Titanium/ Carbon Steel		1	3 357	29 933
HX9	Double Pipe	4	4		Stainless Steel/Stainless Steel		1	3 357	20 046
HX10	Double Pipe	4	4		Stainless Steel/Stainless Steel		1	3 357	20 046
HX11	Double Pipe	4	4		Stainless Steel/Stainless Steel		1	3 357	20 046
HX12	Double Pipe	4	4		Stainless Steel/Stainless Steel		1	3 357	20 046
Total								1 145 869	3 146 134